Development of Fuel Extracting Machine for Converting Plastic Waste into Fuel for Sustainable Waste Management System: A Case of Hossana City

Habtamu Getachew G/Hiwot

A Thesis Submitted to the Department of Mechanical Engineering

School of Mechanical, Chemical and Materials Engineering

Presented in Partial Fulfilment of the Requirement for the Degree of

Master of Science in Thermal Engineering

Office of Graduate Studies

Adama Science and Technology University

May, 2024

Adama, Ethiopia

Development of Fuel Extracting Machine for Converting Plastic Waste into Fuel for Sustainable Waste Management System: A Case of Hossana City

Habtamu Getachew G/Hiwot

Advisor: Dawit Gudeta (PhD)

A Thesis Submitted to the Department of Mechanical Engineering

School of Mechanical, Chemical and Materials Engineering

Presented in Partial Fulfilment of the Requirement for the Degree of Master of Science in Thermal Engineering

Office of Graduate Studies

Adama Science and Technology University

May, 2024

Adama, Ethiopia

DECLARATION

I hereby declare that this Master Thesis entitled “Development of Fuel Extracting Machine for Converting Plastic Waste into Fuel for Sustainable Waste Management System: A Case of Hossana City” is my original work. That is, it has not been submitted for the award of any academic degree, diploma, or certificate in any other university. All sources of materials that are used for this thesis have been duly acknowledged through citation.

Habtamu Getachew	_____	_____
Name of student	Signature	Date

RECOMMENDATION

I, the advisor of this thesis, hereby certify that I have read the revised version of the thesis entitled “Development of Fuel Extracting Machine for Converting Plastic Waste into Fuel for Sustainable Waste Management System: A Case of Hossana City” prepared under my guidance by Habtamu Getachew, submitted in partial fulfilment of the requirements for the degree of Masters of Science in Thermal Engineering. Therefore, I recommend the submission of revised version of the thesis to the department following the applicable procedures.

Dawit Gudeta (PhD)	_____	_____
Major Advisor	Signature	Date

APPROVAL OF BOARD OF EXAMINERS

I, the advisor of the thesis entitled "Development of Fuel Extracting Machine for Converting Plastic Waste into Fuel for Sustainable Waste Management System: A Case of Hossana City" and developed by Habtamu Getachew, hereby certify that the recommendation and suggestions made by the board of examiners are appropriately incorporated into the final version of the thesis.

Dawit Gudeta (PhD)	_____	_____
Major Advisor	Signature	Date

We, the undersigned, members of the Board of Examiners of the thesis by Habtamu Getachew have read and evaluated the thesis entitled "Development of Fuel Extracting Machine for Converting Plastic Waste into Fuel for Sustainable Waste Management System: A Case of Hossana City" and examined the candidate during open defense. This is, therefore, to certify that the thesis is accepted for partial fulfilment of the requirement of the degree of Master of Science in Thermal Engineering.

_____	_____	_____
Chairperson	Signature	Date
_____	_____	_____
Internal Examiner	Signature	Date
Dr. Fitsum Salehu		24.Jun.2024
External Examiner	Signature	Date

Final approval and acceptance of the thesis is contingent upon submission of its final copy to the Office of Postgraduate Studies (OPGS) through the Department Graduate Council (DGC) and School Graduate Committee (SGC).

_____	_____	_____
Department Head	Signature	Date
_____	_____	_____
School Dean	Signature	Date
_____	_____	_____
Office of Postgraduate Studies, Dean	Signature	Date

ACKNOWLEGEMENT

I wish to express my profound gratitude to the Almighty God, the Creator and Sustainer of the Universe, for his invaluable blessings and guidance throughout this journey.

First, I would like to extend my heartfelt appreciation to my advisor, Dr. Dawit Gudeta, for his unwavering support, insightful guidance, generous mentorship, engaging in discussions, and exceptional leadership from the inception to the completion of this study. His contributions have been instrumental in the success of this research.

Moreover, I extend my sincere gratitude to my esteemed instructors, Dr. Addisu Bekele and Dr. Gezahegne Habtamu, for their inspiring lectures, constructive feedback, and encouragement throughout my academic career. Their dedication to imparting knowledge and fostering intellectual growth is a constant source of motivation.

Lastly, I express my heartfelt appreciation to my beloved parents, friends, and colleagues for their steadfast support in making this thesis more meaningful and for their invaluable contributions to my academic pursuits. Their presence and encouragement have been constant sources of strength and inspiration.

TABLE OF CONTENTS

LIST OF TABLES

LIST OF FIGURES

LIST OF ACRONYMS AND ABBREVIATIONS

SPI	Society of Plastic Industry
HDPE	High Density Polyethylene
LDPE	Low Density Polyethylene
PP	Polypropylene
PS	Polystyrene
PET	Polyethylene Terephthalate
PVC	Poly Vinyl Chloride
CAE	Computer Aided Engineering
CAD	Computer Aided Design
CFD	Computational Fluid Dynamics
CFR	Continuous Flow Reactor
AFCIS	Arc Fault Circuit Interrupters
GMAW	Gas metal arc welding
MIG	Metal inert gas
MAG	Metal active gas

ABSTRACT

The exponential growth in plastic production and consumption has led to a significant plastic waste crisis, particularly in developing regions, such as Hossana City, Ethiopia. This study aimed to address the environmental and health challenges posed by plastic waste through the development of a fuel-extracting machine that converts plastic waste into fuel. The primary objective is to create a sustainable waste management solution to mitigate pollution and provide an alternative energy source. This study began by identifying the problem of inadequate plastic waste management in Hossana City, highlighting the environmental degradation and health risks associated with plastic accumulation. The objective of this study is to design and develop a machine that utilizes pyrolysis technology to convert plastic waste into pyrolysis oil, char, and hydrocarbon gas. The methodology includes the conceptual and detailed design of the machine's reactor, condenser system, and body frame, followed by the characterization of the physicochemical properties of the produced fuel and emission tests. The results showed that 49% of the plastic waste was converted into pyrolysis oil, 8% into char, and 43% into gas, thereby demonstrating the efficiency of the process. The properties of the produced pyrolysis oil included a calorific value of 41.318 MJ/kg, a density of 0.789 g/ml at 15°C, and a kinematic viscosity of 2.31 mm²/s at 40°C. These results indicate that the produced pyrolysis oil has a high calorific value and properties comparable to those of diesel fuel, making it a viable alternative. Emission tests confirmed that the fuel met environmental standards, suggesting that the machine can effectively reduce plastic waste while providing a sustainable energy source. The application of this technology extends beyond Hossana City, offering a scalable solution for other regions facing similar challenges. By converting plastic waste into valuable fuel, this innovation promotes environmental sustainability, reduces reliance on fossil fuels, and enhances waste management practices. In conclusion, the development of a fuel-extracting machine represents a significant advancement in sustainable waste management and energy production, addressing critical environmental issues and contributing to a cleaner and healthier future.

Key words: Fuel Extraction Machine; Plastic Waste; Condenser; Reactor

CHAPTER ONE

1. INTRODUCTION

1.1. Background of the study

Plastics are a diverse group of synthetic and semi-synthetic materials, primarily consisting of polymers. Polymers are composed of repeating units called monomers(Desidery & Lanotte, 2022). Plastic products are widely used because of their durability, versatility, light weight, and low cost. However, the increasing demand for plastic products has led to major global concerns, with significant implications for the environment, making it a pressing problem.

The production of plastics has surged since the 1980s, with global production increasing from only two million tons in the 1980s to a staggering 381 million tons in 2015(Sarker, 2012). In the 1980s, virtually all plastic waste was discarded without recycling or incinerating. Fortunately, advancements in technology have made it possible to dispose plastic waste more responsibly. By 2015, only 19.50% of plastic waste was recycled, 55% was still discarded, and 25.50% was incinerated(Ritchie et al., 2023).The surge in the production and consumption of plastic materials has resulted in the growing accumulation of plastic waste, particularly in low-income countries.

As a developing continent, Africa faces unique challenges in managing plastic waste, including limited recycling infrastructure, insufficient waste management systems, and inadequate policies. Based on data from 33 African countries, approximately 172 metric tons (Mt) of plastic waste and polymers were imported between 1990 and 2017, with a value of $285 billion(Babayemi et al., 2019a). Projections indicate that plastic imports to the continent are likely to double within the next five years. Ethiopia, one of the fastest-growing economies in Africa, has experienced a significant increase in plastic consumption due to population growth. However, the absence of a formal system to manage plastic waste has resulted in widespread pollution.

Hossana City, located in the southern region of Ethiopia, is struggling with the plastic waste accumulation crisis caused by rapid urbanization, expansive industrial growth, and inadequate waste management infrastructure(Doboch Wanore et al., 2023).The persistence of non-biodegradable plastics not only spoils the city's aesthetics, but also obstructs drainage

systems, amplifies the proliferation of disease vectors, and poses a risk to local ecosystems, particularly during the rainy season.

Plastic waste management affects both developed and developing countries. Plastics are non-biodegradable and must be continuously removed from the environment using various methods, including reduction, reuse, combustion, incineration (energy recovery), and mechanical recycling(Kaiser et al., 2017).However, conventional mechanical recycling methods, such as sorting, grinding, washing, and extrusion, can only recycle 15-20% of all plastic waste(Darko et al., 2023), and plastic waste management system is as shown in Figure1-1.

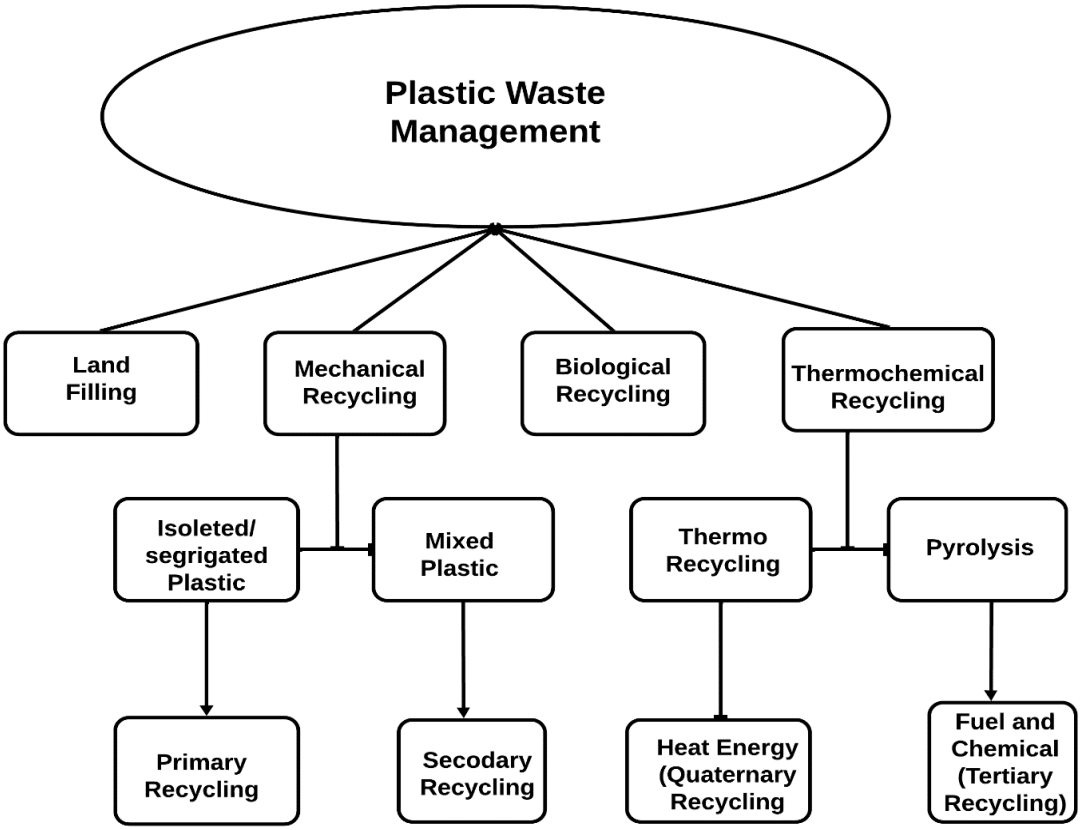

Figure 1-1: Flow chart representation of plastic waste management.

Recognizing this urgent challenge, the development of a fuel-extraction machine capable of converting plastic waste into a viable fuel source has emerged as a crucial solution. The current work focuses on developing a fuel extraction machine that utilizes the pyrolysis to produce fuel oils with a composition similar to that of diesel.

1.2. Statement of the problem

The improper disposal of plastic waste is a major environmental concern in Ethiopia, particularly in Hossana City. It is struggling to handle the increasing amount of plastic waste, owing to more people and higher consumption. This large amount of plastic waste is harmful to the environment and can cause health problems to residents. Because the city does not have good ways to manage this waste, it is piling up in landfills and rivers, causing pollution and hurting the nature. This urgent situation calls for an immediate solution to the problem of plastic waste. A recent study show that Hossana City produces a lot of plastic waste for each person every year(Doboch Wanore et al., 2023). Excessive waste causes pollution and causes people to become sick (Gross and Enck, 2021). Therefore, it is important to develop a machine that can convert plastic waste into fuel for sustainable waste management. This new approach not only aims to reduce the use of fossil fuels, but also to help the environment in the city.

Moreover, mishandled plastic waste not only harms nature, but also affects people's health. Improperly disposing of plastic waste leads to pollution in water, soil, and air, harming plants, animals, and people Also, the dangerous parts in plastics can cause serious health problems for both humans and animals (Pandey et al., 2023). To solve these problems, the development of a fuel extraction machine provides a practical solution for transforming plastic waste into valuable fuel. This machine can effectively reduce plastic waste, mitigate environmental pollution, and contribute to a more sustainable and cleaner city.

1.3. Objectives of the study

This section elaborates on the general and specific objectives of the study. This includes the general objective and the specific, details outlined as follows

1.3.1. General objective

The general objective of this study is to develop machine that extracts fuel from plastic waste, addressing the plastic waste management issues.

1.3.2. Specific objectives

The specific objectives of this study are as follows:

- Designing and developing the reactor.
- Design and development of condenser system.
- Design and development of body of machine
- Characterization of physicochemical properties of extracted fuel.
- Conduct emission test for extracted fuel

1.4. Significance of the study

The development of a fuel-extracting machine to convert plastic waste into fuel for a sustainable waste management system in Hossana is a crucial step towards addressing the challenges of waste management, energy dependence, and environmental pollution. In developing countries, such as Ethiopia, waste management practices are very poor, and plastic waste has been one of the materials with the fastest growth owing to its wide range of applications. This can lead to serious environmental problems. Fuel-extracting machines can significantly reduce the environmental impact of plastic waste by diverting it from landfills and converting it into a usable fuel. This can help improve waste management efficiency and reduce the reliance of a city on imported petroleum.

The machine can also raise public awareness about the value of plastic waste as a resource, encouraging responsible waste disposal practices, and reducing littering. The benefits of this study extend to all members of Hossana City's society. Improvements in environmental conditions, reduced energy costs, and a more sustainable future will benefit the public.

1.5. Scope and Limitation of the study

This study focused on developing a sustainable solution for converting plastic waste into liquid fuel, which is suitable for a sustainable waste management system in Hossana, Ethiopia. The scope begins with a comprehensive analysis of the composition and characteristics of the prevalent plastics (HDPE, LDPE, PP, and PS) found in the city. Subsequently, this research will involve the design and prototyping of a specialized machine/system that can efficiently extract fuel from plastic materials. This was followed by rigorous experimentation, aimed at maximizing fuel yield, maintaining quality, and minimizing environmental impact, with a focus on energy efficiency during the extraction process. Finally, the quality of the extracted fuel was thoroughly assessed to ensure that it

meets the necessary standards for effective and safe use. This is done by considering factors such as the calorific value, density, kinematic viscosity and emissions test. Through these essential stages, this study aimed to provide a viable and environmentally friendly approach for utilizing plastic waste as a valuable resource for fuel production in Hossana, Ethiopia.

This study has several limitations. Only specific types of plastics were processed, excluding PET and PVC, and the machine had a limited processing capacity of 10 kg/batch. Resource constraints such as limited funding, technical expertise, and materials influence the design and fabrication process. Long-term environmental effects and potential safety hazards have not been fully assessed, and the findings may require modifications for different geographical and socio-economic contexts. Additionally, technological constraints such as precision in temperature control and condensation efficiency affect the quality and yield of the produced fuel.

1.6. Organization of the study

This thesis comprises seven chapters, each with a unique purpose and function, to contribute to the comprehensive examination of this study. The first chapter presents an introduction outlining the objectives, significance, and scope of this study. It provides an overview of what will be covered in subsequent chapters. In Chapter Two, a comprehensive literature review is presented, focusing on the development of a fuel- extracting machine from plastic waste. This review synthesizes the existing research and knowledge to provide a solid foundation for this study. The third chapter presents the materials and methodology employed in the preparation of this thesis paper are discussed. This includes the fabrication process of the machine and its components as well as the experimental methods utilized. The fourth chapter discusses the design and theoretical analysis of the machine and its components. The underlying principles and concepts guiding the development of these components are explored. Fifth chapter composes the fabrication of the prototypes, the experimental setup, and the procedures. Chapter six presents the experimental results. This includes laboratory findings and a comprehensive discussion of the results, allowing for deeper understanding and interpretation of the data. The last chapter concludes the thesis by summarizing the main findings and presenting recommendations based on the work conducted. This served as the final stage of the study, providing closure and highlighting areas for further exploration or improvement.

CHAPTER TWO

2. LITERATURE REVIEW

A literature review is a fundamental aspect of any research study or academic paper, as it involves a comprehensive and in-depth examination of the existing literature, which encompasses scholarly articles, books, and other pertinent sources associated with the research topic. The main goal of the literature review is to present a summary, evaluation, and critical analysis of the existing knowledge and research topics. This chapter reviews and assesses the literature relevant to this research topic.

2.1. Classification of plastics

The Society of Plastics Industry (SIP) classifies plastics into different categories based on their applications and chemical structures, resulting in the following groupings:

2.1.1. Polyethylene terephthalate (PET)

Polyethylene terephthalate, commonly referred to as PET, has gained significant popularity in the production of a wide range of plastic packaging materials, particularly for beverages like water, soda, and juice. Its extensive usage can be attributed to its exceptional properties that make it suitable for manufacturing large, lightweight, and pressure-resistant containers. Furthermore, PET has diverse applications, such as electrical insulation, sheet printing, and the production of decorative tapes, X-rays, and photographic films(Nofar and Oğuz, 2019).

2.1.2. High-density polyethylene (HDPE)

Catalysts and low pressure were utilized to produce high-density polyethylene (HDPE), which was initially used in pipes for storm sewers, drains, and culverts. Currently, HDPE is used in a diverse array of products. HDPE is a straight polymer chain with a high degree of crystallinity and minimal branching, leading to its exceptional strength. Its remarkable properties make it a preferred choice for manufacturing items, such as drain bottles, cleaning product bottles, oil containers, toys, and other products. A myriad of applications contribute to approximately 17.6% of plastic waste, making HDPE the third most prevalent type of plastic found in municipal solid waste(Wilke, 2003).

2.1.3. Polyvinyl chloride (PVC)

Polyvinyl chloride (PVC) is a synthetic compound commonly employed in industrial applications. Unlike thermoplastics, such as polyethylene (PE), polystyrene (PS), and polypropylene (PP), which are derived solely from oil and can be melted using heat, PVC is produced by combining 57% chlorine obtained from industrial salt with 43% carbon derived from hydrocarbon feedstocks, such as ethylene obtained from oil or natural gas(Reif-Acherman, 2012).

2.1.4. Low-density polyethylene (LDPE)

LDPE, also known as the first polyethylene to be produced, is often referred to as the "grandfather of the material." Unlike HDPE, which boasts of a greater mass, LDPE is considered a separate material for recycling because of its lower mass. As a thermoplastic made from ethylene monomer, LDPE is commonly used in the production of trays, general-purpose containers, juice bottles, and plastic cartons. LDPE is known for its greater flexibility than HDPE, as it becomes less crystalline and easier to shape when stretched. Additionally, LDPE is highly resistant to water, making it a popular choice for plastic bags, packing foils, trash bags, and more(Ebenezer et al., 2013).

2.1.5. Polypropylene (PP)

PP is a polymer with a saturated linear hydrocarbon chain and is known for its exceptional chemical and heat resistance. Unlike HDPE, PP does not have a melting point below 160°C. Despite having a lower thickness than HDPE, PP has higher hardness and rigidity, making it a popular choice in the plastic industry. Additionally, PP was the largest contributor to the category of plastic waste found in municipal solid waste, accounting for approximately 24.3% (Hogan and Banks, 1986).

2.1.6. Polystyrene (PS)

Polystyrene (PS) is a polymer composed of styrene monomers obtained from liquid petrochemicals. It consists of a long hydrocarbon chain with a phenyl group attached to each carbon atom. Although they are naturally colorless, they can be colored using colorants. Polystyrene is known for its flexibility and offers good strength, durability, and delicacy, which make it an attractive option for use in various fields, including food packaging, equipment development, medical devices, and toys(Rasmussen, 2018).

The Society of the Plastics Industry (SPI) devised a recycling and disposal classification system to facilitate the proper handling of plastics. Manufacturers now follow this coding system and affix a unique number, referred to as SPI code, to each product. This number is typically molded at the bottom of the product, as shown in Table 2-1.

Table 2-1: Plastic identification codes.

Symbol	Acronym	Uses
	PET	Widely used material in the production of fizzy drink bottles and frozen ready-meal packaging.
	HDPE	Used in the production of milk and dishwashing liquid containers.
	PVC	Used in the production of food trays, cling films, bottles for squash, mineral water, and shampoos.
	LDPE	Commonly used in the production of carrier bags and bin liners.
	PP	Used in margarine tubs, microwave-able meal trays.
	PS	Commonly utilized in the production of numerous items, such as yogurt cups, foam meat or fish trays, hamburger containers, egg cartons, vending cups, plastic cutlery, and protective packaging for electronic gadgets and playthings.
	Other	Plastics like melamine, which are commonly utilized in the production of plastic cups and plates, are not classified into any of the previously mentioned categories and are therefore considered to be other plastics.

2.2. Selection of waste plastic

The effectiveness of converting waste plastics into fuel depends on strategic decisions regarding the selection of target plastic types and the characteristics of other waste materials involved in the process. The success of this conversion process is heavily influenced by the

specific technologies chosen, which should be aligned with the local economic, environmental, social, and technical considerations. It is crucial to note that the composition of plastics used as feedstock can vary significantly, with some plastics potentially containing hazardous substances harmful to both humans and the environment, such as nitrogen, halogens, sulfur, and other harmful elements(Pandey et al., 2023).

The type and composition of plastics play a pivotal role in determining pre-treatment requirements, the necessary combustion temperature for conversion, energy consumption levels, fuel quality, and composition of flue gases (including the formation of harmful gases such as NOx and HO), composition of fly ash and bottom ash, and the potential for chemical corrosion of equipment(Babayemi et al., 2019). These factors underscore the importance of meticulous planning and consideration when selecting waste plastics and other materials for fuel conversion processes, as highlighted in Table 2-2.

Table 2- 2: Fuel properties of oils derived from the pyrolysis of various plastics.

Property	**PE**	**PS**	**PP**
Flash point (◦C)	33.6	27.8	26.1
Pour point	2.7	-39	-67
Water content (ppm)	0.18	0.13	0.67
Ash (wt. %)	0.013	0.010	0.006
Viscosity (mm^2/s)	2.19	1.9	1.4
Density (g/ml)	0.858	0.792	0.960

2.3. Methods for Pyrolysis of plastics

The pyrolysis of plastics can be accomplished through several methods, including thermal cracking, catalytic cracking, and cracking-catalytic reforming. Each method has its own set of processes, as illustrated in Figure 2.1. In addition to these three methods, other techniques for the pyrolysis of plastics include hydrogenation, gasification, pyrolysis in supercritical water, and others(Ebenezer et al., 2013).

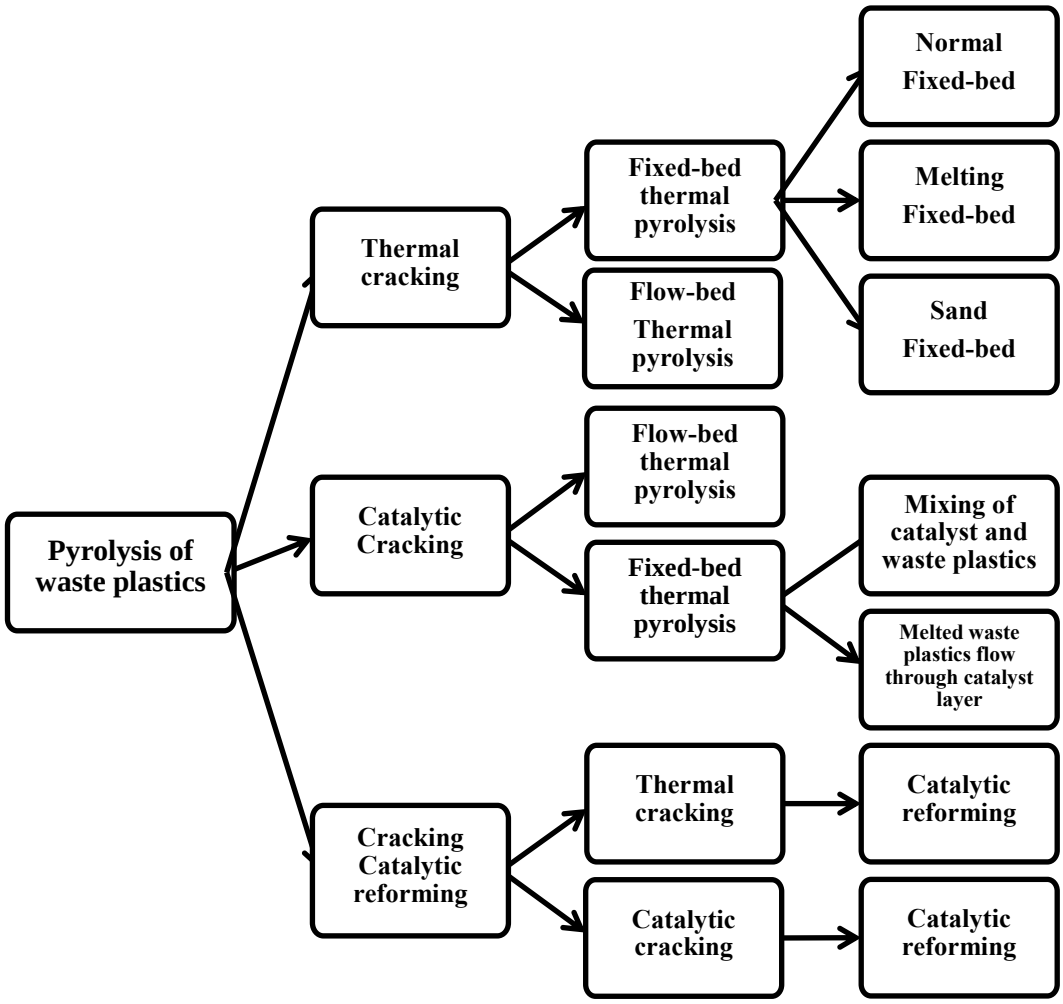

Figure 2-1: Methods for pyrolysis of plastics.

2.4. Factors affecting plastic pyrolysis

Plastic pyrolysis is a thermal decomposition process where plastic waste is converted into valuable products like liquid fuel, gas, and char in the absence of oxygen. This process offers a promising solution for managing plastic waste and recovering energy. Several factors significantly affect the efficiency and outcome of plastic pyrolysis. These factors include the type of plastic feedstock, the temperature of the pyrolysis process, the heating rate, the presence of catalysts, the reactor design, and the residence time of the material in the reactor. The details are as follow:

2.4.1. Reactor type

The choice of reactor in pyrolysis processes significantly influences key factors, such as heat transfer efficiency, mixing effectiveness, residence times of gas and liquid phases, and the prevention of primary product escape(Panda et al., 2010).

In laboratory-scale pyrolysis, various reactor types are employed, including batch, semi-batch, and continuous flow reactors (CFR), sometimes in modified or combined forms. Nitrogen is commonly used in batch and semi-batch operations to purge volatiles continuously from the reactor and vessel, and product collection is achieved by vapor passage through a condensation system. However, this method often results in extended reaction times and can limit catalyst effectiveness compared to thermal product yields under similar conditions. In industrial settings, continuous reaction systems are preferred over batch configurations because of their operational efficiency(Varma & Mondal, 2017).

2.4.2. Temperature

The Temperature plays a vital role in the plastic pyrolysis process, with the required temperature varying depending on the type of plastic and desired product outcome, as illustrated in Table 2-3. At temperatures exceeding 600°C, a mix of fuel gases such as H_2, CH_4, and light hydrocarbons is generated, whereas temperatures ranging from to 400-600°C result in the production of wax and liquid fuel. These liquid fuel derivatives include naphtha, heavy oil, gasoline, diesel, and kerosene. When polyethylene (PE) and polypropylene (PP) undergo pyrolysis, they are mainly transformed into fuel oil and gas, respectively, whereas polystyrene (PS) yields a higher proportion of styrene monomers and light hydrocarbons. Introduction of suitable catalysts can lower the cracking temperature to 200-300°C, thereby enhancing the yield of the liquid products(Murthy et al., 2023).

Table 2-3: Some laboratory experiments of thermal pyrolysis.

Investigator	**polymer**	**Reactor**	**Temperature**	**Products**
(Uddin et al., 1997)	HDPE, PP, PS	Continuous flow stirred reactor	350–450	gas, oil
(Moriya and Enomoto, 1999)	HDPE	Bomb-type autoclave	400–425	gas, oil
(Bockhorn et al., 1999)	HDPE, PP	Closed loop-type reactor	410–480	gas, oil
(Kaminsky et al., 2004)	Mixed waste	Fluidized-bed reactor	600–750	gas, oil, aromatics
(Miskolczi et al., 2004)	Mixed waste	Tube reactor	500–550	Gas, wax, oil

2.4.3. Catalyst

The incorporation of catalysts into the pyrolysis process offers significant advantages, with numerous researchers striving to enhance the yield and quality of light oil derived from waste plastics. As shown in Table 2-4, the inclusion of a catalyst resulted in a substantial reduction in the degradation temperature required to achieve specific conversion levels. In addition, increasing the catalyst content in the waste plastic led to a lower degradation temperature. The liquid product generated from the catalytic degradation contained a greater number of products in the gasoline range and more isoalkanes and aromatics in the C_5-C_{10} range(Sonawane et al., 2014). Furthermore, the reaction rate is significantly accelerated. By carefully selecting and modifying the catalyst, the product distribution during catalytic degradation can be effectively controlled, allowing the targeted optimization of the desired outcomes.

Table 2-4: Literature survey on the effect of catalyst.

Investigator	Polymer	Experimental set-up	Catalyst concentration (%)	Catalyst
(Marcilla et al., 2008)	LDPE HDPE	The thermogravimetric analyzer included a sample mass ranging between 4-25 mg, heating rate of 10 or 40°C/min, and nitrogen environment.	2–9	MCM-41
(Seddegi et al., 2002)	HDPE	The reactor containing 3 g of polymer was connected to a liquid condenser and gas collection bag and analyzed using gas chromatography (GC) for both liquid and gas components.	10–16	MCM-41
(Aguado et al., 2007)	LDPE	The screw kiln reactor, which was outfitted with two furnaces, each measuring 52 cm and 250 g of polymer at a temperature of 300°C under a nitrogen atmosphere, utilized a flow rate of 3.0-15.0 m3/h.	2	Al-MCM-41
(Jalilvand et al., 2007)	HDPE	The quantity of atmospheric HDPE pellets incorporated in the glass batch reactor was 3 g.	3 and 6	MCM-41
(Jung et al., 2010)	PS	A 100.0-gram mixture of PS and 1 g of catalyst was loaded into a Pyrex glass batch reactor.	1	Clinoptilolite, HZSM-5, silica–alumina

The following literature review presents a variety of problems in field pyrolysis technology and design constraints with appropriate solutions given by different scholars. The findings of these researchers have elaborated on their strengths and weaknesses.

Murthy et al., (2023), carried out a comprehensive review of the plastic pyrolysis process in 2023. They investigated the influence of various operational parameters and analyzed the properties of the liquid oil produced. This study revealed that many plastics can produce oil with calorific values comparable to those of conventional fuels.

The distribution of pyrolysis products depends on the reactor used, with Bach-type reactors being commonly studied because of their simple design and operation. On the other hand, continuous fluidized bed reactors can achieve more stable products through the uniform mixing of feedstock and heat carriers or catalysts during operation.

(Damodharan et al., (2019) examined the potential use of waste plastic oil in diesel engines. They utilized pyrolysis, a process involving silica, alumina, ZSM-5, and kaolin catalysts, to produce waste plastic oil with a yield of up to 80 wt.%. This pyrolysis oil has a lower cetane number than fossil diesel, leading to longer ignition delays and higher heat release. Additionally, NOx emissions were higher with plastic pyrolysis oil, while smoke emissions were primarily low and could be further reduced to Euro standards with oxygenated additives. This study found that plastic pyrolysis oil is a feasible substitute for fossil diesel and can operate smoothly in diesel engines.

Shukla et al., (2016) created a machine designed to transform domestic waste plastic, such as polyethylene, polypropylene, or plastic bags, into mixed oil for domestic use. The machine comprises a temperature-controlled electric heater, insulating materials, a closed container with the heater, while water is used for condensation process. The machine produces three out puts: mixed oil, hydrocarbon gas, and carbon black charcoal. This invention can help solve the problem of fuel shortage for local villagers, but is not suitable for PET bottles or PVC pipes. The machine's design is optimized to manage daily domestic plastic waste and provide three types of fuel in return.

Wongkhorsub and Chindaprasert, (2013) conducted a study comparing the use of pyrolysis oil (made from plastic pyrolysis) and diesel oil in a one-cylinder multipurpose agricultural diesel engine. The study aimed to assess engine performance and feasibility. The researchers applied waste plastic pyrolysis oils to the engine and evaluated the results.

Fojt et al., (2020) examined the neglected issues related to the accumulation of micro-plastics in soil. As biodegradable plastic products are gradually replacing conventional ones, composting is recommended for disposing of bioplastics. However, the resulting compost may contain micro-bioplastic particles caused by incomplete biodegradation, which can lead to soil contamination. These researchers proposed solutions by summarizing sample pre-treatments and analytical techniques.

Analytical techniques involve both thermo-analytical (i.e., pre-sorting and respective detection limits) approaches. They concluded that a rapid and suitable method is necessary to determine micro-plastic production rates, fate, sorption properties, and toxicity, as there is limited understanding of these factors. Among the approaches thermo-analytical methods show the most promise.

The rest of the literatures are studied and summarized in a tabular form in order to make easier for the readers of this paper to grasp the required information as shown in Table 2-5.

Table 2-5: Summary of literature.

Authors	**Title**	**Findings**
(Rapsing, 2016)	Design and Fabrication of Machine to Extract Base oil from Waste Plastic.	The hallmark of this design is its suitability for small-scale or domestic use, marking it light weight and compact for easy portability. In the pyrolysis process, the machine operates within a temperature-controlled heater, which is crucial for optimal oil output.
(Singh et al., 2017)	Design and Fabrication of Machine to Extract Base Oil from Waste Plastic an Overview.	The oil derived from the machine can be utilized for daily domestic purposes such as stoves or generators. However, for commercial applications, it requires refining, which, after the process, renders the oil equivalent to diesel and petrol.

(Farayibi, 2017)	Finite element analysis of plastic recycling machine designed for production of thin filament coil.	The successful conceptualization and design of a PET plastic recycling machine have been achieved. The machine features a shredder hopper, two shredder shafts with knife-edge ring cutters, an extruder hopper, an extrusion chamber, and an extrusion auger shaft.
(Mutha et al., 2006)	Design and Analysis of Waste Plastic Pyrolysis Reactor	A comprehensive analysis and design of the pyrolysis system contribute to the development of an efficient and economical system that surpasses other existing processes.

Based on the provided literature review, the following summary can be drawn:

- Thermolysis, a thermochemical decomposition process, effectively converts various types of plastic waste into hydrocarbon fuels. The optimal temperature range for this process is between 450°C and 500°C.
- According to observations made thus far, various types of plastic waste can serve as viable alternatives to petroleum products. A study conducted by (Shehata et al., 2017) found that different plastic products, such as HDPE, LDPE, PP, and PS, possess nearly identical calorific values when compared to diesel, petrol, and LPG.
- Introducing catalysts during thermolysis significantly enhances the conversion efficiency and improves the quality of the produced fuel.
- Catalysts lower the degradation temperature and shorten the reaction time, leading to a more efficient and productive fuel extraction process.
- The use of catalysts can significantly impact the product yield in the thermolysis process. Natural zeolite, for example, has been found to increase product yield from 80% to 86%(Sonawane et al., 2014)
- The properties of the fuel obtained through pyrolysis closely resemble those of conventional diesel and petrol fuel oils. This indicates that plastic-derived fuel holds promise as a viable alternative to traditional fossil fuels.

- In terms of liquid fuel yield, HDPE has been found to produce 77.03% of liquid fuel, while LDPE has been found to produce 90% of liquid fuel(Khan et al., 2016) found 90% from LDPE(Pratama & Winarko, 2020).
- Developing a fuel-extracting machine based on thermolysis technology has the potential to address the growing concerns of waste plastic management and reliance on imported petroleum.

2.5. Research gaps

Research on plastic waste conversion, reveals significant gaps in the existing literature especially in Ethiopia. Firstly, there's a noticeable a few of comprehensive studies dedicated to developing a specialized machine for converting plastic waste into fuel. This specific area requires focused research attention. Additionally, current research overlooks critical aspects such as heat distribution within the reactor and strategies to mitigate heat loss, which significantly affect overall efficiency. Addressing these inefficiencies by emphasizing heat distribution and reducing heat loss should be a priority for future research effort.

Moreover, the prevalent use of wood as the primary heat source leads to deforestation, highlighting the need to explore sustainable alternatives like electricity, an area that remains largely unexplored. Lastly, insufficient attention has been given to the utilization of suitable refractory materials to enhance heat retention within the reactor, which could significantly improve the efficiency of the plastic waste-to-fuel conversion system. Closing these gaps through dedicated research efforts stands to advance and enhance the technology for efficient plastic waste-to-fuel conversion in Hossana City, contributing to sustainable waste management practices in the region.

CHAPTER THREE

3. MATERIALS AND METHODOLOGY

This chapter presents the overall design of the study, including the materials and equipment used for measurement, methodology applied for conducting various tasks, and different phases of the research. This section offers a comprehensive summary of the work carried out at each stage, detailing the tools, techniques, and models applied.

3.1. Methodology

3.1.1. Research procedures and materials

The process of developing a waste-plastic oil converter involves several key stages, including planning, design, fabrication, preliminary testing, modification, final testing, and data collection. Researchers aim to achieve the desired outcomes by reviewing the existing practices and literature on converting plastic waste into a valuable resource, particularly through pyrolysis. The material, tool, equipment, part, and accessory selection for waste-plastic-to-fuel converters is a crucial aspect of the planning phase. The equipment design includes the incorporation of an electric heater with a temperature controller, reactor tank, reactor tank frame, condensing tank, and frame to achieve the required temperature. The proper placement and arrangement of each machine component were carefully considered in the design process. Environmental considerations led to the construction of a smoke cleaning tank to purify smoke and condense the remaining vapor before it was released into the atmosphere. Fabrication commenced after preparing all the necessary materials, such as angle bars, stainless pipes, copper tubes, hoses, hose clips, air chucks, stainless steel pots, electric heaters, thermocouples, temperature controllers, circuit breakers, condensing tanks, and wastewater-collecting tanks.

The testing phase involves two stages: preliminary and final tests. Modifications were made to certain equipment parts after preliminary testing to improve functionality. Subsequently, a final test was conducted to assess the performance of the waste plastic-to-fuel converter. Only the liquid product and char were collected, and the gas was submerged in water before being released into the atmosphere. Finally, the chemical properties of the derived fuels were analyzed, and emission tests were performed.

3.2. Pyrolysis based fuel production flow process methodology and implementation

A machine for producing fuel oils with compositions comparable to those of diesel was developed using pyrolysis, as shown in Figure 3-1. The implemented system comprises the heating, vaporizing, dewaxing, and condensing processes. The heating system provides the heat required to melt and vaporize the solid plastic, which is the field in the reactor. To minimize the heat loss from the system, a refractory brick material was utilized. The temperature inside the reactor was maintained at 450°C by using a temperature controller. After complete vaporization of the plastic, the vapor passed through a piping system and entered the bubbler (dewaxer) to protect the wax from entering the condenser. The condenser was then responsible for changing the fuel from a vapor state to a liquid state.

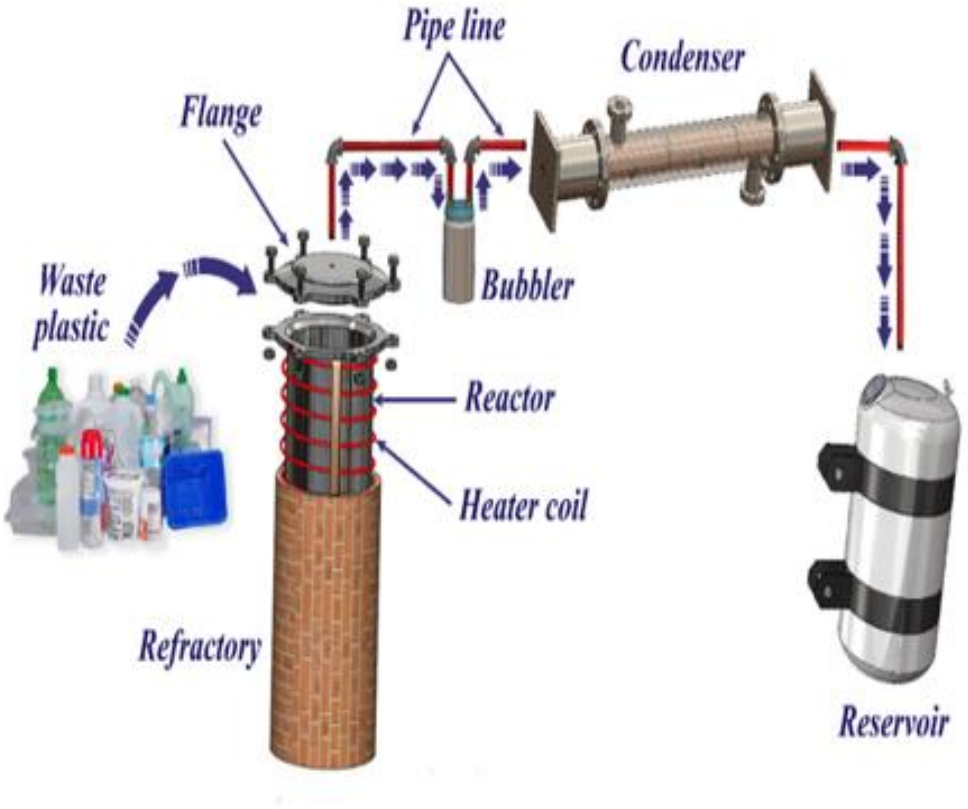

Figure 3-1: Process flow diagram of fuel production by using pyrolysis.

3.3. Study area

Hossana, also known as wachemo, is a significant administrative and commercial center in the Central Ethiopia Regional State. It is located in the Hadiya Zone and serves as its central hub. Hosanna is positioned at a latitude and longitude of 7°33′N 37°51′E and has an elevation of 2177 meters above sea level. It is situated 230 km southwest of the capital, Addis Ababa, and 235 km west of the region of Oromia City, Adama, as depicted in Figure 3-2 below.

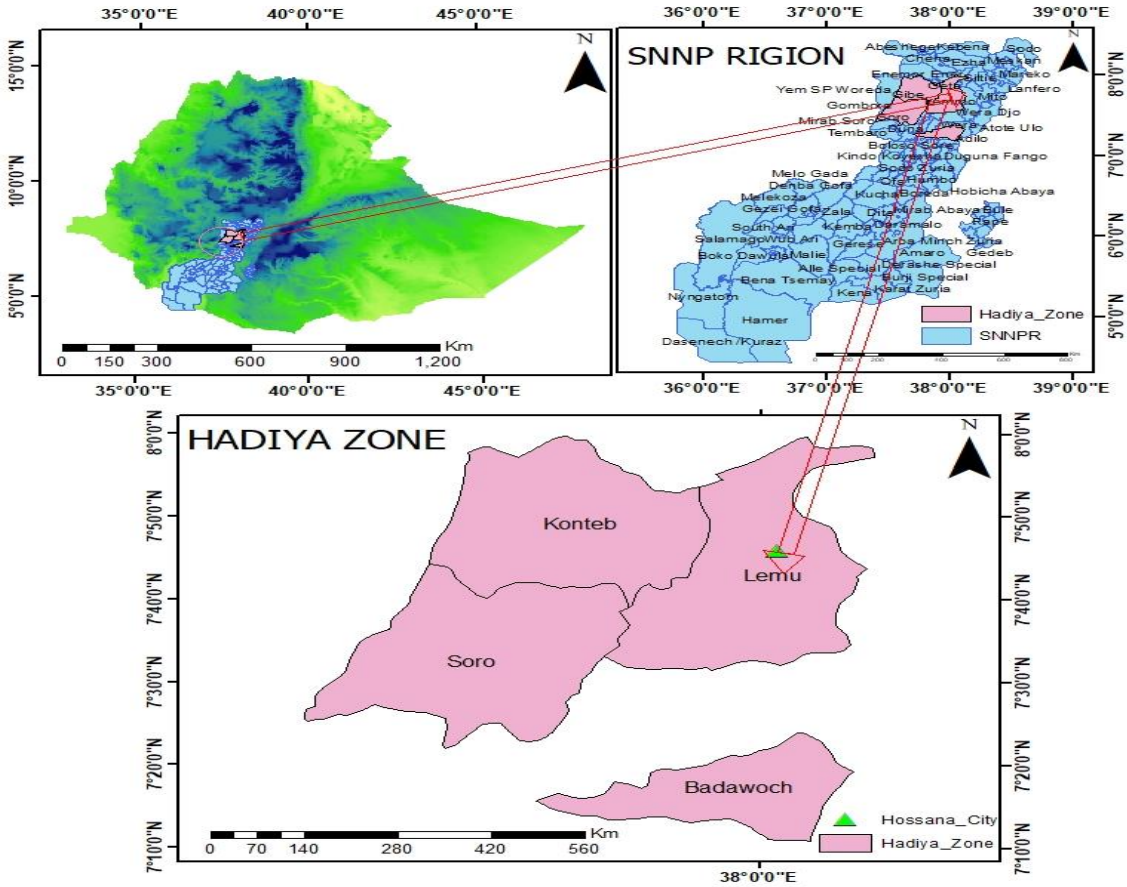

.

Figure 3-2: Location of study area.

The step-by-step methodology used to conduct the study is outlined below and illustrated in Figure 3-3. This flow chart illustrates the general process and sequence of our research approach

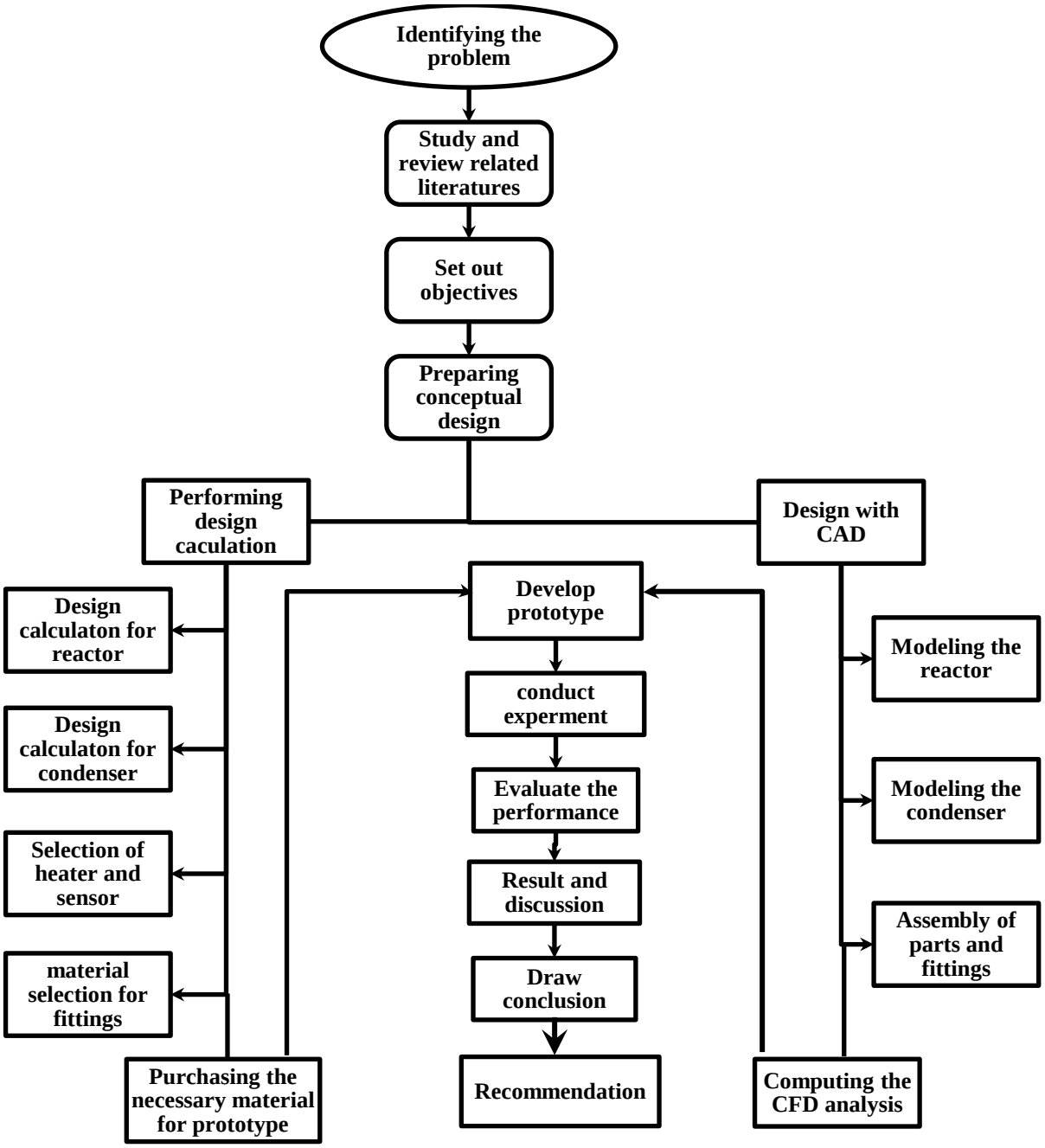

Figure 3-3: Methodology flow chart of the study.

CHAPTER FOUR

4. DESIGN AND THEORETICAL ANALYSIS OF MACHINE

4.1. Conceptual design

The conceptual design of a machine entails presenting various ways in which it operates. To select the most effective design, a decision matrix must be prepared and utilized repeatedly throughout the design process. The decision matrix is an essential design tool that facilitates rational and analytical decision-making rather than relying on personal opinions. This serves as a method for selecting the correct machine model based on specific criteria. The strength of an element in a system plays a critical role in determining its shape and size. Therefore, strength is an important design consideration in these cases. In the design process, certain characteristics must be considered and prioritized. Some important considerations include the following:

Strength	Ergonomics of machine
Stiffness	Manufacturability
Ductility	Maintainability
Machinability	Cost
Fatigue	Safety

Model of the System

This model as shown in Figure 4-1, exhibited rugged construction and good maintainability. The machine was composed of a heater assembled at two positions: at the bottom of the reactor and wound in a helical pattern. The reactor had a cylindrical geometry and its flange was equipped with a chamfer to provide a complete sealing system. The refractory material enhances the heat retention and efficiency. The condenser used in this model was a shell-and-tube type heat exchanger. The control system was a proportional controller with accessories to ensure precise and efficient operation.

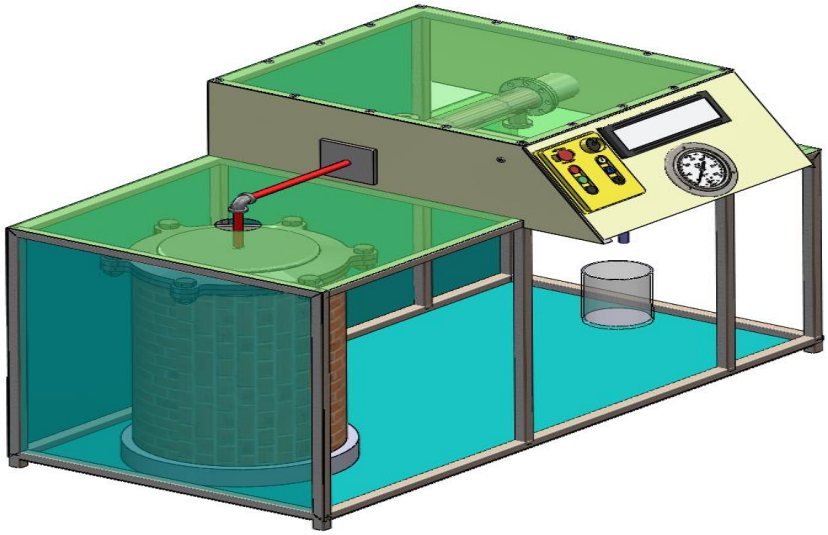

Figure 4-1: Conceptual design of the system

4.2. Detail Design

The development of a top-performing pyrolysis system for fuel production requires a thorough approach to its key components, including the heating element, reactor, condenser, refractory material, and body frame. Each of these crucial components plays a vital role in ensuring the overall performance, efficiency, and durability of the pyrolysis process. A thorough and meticulous design is necessary to optimize the functionality and output of the system. The heating element must be capable of generating sufficient heat to initiate and sustain the pyrolysis reaction, whereas the reactor serves as the primary chamber where the feedstock undergoes thermal decomposition. The condenser is responsible for capturing and condensing the volatile compounds released during the process and converting them into liquid fuels or other valuable products. The refractory material, strategically placed within the system, helps to maintain the desired temperature and minimize heat loss, thereby enhancing the overall efficiency of the pyrolysis process. Finally, the body frame provides structural integrity and support to the entire system, thereby ensuring its stability and durability during operation.

4.2.1. Design of heater

The use of an electric heater was essential for maintaining the furnace temperature in the range of 450–500 °C during pyrolysis. An electric heater was chosen over an LPG gas burner because of its several advantages, including economic viability, cleanliness, pollution-free operation, ease of control, uniform heating, high efficiency, better working conditions, smaller floor area, and safety. Advantages of electric heating include its cost-effectiveness,

as it requires minimal skilled labor and maintenance costs. Electric heating is a clean and pollution-free method of heating that eliminates dust and ash, making it an ideal choice for applications where air quality is a concern. It also provides greater control over the temperature, with the ability to regulate it both manually and automatically. Additionally, electric heating is highly efficient, with the ability to utilize 75-100% of the heat generated, compared to only 40-60% in non-electric heating methods. This leads to a cost-effective and energy-efficient process. Electric heating also provides better working conditions as it produces no noise, making it easier to work in and around. Furthermore, electric furnaces are compact and require less floor area, which is advantageous for applications in which space is limited. Finally, electric heating is safe with no harmful emissions produced during the heating process. Therefore, using an electric heater for the pyrolysis process is a practical and effective choice that provides several advantages over other heating options.

4.2.1.1. Material selection for heating element

The choice of material for a heating element is influenced by the service conditions, such as the maximum operating temperature and the quantity of charge to be heated. However, no single material can fulfil all the requirements of the heating elements. Commonly used materials for heating elements include the following:

1. Nickel–chromium (Ni - Cr)
2. Nickel–chromium–iron (Ni - Cr - Fe)
3. Iron– chromium–aluminium (Fe - Cr - Al)
4. Nickel–copper (Ni - Cu)

Most resistance wire heating elements commonly employ nichrome 80/20 (80% nickel, 20% chromium) in various forms, such as wires, ribbons, or strips. This material is favored for its high resistance, and a protective chromium oxide layer develops when heated, which helps prevent wire damage. Iron-chromium-aluminum alloys share similar electrical resistance properties with nickel-chromium alloys, making them suitable for electrical heating applications. Despite being more cost-effective than Ni-Cr alloys, they are more vulnerable to corrosion. The Fe-Cr-Al electric heating elements have a wide market share. Nickel-copper (Ni-Cu) alloys offer low electrical resistivity, a stable temperature coefficient of resistance, and good resistance to oxidation and chemical corrosion, making them ideal for low-temperature heating purposes.

Criteria for selecting the heater coil

- Cost
- Operating temperature
- Melting point
- Thermal conductivity
- Tensile strength
- Life of coil

In addition to this criterion, the properties of the heater element are also important when selecting. The properties are listed in Table 4-1.

Table 4-1: Properties of material for heating element.

S No.	**Type of alloy**	**Composition**	**Commercial name**	**Max. operating temperature**	**Resistivity at 20°C**	**Specific gravity**
1	Nickel–chromium (Ni - Cr)	80% Ni 20% Cr	Nichrome	1,150^{o}c	1.03 μΩ-m	8.35
2	Nickel–chromium–iron (Ni - Cr - Fe)	60% Ni 16% Cr 14% Fe	_	950^{o}c	1.06 μΩ-m	8.27
3	Iron–chromium–aluminium (Fe - Cr - Al)	70% Fe 25% Cr 5% Al	Kanthal	1,200^{o}c	1.4 μΩ-m	7.20
4	Nickel–copper (Ni - Cu)	45% Ni 55% Cr	Eureka or constantan	400^{o}c	0.49 μΩ-m	8.88

The temperature range for this process is 450–500°C. However, Ni–Cu wire is not applicable because of its maximum operating temperature of 400°C. In contrast, the iron-chromium-iron alloy is more cost-effective than the simple nickel-chromium alloy because it reduces the overall cost of the final product. However, the use of iron in the alloy results in a shorter lifespan because it is prone to oxidation. On the other hand, Ni-Cr heater coils are suitable for this study because of their high melting point, operating temperature, thermal conductivity, and tensile strength.

The elected material of heater coil is Nichrome (Ni-80%, Cr-20%).

4.2.1.2. Design of heating element

The construction of a heating component for an electric oven necessitates the evaluation of the dimensions and length of the component based on the voltage and electrical power input. The wire can be fashioned as a circular or rectangular ribbon. The circular type is optimal for cylindrical reactors. Upon initially connecting the heating component to the power supply, the temperature increased and ultimately reached a high temperature.

According to Stefan's law, heat dissipated per unit area (Hollands, 2004) :

$$H = 5.72 \times 10^4 ke\left[\left(\frac{T_1}{1{,}000}\right)^4 - \left(\frac{T_2}{1{,}000}\right)^4\right] \quad \text{.....4.1}$$

Where T_1 is the absolute temperature of the element (K), T_2 is the absolute temperature of the charge (K), *e* is the emissivity, and *k* is the radiant efficiency.

Temperature of the heat source $(T_1) = 1000^0 c + 273 = 1273K$

Temperature of the charge $(T_2) = 25^o c + 273 = 298K$

For nichrome wire radiating efficiency and emissivity can be taken as 1 and 0.9 respectively.

$$H = 5.72 \times 10^4 (1)(0.9)\left[\left(\frac{1273}{1{,}000}\right)^4 - \left(\frac{298}{1{,}000}\right)^4\right]$$

$$H = 134786.4\, W/m^2 \approx 135K\, W/m^2$$

The power capacity of the heater is 3KW and it requires 220V input supply.

$$P = \frac{V^2}{R} \quad \text{.....4.2}$$

$$R = \frac{\rho l}{A}, Wher\ A = \frac{\pi d^2}{4} \quad \text{.....4.3}$$

$$P = \frac{V^2 \pi d^2}{4\rho l}$$

$$\frac{d^2}{l} = \frac{4\rho P}{V^2 \pi} \quad \text{.....4.4}$$

$$\frac{d^2}{l} = \frac{4(1.03 \times 10^{-6})(3000)}{(220)^2 \pi} = 8.13 \times 10^{-8}$$

Where

P is the electrical power input per phase (watt)

A is the area of cross-section (m^2),

V is the operating voltage per phase (volts)

d is the diameter of the element (m),

R is the resistance of the element (Ω)

ρ is the specific resistance (Ω-m)

The surface area of the circular heating element:

$$S = \pi dl \quad \text{.....4.5}$$

$$Total\ heat\ dissipated = S \times H$$

Under thermal equilibrium,

$$Power\ input = heat\ dissipated$$

$$P = \pi dl \times H \quad \text{.....4.6}$$

$$dl = \frac{P}{H} \quad \text{.....4.7}$$

$$dl = \frac{3000}{134786.4} = 0.022 \qquad d = \frac{0.022}{l}$$

Substituting the value of d

$$\frac{0.022^2}{l^3} = 8.13 \times 10^{-8}$$

$$l = 18m$$

$$d = \frac{0.022}{18} = 8.8 \times 10^{-4}\, m \approx 0.9mm$$

The next step is to arrange 18m of nichrome wire uniformly throughout the reactor.

$$C = 2\pi r_o = \pi d_o$$

The outer diameter of the reactor is 360mm(Kurniawan et al., 2020)

$$C = \pi 360 = 1131\text{mm}$$

$$Number\ of\ coils(N_c) = \frac{l}{C} = \frac{18{,}000}{1131} = 16$$

Now 16 number of coils are arranged in a helical pattern with a pitch (p):

$$L = N_c(d_w) + (N_c + 1)p \quad \text{.....4.8}$$

Were

L is length of reactor = 750mm,(Kurniawan et al., 2020) and d_w is diameter of wire = 0.9mm

$$p = \frac{L - N_c(d_w)}{(N_c + 1)} = \frac{750 - 16(0.9)}{(16 + 1)} = 43.27mm$$

The pitch can be taken as 50 mm

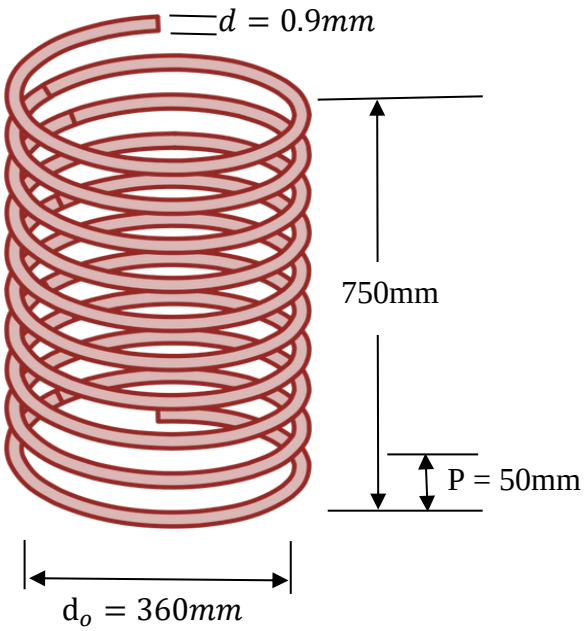

Figure 4-2: Helical arrangement of heater coil.

4.2.2. Design of reactor

4.2.2.1. Classification of reactors

The selection of the reactor used in the pyrolysis process had a significant impact on the mixing of plastics with pyrolysis by-products, heat transfer efficiency, levels of primary product reflux, and residence time. The classification of chemical reactors is based on various factors, such as the operation mode, phases involved, process type, pressure and temperature conditions, geometry, orientation, wall thickness, heating method, material, fabrication technique, and location. Reactors for pyrolysis can be categorized into batch, continuous, fixed-bed, fluidized bed, or variations of these types. In a batch reactor, feedstock is introduced in batches, either at the beginning or after the process begins. Continuous reactors involve continuous input of feedstock and product output. Semi-batch reactors continuously remove the pyrolysis products while adding feedstock before the pyrolysis process begins. Some semi-batch reactors use inert gases to facilitate the removal of products.

4.2.2.2. Determination of vessel geometry

Reactors can be classified based on their geometric shapes as cylindrical, spherical, or rectangular. Cylindrical reactors, which are the most commonly used type in process plants, are less expensive to fabricate than spherical reactors; however, they are not as strong. Spherical reactors, on the other hand, are ideal type of reactor, but their high cost makes them less commonly used. They are typically used to store gases and in high-pressure industrial processes. Rectangular reactors are not frequently used because the stress is not evenly distributed, although they do have some industrial applications for storage and mixing.

The pyrolysis reactor was designed with a vertical cylindrical cross-section called a shell, and the end caps or heads were flat to reduce fabrication costs, ensure easy maintenance, and facilitate heat transfer. This reactor was designed to operate at normal atmospheric pressure, and specific locations were identified for attaching a pressure gauge and connecting piping to guide vapor to the condenser and to remove char.

4.2.2.3. Design specification or factors to consider include: -

- The ability to withstand high temperatures
- Material with low density to facilitate easier vaporization of plastic and increased oil output
- Sufficient reactor size to optimize pyrolysis oil yield
- Low moisture content in the plastics to enhance oil production
- High heating rate to attain maximum yield.

4.2.2.4. Analysis of heat required

The reactor used in the experiment was cylindrical and operated as a batch-type fixed-bed system. To feed the raw material, the top of the reactor was left open, and the solid residue (also known as char) was removed at the end of the experiment. A cover plate was tightly secured to the flanged opening on top of the reactor, preventing atmospheric air from entering and ensuring that the pyrolysis conditions were maintained. The energy required to heat, melt, boil, pyrolyze, and vaporize 10 kg of plastic waste was estimated, and the appropriate heat transfer rate and electrical heater capacity were also established. The production of plastic vapor was calculated and used in the condenser design. Dimensional specification of reactor given as follows: Inner diameter is 350mm, height of reactor is 750mm, Capacity/Volume is 72 litters, specific heat capacity is 2023.5J/kg. k and Convection heat transfer coefficient = 10.42W/(m ^{2}.k(Kurniawan et al., 2020).

Process 1: Heat is required to increase the temperature of the material and heat the reactor.

The heat transfer mode was conducted during the initial stage of the heating process. The heater was provided with the required wattage, and it heated the heat transfer from the hot heater surface to the reactor. When the plastic is in direct contact with the reactor, it absorbs heat. This heating process is referred to as sensible heating. For this process, it is logical to consider a one-dimensional transient conduction with certain assumptions. These assumptions include a constant surface temperature, one-dimensional conduction in the x-direction, constant and uniform properties, and negligible contact resistance. The necessity for varying the quantities of heat to alter the temperature of different materials is due to their distinct thermal properties. The specific heat capacity of a substance is the amount of heat

required to raise the temperature of a unit quantity of the substance by one degree. If the amount of heat added is represented by Q, which causes a change in temperature ΔT in a mass of substance m with a specific heat of mixed plastic c_p, (Cengel, 2015)then heat taken by 10kg of solid plastics until it starts melting at Temperature, T = 260^0c.

$$Q_1 = \mathrm{m}c_p\Delta\mathrm{T}\text{……...……....}4.9$$

$$Q_1 = (10)2.02353(260 - 25) = 4755.5\ KJ$$

This value indicates that $4755.5\ KJ$ of energy is required to raise the temperature of the plastic from its ambient temperature of 25^0C to the average melting point of the mixed plastic which amounts to 260^0C.

Process 2: Heat required to melt the plastic

When adding heat to a substance, it is essential to foresee potential alterations in its state, including melting and vaporization. The heat required to melt a substance is referred to as the latent heat of fusion and is denoted by hf, with a value of $143.3\frac{KJ}{Kg}$.

Heat required to completely melt 10kg of plastics at temperature, T = 260^0c

$$Q_2 = mh_f \text{ …….}4.10$$

$$Q_2 = \ (10)143.3 = 1{,}433\ KJ$$

After complete melting the mode of heat transfer will change to convection. In this stage the heat starts to flow from the heater to the liquid plastic by convection. The rate of convection heat transfer can be calculated as

$$q = h_c\mathrm{A}\Delta\mathrm{T}\text{…….}4.11$$

$$A = \pi\frac{d^2}{4} + \ 2\pi\mathrm{rL}\ \text{……..……..……...}4.12$$

$$A = \pi\frac{0.35^2}{4} + \ 2\pi(0.175) \times 0.75 = 0.92m^2$$

$$q = (10.42)0.92(320 - 260)$$

$$q = 575.2\ W$$

The nature of mixed plastic after it melts resemble with the property of diesel(Khan et al., 2016). Hence the boiling point of diesel ranges from (150^0c – 390^0c). By taking the average value the plastic starts to boil at a temperature of 320^0c. The convection heat transfer coefficient of mixed plastic is $10.42\ W/m^2\ k$.

Process 3: Heat required for boiling

Heat required for the boiling of 10 kg of waste plastic can be calculated as:

$$Q_3 = \mathrm{m}c_p\Delta\mathrm{T} \quad \text{.....4.13}$$

$$Q_3 = 10 \times 2.02353 \times (450 - 300) = 3035.3\ KJ$$

Process 4: Heat required for complete vaporization

The energy required to transform a substance from liquid to vapor is known as the latent heat of vaporization, which is denoted by the symbol h_v. This energy is also released when the vapor undergoes a reverse process and condenses back into a liquid.

$$Q_4 = mh_v \quad \text{.....4.14}$$

$$Q_4 = 10 \times 180.46 = 1804.6\ \mathrm{KJ}$$

The latent heat of vaporization is taken as 180.46KJ/Kg

Total heat required for pyrolysis:

$$Q_{total} = Q_1 + Q_2 + Q_3 + Q_4$$

$$Q_{total} = 4770.5\ KJ + 1{,}433\ KJ + 3045\ KJ + 1804.6\ \mathrm{KJ} = 11{,}028.4KJ$$

Total time required for complete process is

$$t_{total} = \frac{Q_{total}}{P\ required} \quad \text{.....4.15}$$

$$t_{total} = \frac{11{,}028.4KJ}{3KW} = 1.15\mathrm{hr}$$

$$\text{Heat transfer rate required} = \frac{Total\ heat\ required}{time\ taken} \quad \text{.....4.16}$$

$$\text{Heat transfer rate required} = \frac{11028.4}{1.15} = 9589.9\mathrm{KJ/hr}$$

$$\text{Mass flow rate of oil vapor} = \frac{Heat\ transfer\ rate}{Latent\ heat\ of\ vaporization} \quad \text{.....4.17}$$

$$\text{Mass flow rate of oil vapor} = \frac{9589.9}{1047.62} = \frac{0.0025Kg}{sec}$$

Sizing of The Reactor

According to the ASME Boiler and Pressure Vessel code, the thickness of the cylindrical shells can be determined by the equation.

$$t = \frac{PR}{SE - 0.6P} \quad \text{.....4.18}$$

Where,

R is inside radius of the cylinder — E is weld joint efficiency

P is design pressure — t is theoretical thickness of the shells

S is maximum allowable stress

Most commonly used materials for the manufacturing of reactor are stainless steel 304, stainless steel 316, and mild steel. The yield stress value of this materials is given below

Mild steel = 460 Mpa

Stainless steel 304 = 276 Mpa

Stainless steel 316 = 138 Mpa

$$Factor\ of\ safety\ (FOS) = \frac{Yiel\ stress}{Allowable\ stress} \quad \text{.....4.19}$$

$$Allowable\ stress(S) = \frac{Yield\ stress}{FOS} \quad \text{.....4.20}$$

Taking factor of safety value of 4. The thickness of the reactor can be calculated for each material.

$S_{mild\ steel} = 115Mpa, S_{ss304} = 69Mpa,\ S_{ss316} = 34.5Mpa$

Now the thickness of the reactor for three different materials can be calculated as:

$$t_{mild\ steel} = \frac{PR}{S_{mild\ steel}E - 0.6P} = \frac{(1.08)(0.175)}{(115)0.7 - 0.6(1.08)} = 3.03\text{mm}$$

$$t_{ss304} = \frac{PR}{S_{ss304}E - 0.6P} = \frac{(1.08)(0.175)}{(69)0.7 - 0.6(1.08)} = 3.966\text{mm}$$

$$t_{ss316} = \frac{PR}{S_{ss315}E - 0.6P} = \frac{(1.08)(0.175)}{(34.5)0.7 - 0.6(1.08)}$$

$$t_{ss316} = 8.042\text{mm}$$

4.2.2.5. Material selection for the reactor

Material selection is a crucial aspect of the mechanical design of reactors as it determines both safety and economic viability. A poor choice of material can result in catastrophic failure if it cannot withstand operating temperature, pressure, and other conditions. However, selecting a material that is far beyond the required specifications results in an extended payback period for the machine. When selecting a material, it is necessary to evaluate various factors, including operating conditions (such as temperature, pressure, and corrosion resistance), ease of fabrication, thermal conductivity, high service performance, market availability, and design life. The process of converting plastic into fuel oil and gas is analogous to the refining of crude oil, as described by(Jayswal et al., 2017) The same standards used for selecting materials in crude oil refineries can also be applied to the selection of materials for the conversion of plastics into fuel oil and gas. Carbon steel, which accounts for 80% of the components of petroleum refineries, is the most commonly used material(Rapsing, 2016). Low-alloy steels are utilized in applications with average temperatures, whereas stainless steels are used in high-temperature sulfidic and naphthenic acid conditions, which are more expensive and have slightly reduced strength.

Stainless steel has emerged as the optimal material for constructing batch reactors, considering the operating temperature, operating pressure, and corrosion resistance. Although Monel and Inconel are appealing because of their higher temperature ranges, various types of stainless steel, such as 304, 316, and mild steel, as shown in Table 4-2, must be evaluated to determine the most suitable metal for the fabrication of the batch reactor. To make this determination, the following factors should be considered: the batch reactor is a fired vessel, the reactor's maximum operating temperature is approximately 500°C, the operating pressure is approximately 1.08 MPa, the possibility of operating under sulfidic and naphthenic acid conditions, ease of fabrication, and good market availability.

Table 4-2: Properties of materials.

Criteria	**Mild steel**	**SS 304**	**SS 316**
Thickness (t)	3mm	4mm	9mm
Melting point	1350^0c – 1530^0c	1400^0c – 1450^0c	1375^0c – 1400^0c
Thermal conductivity	50 W/m. k	16.2 W/m. k	15.9 W/m. k
Price per Kg in birr	72	360	432
Specific heat capacity	470 J/Kg-k	490 J/Kg-k	500 J/Kg-k

Based on the above criteria mild steel is less expensive and it can withstand the temperature with in the reactor so Mild steel is used for the manufacturing of the reactor. The thickness is 4mm considering safety allowance. And model of the reactor assembly as shown in Figure 4-3 below.

Figure 4-3: Model of reactor assembly.

4.2.3. Design of flange

The design of flange comprises both the design of bolts and cover plate as shown in Figure 4-4.

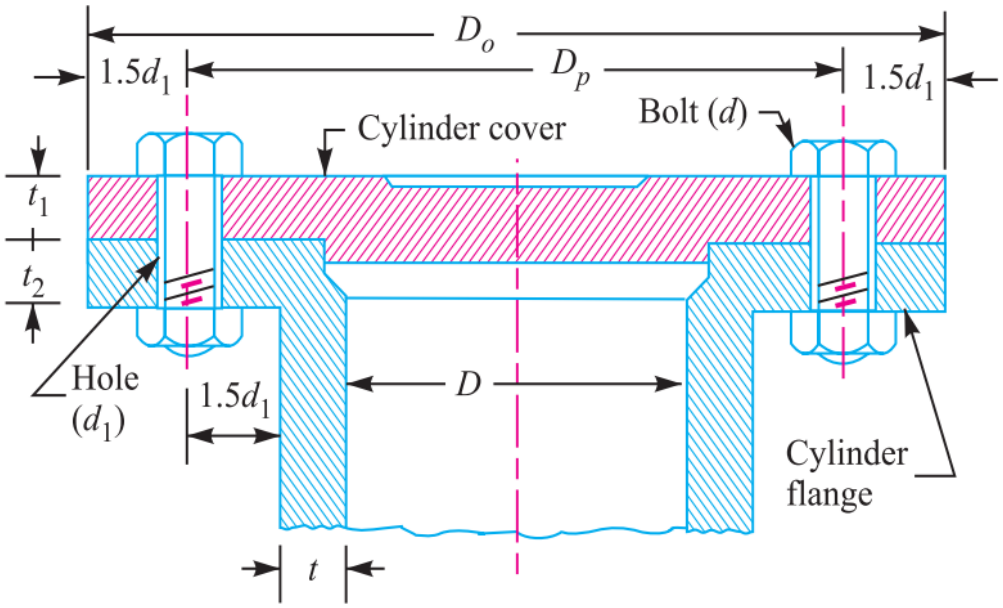

Figure 4-4: Nomenclature of the flange assembly.

Design of bolts

The upward force acting on the cylinder cover can be calculated as:

$$F = \frac{\pi}{4}(D)^2 P \quad \text{.....4.20}$$

$$F = \frac{\pi}{4}(350)^2 1.08 = 103{,}908.177N \approx 104\text{KN}$$

The cover is secured using n bolts, which provide resistance against external forces. The bolts or studs are tightly screwed in, along with either a metal gasket or asbestos packing, to form a leak-proof joint. As a result of tightening the bolts, tensile stress is generated in the bolts, which can cause them to break before any external load is applied due to internal pressure. Consequently, bolts with a diameter less than 16mm should not be used under any circumstances.

$$F = \frac{\pi}{4}(d_c)^2 \sigma_t n \quad \text{.....4.21}$$

Assume that bolts of nominal diameter 20 mm are used. The corresponding core diameter (d_c) is found to be 16.933mm.

$$n = \frac{4F}{\pi(d_c)^2\sigma_t} = \frac{4(104K)}{\pi(16.933)^2 83}$$

$$n = 7.56 \approx 8\ bolts$$

Taking the diameter of the bolt hole (d_1) as 21 mm, the pitch circle diameter of the bolts can be calculated as.

$$D_p = D + 2t + 3d_1 \text{……4.22}$$

$$D_p = 350 + 2(5) + 3(21) = 423mm$$

Design of cover plate

bending moment,

$$M = 0.053\text{F}\frac{D_p}{2} \text{……4.23}$$

$$M = 0.053(104\text{K})\frac{423}{2} = 1{,}165{,}788Nmm$$

Outside diameter of the cover plate,

$$D_o = D_p + 3d_1 \text{……...4.24}$$

$$D_o = 423 + 3(21) = 486mm$$

Width of the plate,

$$w = D_o - 2d_1 \text{……4.25}$$

$$w = 486 - 2(21) = 444mm$$

Section modulus,

$$Z = \frac{1}{6}w(t_1)^2 \text{……4.26}$$

$$Z = \frac{1}{6}(444)(t_1)^2 = 74(t_1)^2 mm^3$$

bending (tensile) stress,

$$\sigma_t = \frac{M}{Z} \text{……...4.27}$$

$$\sigma_t = \frac{1{,}165{,}788Nmm}{74(t_1)^2}$$

$$t = 9.22mm \approx 10mm$$

The selected material is AISI 1018 mild steel Where, σ_t is tensile strength of the plate material. $\sigma_t = 185Mpa$ taking safety factor of 2.

Stress analysis of the reactor

The total force acting on a longitudinal section of the shell:

Longitudinal stress:

$$\sigma_l = \frac{Pr}{2t} \quad \text{....4.28}$$

$$\sigma_l = \frac{(1.08)(175)}{2(4)} = 18.9\ Mpa$$

Hoop stress:

$$\sigma_h = \frac{Pr}{t} \quad \text{.....4.29}$$

$$\sigma_h = \frac{(1.08)(175)}{4} = 37.8\ Mpa$$

Where,

P is intensity of pressure t is thickness of cylinder

r is internal radius of reactor

Maximum shear stress theory suggests that the maximum shear stress is equal to half the algebraic difference between the maximum and minimum principal stresses. The maximum principal stress is the hoop stress (σ_h) the minimum principal stress is the longitudinal stress (σ_l). Therefore, the maximum shear stress was determined.

$$\tau_{max} = \frac{\sigma_h - \sigma_l}{2} \quad \text{.....4.30}$$

$$\tau_{max} = \frac{37.8 - 18.9}{2} = 9.45\ Mpa$$

The selected material is mild steel, so the allowable stress = 115Mpa and since

$\sigma_{all} > \tau_{max}$

The design is safe.

4.2.4. Design of Refractory

Refractory materials play a critical role in industries that involve high temperatures and corrosive environments, such as pyrolysis. To design effective refractory materials to reduce heat loss during pyrolysis, it is crucial to have a good understanding of the fundamentals of refractory materials. In processes such as pyrolysis, where the temperature surpasses 1500°C, refractory materials are indispensable for minimizing heat loss and ensuring operational efficiency. By selecting appropriate refractory materials with high thermal resistance and insulating properties, industries can limit the heat loss through the refractory lining, thereby improving the energy efficiency and process effectiveness. Refractory materials are not only essential for reducing heat loss but also play a significant role in protecting the furnace and reactor lining from wear and tear caused by high temperatures and corrosive environments. By selecting the appropriate refractory materials, industries can ensure the longevity of their equipment and reduce maintenance costs(Jastrzębska & Szczerba, 2024).

A thick layer of refractory material was utilized to insulate the apparatus and offer improved resistance to thermal shock, as illustrated in Figure 4-5. This is achieved through the thermal conduction process of heat.

$$\text{Heat current} = \frac{\text{Temperature differnce}}{\text{Heating resistance}} \quad \text{.....4.31}$$

The heating resistance:

$$R = \int_{r}^{r+t} \frac{d_x}{2\pi K x H} \quad \text{.....4.32}$$

$$\mathrm{R} = \frac{\log\left[1 + \frac{\mathrm{t}}{\mathrm{r}}\right]}{2\pi\mathrm{KH}}$$

$$\text{Heat current} = \frac{2\pi\mathrm{KH}(\mathrm{T} - \mathrm{T}_0)}{\log\left[1 + \frac{\mathrm{t}}{\mathrm{r}}\right]}$$

$$\text{Heat current} = \frac{2\pi \times 1.31 \times 0.282(460 - 25)}{\log\left[1 + \frac{5}{0.37}\right]} = 869\ \mathrm{W}$$

Where: R- represents the heating resistance

K- represents the thermal conductivity

r- denotes the inner radius of the furnace

H- denotes the height of the furnace.

t- refers to the thickness of the refractory material and

T- represents the temperature of the furnace.

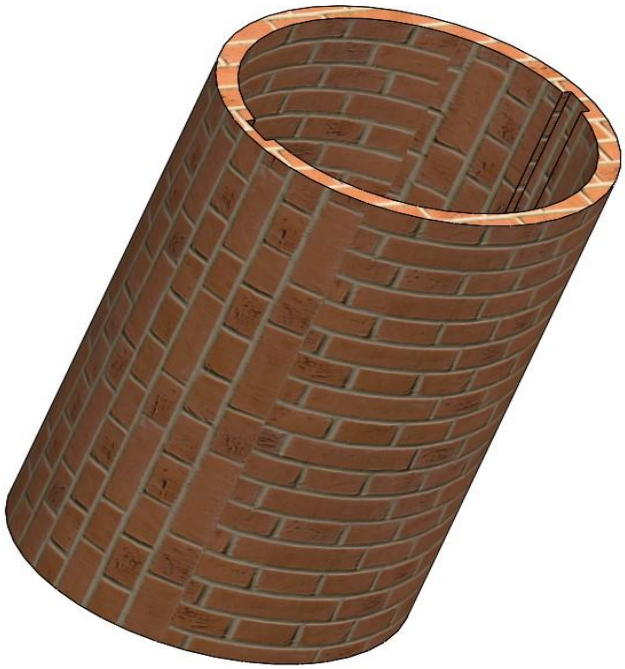

Figure 4-5: Design of refractory material.

4.2.5. Design of Pipe

Pipping system is required in this machine to connect the reactor with the condenser. It carries the vaporised plastic and delivers it to the condensing medium. The design of a pipe involves the determination of inside diameter of the pipe and the wall thickness. More over the thermal analysis of the piping system plays a great role for the proper working of the machine.

4.2.5.1. Sizing of Pipe

The inside diameter of the pipe depends up on the quantity of fluid to be deliver. The volumetric flow rate can be obtained from the relation.

$$Q = \frac{\dot{m}}{\rho} \quad \text{.....4.33}$$

Where:

Q is volumetric flow rate

V is average velocity of fluid

A is area of flow pipe

$\dot{m}$ is mass flow rate

ρ is average density of evaporated mixed plastic

The density is taken as the average of mixed plastic which is found to be 1050 Kg/m^3.The mass flow rate of the vapour is assumed to be uniform. Hence it has the same value inside the pipe and in the reactor. $\dot{m}$ is 0.0025 Kg/sec

$$Q = \frac{0.0025}{1050} = 2380m\,m^3/sec$$

Schedule =$1000\frac{p}{s}$.....4.34

Where:

P is internal pressure

S is allowable stress

Schedule =$1000 \times \frac{1.04\times10^6}{205\times10^6}$

Schedule = 5

After finding the schedule the outside diameter of pipe for stainless steel pipes can be found from Appendix A and it is found to be 20mm.

$$t = \frac{DP}{2S} \quad \text{.....4.35}$$

Where:

t is wall thickness D is outside diameter

S is allowable stress P is internal pressure

$$t = \frac{21mm \times 1.08Mpa}{2 \times 205Mpa} = 0.06\text{mm}$$

A little consideration will show that the thickness of wall as obtained by the above relation is too small.

Therefore, for the design of pipe a certain constant is added to the above relation. Now the relation may be written as

$$t = \frac{P \times D}{2S} + \text{c} \quad \ldots\ldots 4.36$$

Where: c is constant, the value of "c" is as shown in Table 4-3.

Table 4-3: The value of constant "c" according to Darcy- Weisbeck.

Material	Cast iron	Steel	Zink and copper	Lead
Constant(c)in mm	9	3	4	5

Now the thickness becomes:

$t = 0.06 + 3 = 3.06$ mm $\approx$ 3mm

The inner diameter is given by;

$$D_i = Do - 2\text{t} \quad \ldots\ldots 4.37$$

Where: $D_i\ is$ Inner diameter

$t\ is$ Thickness of pipe

$$D_i = 21 - 2(3) = 15mm$$

The flow area of the pipe can be calculated as

$$A = \frac{\pi}{4} D_i^2 \quad \ldots\ldots 4.38$$

$$A = \frac{\pi}{4} \times 15^2 = 176.7mm^2$$

Average velocity of mixed plastic

$$V = \frac{Q}{A} \text{.....4.39}$$

$$V = \frac{2380}{176.7} = 13.47 \times 10^{-3}\, m/sec$$

Energy Loss in Pipe

The total energy losses are major energy (friction) losses, and Head loss due to friction in pipe flow;

Using Darcy- Weisbeck equation;

$$h_f = \frac{f \times L \times v^2}{2g \times D_i} = \frac{K_L \times V^2}{2 \times g} = \text{.....4.40}$$

Where:

h_f is Friction loss L is pipe length

V is average velocity of mixed plastic D_i is inner diameter of pipe

g is Acceleration due to gravity

The friction factor (f) depends on the types of flow

For circular pipe with turbulent flow

$$f = \frac{0.0791}{Re^{1/4}} \text{.....4.41}$$

Where: R_e is Reynolds number

The Reynolds number for flow in pipe is define as

$$R_e = \frac{Di \times v \times \rho}{\mu} \text{.....4.42}$$

$$R_e = \frac{15 \times 3.09 \times 10^{-3} \times 1050}{0.024} = 2433.375$$

Where: μ is viscosity of fluid which is 0. 024Ns.m^2

$$f = \frac{0.0791}{Re^{1/4}} = 0.011$$

From the above Darcy- Weisbeck equation:

$$L = \frac{K_L \times D}{f} \text{.....4.43}$$

Where; k_L is Loss coefficient for pipe

The suitable loss coefficient for pipe elbows Regular90, threaded is selected and k_L is 1.5

$$L = \frac{1.5 \times 15mm}{0.011} = 2045\text{mm}$$

$$h_f = \frac{0.011 \times 2.045 \times 0.00309^2}{2 \times 9.81 \times 0.015} = 2.36 \times 10^{-4}\text{m}$$

Heat loss through un insulated pipe

The heat loss from un insulated pipe is basically made of two components

- Heat loss through convection, and
- Heat loss through radiation

$Total\ heat\ loss\ = convection\ heat\ loss\ +\ radiation\ heat\ loss$

convection heat loss

$$q_{conv} = h \times (\pi \times D_o \times L(T_\infty - T_s\ ) \qquad \text{.......................................4.44}$$

T_s is surface temperature

Hence (T∞ -T_S) becomes negative which indicates that heat loss.

$$q_{conv} = 1.74\text{W}$$

Radiation heat loss

$$q_{rad} = \varepsilon\sigma(\pi D_o L)(T_s^4 - T_{sur}^4) \qquad \text{..4.45}$$

$$q_{rad} = 200\ \text{W}$$

Total heat loss in the pipe (q_{tot})

$$q_{tot} = q_{conv} + q_{rad} = 201.74\text{W}$$

Stress in pipe

Hoop stress: σ_h

$$\sigma_h = \frac{p \times ri}{t} \qquad \text{.. 4.46}$$

$$\sigma_h = \frac{1.08 \times 7.5}{3} = 2.7Mpa$$

Longitudinal stress

$$\sigma_t = \frac{p \times r_i}{2t} \qquad \text{..4.47}$$

$$\sigma_t = \frac{1.08 \times 7.5}{2 \times 3} = 1.35 Mpa$$

Factor of safety

For the design of piping the general range of factor of safety is in between 3.5 -4. Since the pipe is not exposed to much mechanical and thermal load smaller value of safety is adequate for the design calculation. Taking 3.5 In order to minimize the cost of production of the piping element.

To check the yield stress of the design

$$FOS = \frac{yield\ stress}{design\ stress} \quad \text{.....4.48}$$

Where: Design (hoop) stress (σ_h)is 2.7Mpa

$yield\ stress = FOS \times design\ stress$

$yield\ stress$ =9.45Mpa

The yield stress is less than the allowable stress

$i.e$ 9.45 $Mpa < 205\ Mpa$ (Allowable stress of SS304)

The design is safe.

Selection of materials

The selection of pipe materials is based on

- Carrying capacity
- Strength
- Life of durability
- Local availability
- Safety
- Cost

For the designing of pipe stainless steel pipe (SS304) is selected;

Because;

- Stainless steel is frequently used for fluid pipes especially for pipelines where pressure is high.
- SS304 being much stronger than other related types of stainless steel and can be easily transported

- Joint by welding or riveting.
- SS304 are excellent resistance to weather-chemical and corrosion.
- High strength with low weight.
- Formability and easy maintenance.
- Better corrosion resistance and relatively low

4.2.6. Design of condenser

A condenser is a vital component in a pyrolysis plant because it is responsible for transforming the vapor-gas mixture generated during the pyrolysis process into liquid biofuel. The primary function of the condenser is to cool and condense the pyrolysis vapors, thereby separating the liquid biofuel from non-condensable gases.

4.2.6.1. Thermal design considerations

The thermal design of shell and tube heat exchangers entails the evaluation of the flow rates, terminal temperatures, and fluid properties of both hot and cold streams. The central components of the typical thermal design process include determining the heat transfer area, number of tubes, tube length and diameter, tube layout, number of shell and tube passes, type of heat exchanger tube pitch, and number of baffles.

The tube bundle, which functions as a fluid container, is housed within the shell, stressing the importance of selecting a shell diameter that snugly accommodates the tube bundle. The clearance between the tube bundle and inner shell wall varies based on the type of exchanger, with shells commonly made from standard steel pipes with a suitable corrosion allowance.

To improve the heat transfer efficiency, it is crucial to increase the number of tubes in the shell. The tube thickness should be adequate to withstand internal pressure and provide corrosion protection, typically measured using the Birmingham Wire Gauge (BWG) and true outside diameter (OD). Longer tubes reduce the shell diameter but increase the shell pressure drop. Finned tubes are preferred for low heat transfer coefficient fluids on the shell side, and materials such as stainless steel, admiral brass, copper, bronze, and copper-nickel alloys are commonly used.

The tube pitch, which is the shortest center-to-center distance between adjacent tubes, plays a significant role in heat exchanger performance. Tubes are usually arranged in square or

triangular patterns, and the tube count is influenced by factors such as the shell ID, tube OD, tube pitch, layout, number of passes, heat exchanger type, and design pressure.

The tubes within an exchanger were designed with a specific number of passes to attain the necessary fluid velocity and enhance heat transfer while minimizing scale formation. The number of passes can range from 1 to 16, with common applications utilizing one, two, and four passes. The exchanger head includes a partition plate, also known as a pass partition, which directs tube-side flow.

Baffles are a critical component in increasing fluid velocity and promoting heat transfer efficiency, and are a crucial element in thermal design, as they influence the turbulence and heat transfer efficiency of the tube bundle. Typically, a baffle spacing of 0.2 to 1 time the inside shell diameter is employed. By increasing the distance between the baffles, the turbulence and heat transfer efficiency were improved, but there was also an associated increase in the pressure drop. To maintain an optimal balance between these factors, baffles were secured in place with baffle spacers.

4.2.6.2. Thermal design procedure

The thermal design procedure involves several key steps:

1. Identifying the application area, including factors such as temperature and heat load.
2. Deciding on a construction type based on the specific requirements of the application.
3. Evaluating the log mean temperature difference (LMTD), q, and F.
4. Determining the dimensions of the exchanger.
5. Evaluating the heat transfer coefficient on both the hot and cold sides.
6. Determining the overall heat transfer coefficient.
7. Determining the length of the exchanger and iterating the design as needed.

Procedure 1: Identifying application and define the essential process requirements

There are certain process parameters which must be fixed. The inlet and outlet temperatures of the condenser can be fixed as shown below Table 4-4.

Table 4-4: Temperature specification of condenser.

Position	Temperature	
Oil Outlet temperature (T_{oo})	50°C	(Jayswal et al., 2017)
Oil inlet temperature (T_{oi})	450°C	
Water Inlet temperature (T_{wi})	25°C	
Water Inlet temperature (T_{wi})	45°C	

Procedure 2: Select suitable type of heat exchanger.

Condensers are typically classified based on the cooling medium utilized, into three main types: air-cooled condensers, water-cooled condensers, and evaporative condensers. Air-cooled condensers, commonly found in smaller machines such as refrigerators and portable water coolers, use vertical coils, tubes, and plates with natural circulation to dissipate heat through air via natural or forced circulation. These condensers are constructed using steel, copper, or aluminum tubing with fins to enhance the heat transfer. The refrigerant flowed through the tubes while the air was circulated externally. Water-cooled condensers, on the other hand, come in three variations: shell and tube condensers, shell and coil condensers, and tube-in-tube or double-tube condensers. Shell-and-tube heat exchangers provide several advantages, such as cost-effectiveness, suitability for higher temperatures and pressures, minimal pressure drop, easy leak identification and repair, and ability to function as receivers in refrigeration systems. In addition, they offer protection against corrosion through sacrificial anodes.

Procedure 3: Evaluating heat load in the condenser (q), Logarithmic mean temperature difference (LMTD), and correction factor (f).

Heat load in the condenser:

$$q = \left(\dot{m}c_p\right)_o \Delta T, where\ \Delta T = T_{oo} - T_{oi} \quad \text{.....4.49}$$

Mass flow rate of water can be found as:

$$q = \left(\dot{m}c_p\right)_w \Delta T, where\ \Delta T = T_{wo} - T_{wi} \quad \text{.....4.50}$$

$$\dot{m}_w = \frac{q}{c_{pw}(T_{wo} - T_{wi})} \quad \text{.....4.51}$$

Logarithmic mean temperature difference (LMTD),

$$LMTD = \frac{\Delta T_2 - \Delta T_1}{ln\left({}^{\Delta T_2}/_{\Delta T_1}\right)} \quad \text{.....4.52}$$

$$\Delta T_1 = T_{oi} - T_{wo} \quad \text{.....4.53}$$

$$\Delta T_2 = T_{oo} - T_{wi} \quad \text{.....4.54}$$

$$LMTD = \frac{25 - 405}{ln\left({}^{25}/_{405}\right)} = = 136.44^o c$$

Correction factor:

$$F = \frac{\sqrt{R^2+1}\ln\left(\frac{1-S}{1-RS}\right)}{(R-1)\ln\left[\frac{2-S\left(R+1-\sqrt{R^2+1}\right)}{2-S\left(R+1+\sqrt{R^2+1}\right)}\right]} \quad \text{.....4.55}$$

$$R = \frac{T_{oi} - T_{oo}}{T_{wo} - T_{wi}} = \frac{450 - 50}{45 - 25} = 20$$

$$P = \frac{T_{wo} - T_{wi}}{T_{oi} - T_{wo}} = \frac{45 - 25}{450 - 45} = 0.049$$

$$\alpha = \left(\frac{1-RP}{1-P}\right)^{1/N} \quad \text{.....4.56}$$

$$\alpha = \left(\frac{1 - (20)(0.049)}{1 - 0.05}\right)^{1/1} = 0.013$$

Where N is number of shell side passes,

$$S = \frac{\alpha - 1}{\alpha - \mathrm{R}} \quad \text{.....4.57}$$

$$S = \frac{0.013 - 1}{0.013 - 20} = 0.049$$

$$F = \frac{\sqrt{20^2+1}\ln\left(\frac{1-0.049}{1-(20)(0.049)}\right)}{(20-1)\ln\left[\frac{2-0.049(20+1-\sqrt{20^2+1})}{2-0.049(20+1+\sqrt{20^2+1})}\right]} = 0.775$$

$$Corrected\ LMTD = F(LMTD) \ldots\ldots\ldots\ldots\ldots\ldots\ldots\ldots\ldots\ldots\ldots\ldots\ldots\ldots\ldots\ldots 4.58$$

$$Corrected\ LMTD = 0.775(136.44^o c) = 105.741^o c$$

Procedure 4: Define a tentative geometry and determine dimensions

The configuration of tubes in a bank can be either in an aligned or staggered pattern, which is determined by the tube diameter D, transverse pitch St, and longitudinal pitch SL, which is the distance between the centers of the tubes. The flow within the bank is significantly influenced by the boundary layer separation and wake interactions, which ultimately affect the convective heat transfer.

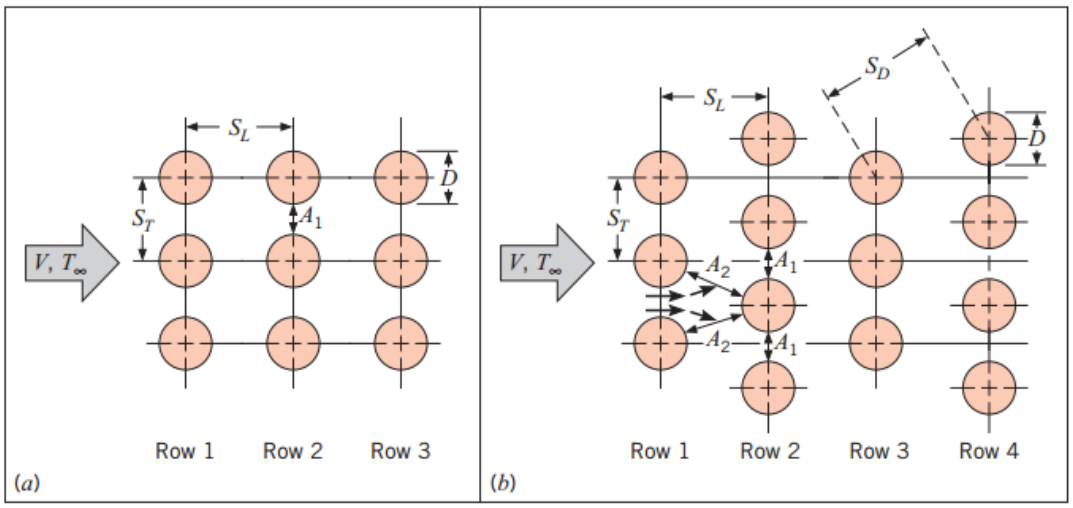

Figure 4-6: Tube arrangements in a bank. (a) Aligned. (b) Staggered. (Cengel, 2015).

Studies have suggested that a staggered layout for equipment results in an increase in the pressure drop and overall heat transfer coefficient. This increase in the pressure drop minimizes the generated power and consequently boosts operational expenses. From a thermodynamic perspective, an inline arrangement appears to be a more logical choice.

For the first iteration the values of:

$$D = 15mm \quad S_L = 20mm \quad S_T = 20mm$$

$$W = S_T(N+2) \ldots\ldots\ldots\ldots\ldots\ldots\ldots\ldots\ldots\ldots\ldots\ldots\ldots\ldots\ldots\ldots 4.59$$

Where, N is number of tubes

$$W = 22(8+2) = 220\,mm = 0.22m$$

Choose baffle spacing, $BF = {}^{2}/_{3}\,W = 146.67mm = 0.1467m$

Flow area, $A = (BF)(W) = 0.02m^2$

Procedure 5; Evaluate heat transfer coefficient outside the tube.

$$\overline{N_{u_d}} = Re_{D,max}^{m} Pr^{0.36} \left(\frac{Pr}{Pr_s}\right)^{1/4} \text{.....4.60}$$

$$\begin{bmatrix} N_L \geq 20 \\ 0.7 \leq \Pr \leq 500 \\ 10 \leq Re_{D,max} \leq 2 * 10^6 \end{bmatrix}$$

For $N_L < 20$, $\overline{N_{u_d}}|_{(N_{L<20})} = C_2 \overline{N_{u_d}}|_{(N_{L>20})}$ 4.61

The Reynolds number $Re_{D,max}$ for the foregoing correlation is based on the maximum fluid velocity occurring within the tube bank.

For aligned tubes from continuity equation we have

$$V_\infty S_T = V_{max}(S_T - D) \text{.....4.62}$$

$$V_{max} = \frac{S_T}{S_T - D} V_\infty$$

$$V_\infty = \frac{\dot{m}}{\rho A} \text{.....4.63}$$

$$V_\infty = \frac{0.07165}{(1000)0.02} = 2.17 \times \frac{10^{-3}m}{s}$$

$$V_{max} = \frac{0.02}{0.02 - 0.015} \times 2.17 \times 10^{-3} = 8.68 \times \frac{10^{-3}m}{s}$$

For flow outside the tube the properties of water can be adopted.

$$Re_{D,max} = \frac{\rho V_{max} D}{\mu} \text{.....4.64}$$

Were, $\rho_w = 10^3\,kg/m^3$

$$\mu_w = 8.55 \times 10^{-4}\,Ns/m^2$$

$$Re_{D,max} = \frac{1000 \times 8.68 \times 10^{-4} \times 0.015}{8.55 \times 10^{-4}} = 1523$$

$\frac{S_T}{D} = \frac{S_L}{D} = 1.34$ Using this value and referring to table given in the appendix it is possible to get the constants.

$$\overline{N_{u_d}} = 0.8 \times 0.96 \times 1523^{0.4} 6.146^{0.36} \left(\frac{6.146}{88}\right)^{1/4} = 14$$

$$h_o = \frac{\overline{N_{u_d}} K_f}{D} \quad \text{.....4.65}$$

$$h_o = \frac{14 \times 0.598}{0.015} = 558.14 \ W/m^2 \cdot K$$

Procedure 6: Evaluate heat transfer coefficient inside the tube.

Mean velocity inside the tube

$$V_{m,tube} = \frac{\dot{m}}{\rho_o A_{tube} N} \quad \text{.....4.66}$$

$$A_{tube} = \frac{\pi D^2}{4} \quad \text{.....4.67}$$

$$V_{m,tube} = \frac{5.84 \times 10^{-4}}{1050 \times 1.77 \times 10^{-4} \times 8} = 3.93 \times 10^{-4} \frac{m}{s}$$

$$Re_D = \frac{\rho_0 V_m D}{\mu} \quad \text{.....4.68}$$

$$Re_D = \frac{1050 \times 3.93 \times 10^{-4} \times 0.015}{0.07 \times 10^{-2}} = 88.425$$

$$\overline{N_{u_d}} = 0.23 Re_{D,max}^{4/5} Pr^n, where\ n = 0.3\ for\ cooling \quad \text{.....4.69}$$

$$\overline{N_{u_d}} = 0.23(88.425)^{4/5}(0.55)^3 = 1.38$$

$$h_i = \frac{\overline{N_{u_d}} K_i}{D} = \frac{1.38 \times 0.62}{0.015} = 57.04 \ W/m^2 \cdot K$$

Procedure 7: Determine overall heat transfer coefficient.

Assuming thin wall and no fouling effect;

$$\frac{1}{U} = \frac{1}{h_o} + \frac{1}{h_i} \quad \text{.....4.70}$$

$$U = \frac{h_i h_o}{h_i + h_o} = \frac{57.04 \times 558.14}{57.04 + 558.14} = 51.72 \ W/m^2 \cdot K$$

Procedure 8: Determine length of the tube.

$$q = UAF \times LMTD \quad \text{.....4.71}$$

$$A = N \times \pi \times DL \quad \text{.....4.72}$$

$$A = 8 \times \pi \times 0.015 = 0.377m^2$$

$$L = \frac{q}{U * AF * LMTD}$$

$$L = \frac{4 \times 10^3}{51.72 \times 0.377 \times 0.775 \times 409.44} = 0.65m$$

Therefore, the total length of the condenser is taken as 65cm.

Required number of baffles, m

$$m = \frac{L}{BF} - 1 \quad \text{.....4.73}$$

$$m = \frac{0.65}{0.1467} - 1 = 4$$

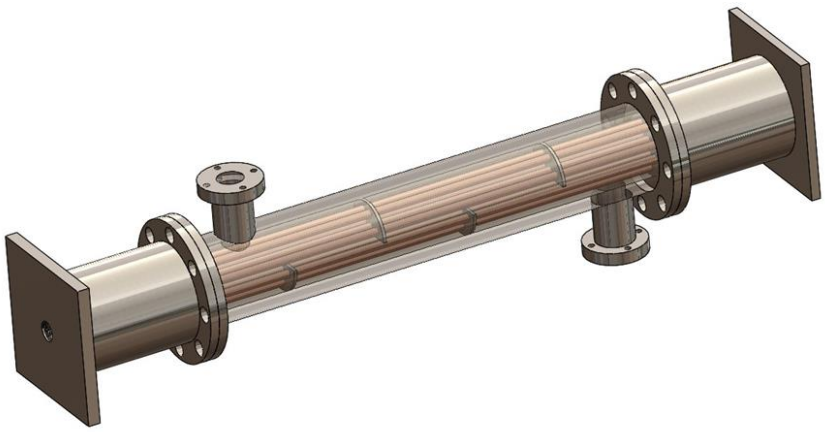

Figure 4-7: Design of condenser.

4.3. Temperature sensor selection

It is crucial to evaluate various factors when choosing a temperature device suitable for a specific application, such as:

- The required temperature ranges
- Accuracy level
- Response time

- Stability
- Linearity
- Sensitivity.

The comparison of the temperature sensor type based on the above selecting criteria is illustrated in Table 4.5.

Table 4-5: Comparison of Sensor Types.

	Thermocouple	Platinum Resistance	Thermistor
Sensor	Thermoelement, two dissimilar metals/alloys	Platinum - wire wound or flat film resistor	Ceramic (metal oxides)
Accuracy (typical values)	0.5 to 5.0°C	0.1 to 1.0°C	0.1 to 1.5°C
Long term Stability	Variable, Prone to ageing	Excellent	Good
Temperature range	-200 to1750°C	-200 to 650°C	-100 to 300°C
Characteristic	Thermo voltage	PTC resistance	NTC resistance (some are PTC)
Output/ characteristic	From 10 µV/°C to 40 µV/°C depending on type	approx. 0.4 W/°C	-4% / °C
Extension Leads	Compensating cable	Copper	Copper
Cost	Relatively low cost	Wire wound – more expensive Film – cheaper	Inexpensive to moderate

Various types of thermocouples are available based on the temperature range and sensitivity. These types include:

- Type K - Chromel-Alumel: This is the most commonly used and well-known thermocouple in the chromium-nickel-aluminum group. I have an extended temperature range of -200 to 1100°C, and its output voltage/temperature curve is relatively linear. The sensitivity was 41 µV/°C.
- Type J-Iron-Constantan: Although it is still widely used in traditional thermometry, its limited temperature range (-200°C to +750°C) makes it less important in the Mineral Insulated form. The sensitivity was 55 µV/°C.
- Type E - Chromel-Constantan thermocouples have a high level of sensitivity, making them suitable for low-temperature applications ranging from -200°C to +900°C. Their nonmagnetic properties may also be advantageous in certain specialized situations.
- Type N-Nicrosil-Nisil thermocouples have excellent stability and oxidation resistance, making them well suited for accurate temperature measurements in air up to 1200°C. They can withstand temperatures over 1200°C in a vacuum or controlled atmosphere. Although their sensitivity at 900°C was slightly lower than that of the Type K thermocouples, they had the same level of interchangeability tolerance.
- Type T-Copper-Constantan thermocouples are less commonly used because of their limited temperature range of -200°C to +350°C. However, they are also useful in food, environmental, and refrigeration applications. The tolerance class of Type T thermocouples is better than that of other base metal types, and close-tolerant versions are readily available. The output voltage/temperature curve of the Type T thermocouples is highly nonlinear, especially around 0°C, with a sensitivity of 42 µV/°C.
- Type S and Type R thermocouples are both made of platinum rhodium and have sensitivities ranging from 6 to 12 µV/°C and 6 to 14 µV/°C, respectively. Type S can be used in oxidizing atmospheres up to 1600°C, whereas Type R is similar but has a slightly higher temperature range.

- Type B, on the other hand, is made with a higher percentage of platinum rhodium and can measure up to 1700°C; however, it has a lower sensitivity in the lower range and produces negligible output at room temperature.

Historically, Type N thermocouples have been the go-to choose for high-temperature measurements, although they have a high-price tag and low thermoelectric power. However, with the advent of Nicrosil-Nisil thermocouples, there is now a more cost-effective option that provides good thermoelectric stability.

Despite being the most accurate, Type E thermocouples are also the most expensive. On the other hand, Types K, J, and M are less accurate, but more affordable. Considering that the accuracy level was not a critical factor in this study, a cost-effective sensor was preferred. Additionally, Type K thermocouples have a longer lifespan than the J and M types, making them the ideal choice. Therefore, a Type-K thermocouple was selected as it met all the necessary criteria.

Selected temperature sensor: Type-K thermocouple.

4.4. Selection of temperature controller

When opting for a temperature controller, there are three primary types to consider: on/off, proportional, and PID (proportional-integral-derivative).

The on/off temperature controller is a fundamental control device that functions with its output either entirely on or entirely off without intermediate states. It switches its output only when the temperature reaches the set point. In heating control, the output is activated when the temperature is below or above the setpoint. This type of controller causes the process temperature to cycle continuously, as it needs to cross the setpoint to change the output state. On/off controllers are suitable for situations where precise control is not crucial, in systems incapable of handling frequent on-off energy changes, or in systems with significant mass leading to slow temperature changes.

The proportional temperature controller addresses the cycling issue observed in the on/off control. They adjust the power supplied to the heater as the temperature approaches the setpoint, slowing down the heater to prevent overshooting, and maintaining a stable temperature. This proportional action was achieved by cycling the output on and off for short periods.

A PID temperature controller is a sophisticated device that integrates proportional control with two additional adjustments, integral and derivative, to automatically compensate for system changes. These adjustments, expressed in time-based units such as RESET and RATE (reciprocals of integral and derivative terms), require trial-and-error tuning for optimal system performance. PID controllers provide the most precise and stable control among the three types, and are ideal for systems with relatively low mass.

Key Considerations for Selecting Temperature Controllers

- Cost
- Accuracy

The on/off temperature controller is very cheap but has poor accuracy. The proportional temperature controller is accurate, but lower than the PID temperature controller in terms of accuracy. PID temperature controller is the best in terms of accuracy but is very expensive.

For this study, the proportional temperature controller had sufficient accuracy; therefore, a proportional temperature controller was selected.

4.5. Selection of Circuit Breakers

Circuit breakers are essential devices that protect electrical systems from overload, short circuits, and other hazards. Three primary types of circuit breakers are commonly used in homes and businesses.

- Standard circuit breakers are categorized into single-pole and double-pole types. Single-pole circuit breakers are the most widely used in residential settings, monitoring the current flow in a single wire and tripping in response to shorts or electrical overloads. These breakers operate within a voltage range of 15 to 30 amps and supply 120 volts to the circuit. Double-pole circuit breakers, on the other hand, simultaneously monitor the electrical flow through two wires. They are easily identifiable by their dual, interconnected switches. These breakers trip if either or both wires experience a short or overload, accommodating current ratings from 15 to 200 amps and delivering either 240 volts or 120/240 volts to an electrical circuit.
- Ground-fault circuit interrupters (GFCIs) are crucial safety devices that protect against line-to-ground faults and electrical overloads, especially in damp areas such as bathrooms, laundry rooms, and outdoor spaces. These circuit breakers are mandated by electrical codes to increase the safety in residential settings.

- Arc-fault Circuit Interrupters (AFCIs) are specialized breakers that detect arcing in electrical wiring, which is a common issue caused by damaged cords or thin insulation. AFCIs are required in newer homes to address electrical arc faults that standard circuit breakers may not consistently detect, thereby ensuring enhanced fire prevention measures in modern electrical systems.

It is important to choose the right type of circuit breaker for each electrical circuit to ensure the safety of the system and to prevent damage or fire. The comparison of circuit breaker is illustrated in Table 4-6 below

Table 4-6: Comparison of circuit breaker.

Criteria	Single-pole circuit breaker	Double-pole circuit breakers	Arc fault circuit interrupter	Ground fault circuit interrupter
Safety	won't always detect electrical arcs because they're only tripped by excessive heat.	won't always detect electrical arcs because they're only tripped by excessive heat.	are designed to trip when arcing is detected within electrical wiring.	This is when a dangerous electrical path occurs between a grounded element and an electrical current.
Cost in birr	329	879.5	3812.25	4362.38

Based on the criteria of cost single-pole and double-pole circuit breakers are preferable but in case of safety AFCIS & GFCIS circuit breakers are recommendable. The main priority is safety so GFCIS & AFCIS should be considered.

GFCIS is used when dangerous electrical path occurs between ground element and an electric current. AFCIS are designed to trip when arcing is detected within electrical wiring. Our project relates with AFCIS not with GFCIS. This project uses heat in high amount in this operation arcing can be detected, circuit breaker that trip when arcing is required, so AFCIS circuit breaker is selected.

4.6. Design of body Frame

4.6.1. Force Analysis

To select the best material for the designing components the distribution of forces in each component must be known. If not, the design is easily faced by many failures during service. In the engineering practice, the machine parts are subjected to various forces which may be due to one or more of the following.

- Energy transmitted
- Weight of the machine
- Change of temperature
- Lack of balance of moving parts
- Types of loads applied to the machine etc.

The various forces that affect a machine create different types of stresses such as bending stress, axial compressive stress, and shear force. When external forces or loads act on a body, internal forces (equal and opposite) arise at different sections of the machine to resist external forces. The internal force per unit area is referred to as unit stress.

Generally, there are four types of loads;

- Dead or stead load
- Live or variable load
- Suddenly load
- Impact load

Among these loads, the machine is subjected to a dead or steady load that can't change in its magnitudes and direction. Since the force analysis is the part of the design which contain the calculation of the load that exerts on each component according to their arrangement and how they must resist the external load (bending, shear, and compressive forces) for available function like; quality, competence, durability, reliability, efficiency, and strength of the designed machine.

Assumptions

- The load or weight of machine components are acting on the base plate and frame.
- Homogeneous cross-section of the frame reinforced.
- A load of machine components is to be 65kg.

4.6.2. Stress analysis

Body frame beams

Beams serve as structural components that support loads by resisting loads parallel to their axes. When designing beams, it is essential to evaluate the permissible shear and bending stresses. Typically, the maximum bending stress in a beam is greater than the localized stress caused by the application of loads on the beam surface.

Procured for stress analysis

The following procedure outlines a rational method for designing a beam based on strength.

Procedure 1: Shear and Moment Diagrams

- To determine the maximum shear and moment in a beam, shear and moment diagrams are utilized by plotting V versus x and M versus x, where V represents the shear force and x denotes the distance from the beam. Positive values of V and M are shown above the x-axis, whereas negative values are displayed below. Typically, it is more practical to present shear and moment diagrams below the free-body diagram of the beam.

Procedure 2: Bending Stress

- The flexure formula can be applied to calculate the section modulus of a long beam as Sreq'd = Mmax/σallow, where Sreq'd is the required section modulus, Mmax is the maximum beam moment, and σallow is the allowable bending stress. Once the section modulus is determined, the dimensions of the simple shapes can be computed using the formula Sreq'd = I/c. Here, "I" represents the moment of inertia of the cross-sectional area about the natural axis, and "c" is the perpendicular distance from the natural axis to a point farther from the natural axis, where σallow acts.
- When selecting a steel section, the American Institute of Steel Construction (AISC) manual offers a table of options that meets the requirements (S > Sreq'd). The most economical and lightest option was chosen, with the smallest cross-sectional area. The chosen section modulus S should slightly exceed Sreq'd to accommodate the additional moment from the weight of the beam.

Procedure 3: Shear stress

- Steel beams used to transport heavy loads are usually designed to first withstand shear stress and then check for compliance with the permissible bending stress

requirement. To ensure that the designed shear stress is lower than the permissible shear stress, the shear formula can be utilized.

Body frame columns

Columns are typically long and slender, and are designed to bear axial compressive loads. The crucial load denotes the maximum axial force that a column can endure prior to buckling. This occurred when the column reached a neutral equilibrium state. An idealized column is initially straight and made of uniform material, with the load applied through the centroid of its cross section.

4.6.3. Material selection

Commonly used materials for body frame are steel, aluminium, and carbon-fibre. Comparison between those materials described in Table 4-7 as follow.

Table 4-7: Different material properties.

Steel	Aluminium	Carbon fibre
• Strong, predictable, repairable, long time use: heavy • Durability-high, fails gently, corrodes • Cost-low to moderate to high (grade and joints) • Readily recycled • Uses-Touring, off-	• Light weight, moderate use, brittle • Durability-non corroding, poor resilience • Readily recycled • Cost-low to high • Uses- off-road, racing, general	• Lightest-weight, least use history, fractures andsplinters • Durability-low, catastrophic failure, UV deterioration • Cost-high to extreme • Non-recyclable; down recycling possible • Limited off-road,

Material selection for base, column, and frame are based on mechanical properties such as high bending strength; tensile strength, easy of availability easy of machining, welding, finishing, cutting and cost factor. Compared to aluminium and carbon fibre, steel has the greatest ability to maintain strength and integrity during tough event.

Types of Steel

1. Carbon Steel

Carbon steel has a dull and matte appearance and is prone to corrosion. It is divided into three subcategories: low, medium, and high carbon steel. Low carbon steel contains approximately 0.30% carbon, medium contains 0.60%, and high contains 1.5%.

2. Alloy Steel

Alloy steel is a type of metal that is made by combining different metals, including nickel, copper, and aluminum. This type of steel is highly resistant to corrosion and is commonly used in a variety of applications, such as car parts, pipelines, ship hulls, and mechanical projects. The strength of alloy steel is determined by the concentration of its constituent elements.

3.Tool steel

Tool steel is a type of metal that is known for its exceptional hardness and resistance to heat and wear. This makes it an ideal material for creating metal tools, such as hammers. Tool steel is composed of elements like cobalt, molybdenum, and tungsten, which are responsible for its remarkable durability and heat resistance properties. The name "tool steel" is derived from its common use in making metal tools.

4. Stainless steel

Stainless steel is the most widely used type of steel, which typically comprises 10 to 20% chromium as its main alloying element. This composition enables the steel to be resistant to corrosion and easily molded into various forms. In contrast, mild steel or plain carbon steel is a better option for machine frames compared to other types like stainless steel, alloy steel, and tool steel. Mild steel is primarily composed of carbon with small amounts of silicon, manganese, copper, nickel, molybdenum, aluminum, and chromium. AISI 1025 carbon steel (UNS G102500) is commonly used for body frame construction.

Physical and mechanical properties of AISI 1025 carbon steel.

The physical and mechanical properties of AISI 1025 Carbon steel illustrated at Table 4-8 and Table 4-9 below.

Table 4-8: Physical property of AISI 1025 carbon steel.

Property	**Metric**	**Imperial**
Density	7.858 g/cm^3	0.2839 lb/in^3

Table 4-9: Mechanical property of AISI 1025 steel.

Properties	**Metric**	**Imperial**
Tensile strength	440 Mpa	63800 psi
Yield strength	370 Mpa	53700 psi
Shear strength	290-310 Mpa	44000 psi
Bulk modulus (typical for steel)	140 GPa	20300 ksi
Shear modulus (typical for steel)	80.0 GPa	11600 ksi
Elastic modulus	190-210 GPa	27557-30458 ksi
Poisson's ratio	0.27-0.30	0.27-0.30

Factor of safety

The concept of safety is important in the design of machine components. To ensure reliable and safe operation of a component, it is crucial to prioritize safety during the design phase. By designing components to withstand loads beyond their actual operating loads, a margin or buffer is established to ensure item safety. This margin was determined during the design phase by considering a suitable safety factor. The safety stress or yield stress, which is the amount of stress at the safety load, and the working stress or allowable stress, which is the

amount of stress at the designated design load, are the two key parameters in determining the safety factor.

The ratio of the safety stress to the working stress was used to calculate the safety factor. It is essential to adhere to the established safety factors to ensure the safe operation of a component. The range of Factor of safety illustrated in Table 4-10 below.

Table 4-10: Typical Factor of Safety Range for different machine component.

Member	**Typical Factor of safety range**
Materials that exhibit a high level of reliability under moderate loading and environmental conditions.	1.3 to 1.5
Materials that are dependable under moderate loading and environmental conditions.	1.5 to 2
Materials that are routine and function effectively under moderate loading and environmental conditions.	2 to 2.5
Materials that are suitable for use with untested or brittle items and under average environmental conditions.	2.5 to 3
Materials that are appropriate for use with items that lack dependability and are subjected to moderate loading and environmental conditions or when reliable materials are utilized in challenging environments.	3.0 to 4.0

Due to typical factor of safety range above mentioned the machine is subjected to difficult environmental condition. The body is exposed to high thermal condition and for corrosion. For the machine body component safety factor is mentioned in Table 4-11 as follow.

Table 4-11: Summery of factor of safety.

Body component	**Safety factor (F.S)**
Frame beam	4
Frame column	3

4.6.4. Shape of body frame structure

Selecting the appropriate frame shape, whether it be a profile or beam type, is crucial for different purposes. Every beam shape possesses distinct characteristics and a variety of sizes. There are numerous standard beam types available. The table 4-12 below provides a ranking for each property, with the range of numbers from 1 to 5 indicating general ratings. A higher number signifies stronger, more efficient, or more durable properties, while a lower number suggests weaker or less desirable properties in comparison to others. It is important to note that the comparative nature of the rating system means that a lower number does not necessarily equate to a poor rating.

Table 4-12: Comparison of standard beam shapes.

Beam Profile >>>> Functional Property	**HSS** 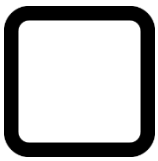	**Round Tube** 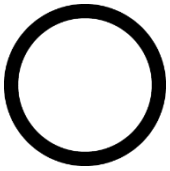	**C-Channel** 	**L-Angle** 	**I-Beam** 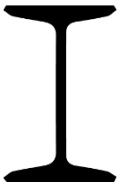
Vertical Strength Per Weight (Bending)	4	3	4	2	5
Horizontal Strength Per Weight (Bending)	3	3	2	2	2
Torsional Strength Per Weight	4	5	2	2	3

Open / Closed Section	Closed. Convex	Closed. Convex	Open. Concave	Open. Concave	Open. Double Concave
Ease of Work (Cutting Angles, Holding, Fixture setup.)	5	3	4	4	3
Ease of Protecting (From Corrosion)	4	3	5	5	5
Easy Bolting (Angles / Squish)	3	2	3	5	3
Total	23	19	20	20	21

From the above chart a rectangular hallow section profile is the most rated profile due to different functional property of the mentioned profiles. Most important machinability qualities for the machine body construction are: -

1. Easy for cutting of angle
2. Suitable for welding
3. Handy for holding fixture
4. Easy for bolting

Square hallow section profile is the selected profile which is full fill the machinability quality for the body frame construction compared to other profiles.

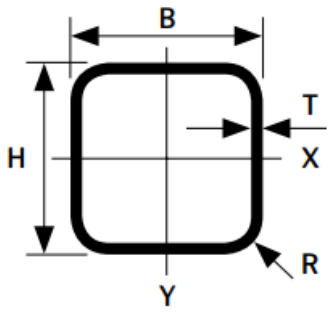

Figure 4-8: Section and dimension of the RSH.

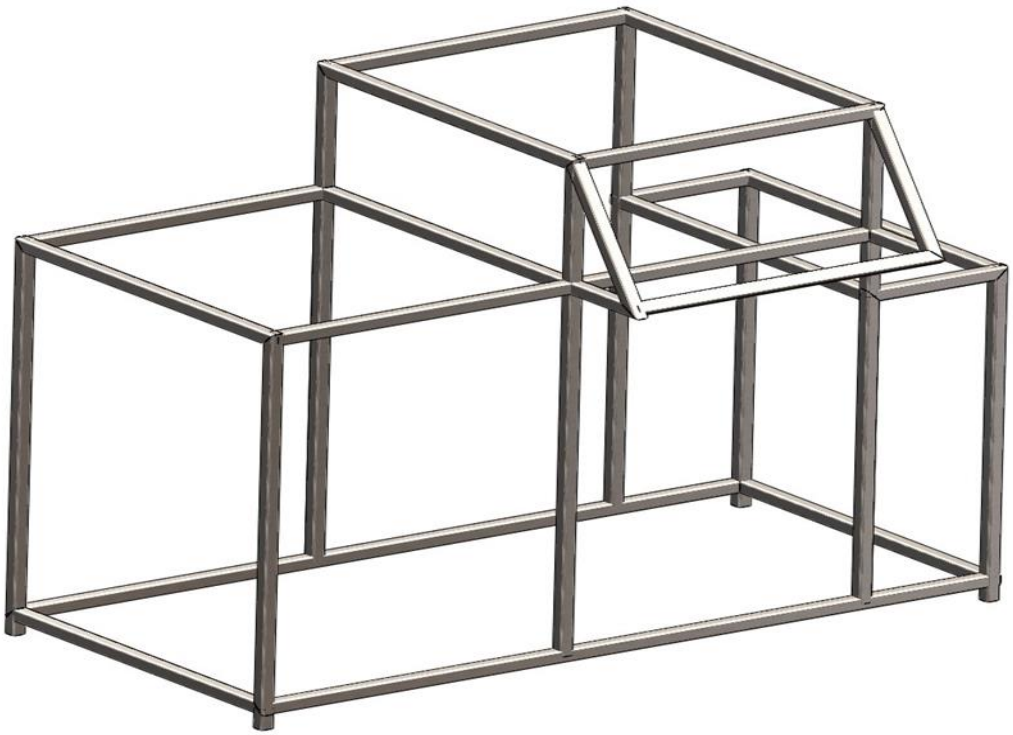

Figure 4-9: Design of body frame.

CHAPTER FIVE

5. EXPERIMENTAL SETUP AND PROCEDURE

5.1. Introduction

This section offers a detailed account of the experimental procedures and the comprehensive development process of the experimental setup. It delves into the fabrication of each individual component of the fuel extracting machine, assembly of the final experimental setup, and measuring equipment employed throughout the study. By providing this thorough overview, the reader gains a clear understanding of the methodological approach and the technical aspects involved in the development of the fuel extraction machine.

5.2. Manufacturing Process

The components of the fuel extracting machine were built using materials obtained from the local market, considering the cost and availability of each material. The dimensions of the components were depicted in a theoretical analysis of the machine, which is employed to extract fuel from waste plastic.

5.2.1. Pyrolysis of reactor and its flange

The metal sheet was then rolled and welded to form a cylinder, with circular sheets welded onto the top and bottom to cover them. After construction, the entire reactor was checked for leakage by filling it with water and observing where it leaked. This was done to ensure a safe and precise experiment, as leakages could have caused an explosion and prevented the experiment from achieving its aim. A bore was made on the top surface of the cylinder for the entrance of raw material. The flange was then fabricated by cutting a circular plate of specified dimensions and drilling eight holes for the bolts. To ensure a complete seal between the flange cover plate and reactor, a gasket was used, as shown in Figure 5-1.

Figure 5-1: The pyrolysis reactor with flange.

5.2.2. Refractory material

As shown in Figure 5-2, the refactor material was constructed using brick and cement materials that could withstand high temperatures without deformation or degradation.

Figure 5-2: Fabricated refractory material.

5.2.3. Condenser system

The manufacturing process of a condenser system begins with cutting the sheet metal to the appropriate dimensions using grinders. The length of the metal sheet is equal to the circumference of the shell, whereas the width matches the length of the shell. Subsequently, the metal was subjected to a rolling process to reduce its thickness and ensure uniformity. Rolling can be classified into two categories: hot rolling, in which the metal is above its recrystallization temperature, and cold rolling, in which the metal is below its recrystallization temperature. Hot rolling is the most extensive manufacturing process, whereas cold rolling leads to tonnage production during cold working processes. Surface grinding was then employed to create a flat surface on the metal, with tolerances typically achieved within $\pm 2 \times 10{-}4$ in for flat materials and $\pm 3 \times 10^{-4}$ in for parallel surfaces. Drilling is a process used to create circular holes in solid metal components. On the other hand, gas metal arc welding (GMAW), also known as metal inert gas (MIG) welding, is a technique used to join metal components. In GMAW, an electric arc is formed between a consumable wire electrode and workpiece metal, causing it to melt and fuse. A shielding gas was used to protect the welding process from air contaminants. These processes, including cutting, rolling, grinding, drilling, and welding, are crucial steps in the manufacturing of condenser systems, as shown in Fig. 5.3.

Figure 5-3: Constructed condenser system.

5.2.4. Body frame

The manufacturing process can be used to process available raw materials into components. The selection of the manufacturing process considers factors, such as the materials of the components, geometric shape of the components, cost of manufacturing, surface finish, and required tolerance. As shown in Figure 5-4, the body frame is the part of the machine used to support the entire machine. The machine frame must be sufficiently rigid to carry an applied load. The materials required for the manufacturing process of the body frame are hollow cross-sectional beams and electrodes for weld joining of steel beams to form the required body frame structure. The reason for selecting weld joining is that it is more rigid than other fastening methods such as temporary and permanent fastening.

Figure 5-4: Constructed Body frame.

5.3. Feed stock pre-processing and preparation for experiment

Identifying and gathering municipal solid wastes that can be used in pyrolysis: Among the different types of municipal solid wastes, glass, bones, metals, ceramics, ash, dust, and non-combustible wastes are not suitable for pyrolysis due to their high melting points and non-combustible properties. However, materials such as vegetables, paper, wood, and textiles have low calorific values and are prone to decay, making pyrolysis an unviable option. However, plastics are the most suitable feedstock for pyrolysis because of their high calorific

value and significant environmental impact if not disposed properly. The primary focus of the target feedstock was on HDPE and LDPE waste plastics, plastic bags, PP, and PS derived from yogurt cups. A total of 10 kg of sample was collected from the daily disposal waste of city residents and used for pyrolysis. PVC was excluded from the study because of its insignificant contribution to the waste stream and the high yield of corrosive hydrogen chloride produced during its conversion through pyrolysis. After collecting the feedstock, it was cleaned to remove any dirt and washed before drying at ambient temperature. The cleaned feedstock was then shredded into small pieces for easier feeding and pyrolysis, as shown in Figure 5-5.

Figure 5-5: Shredded waste plastic for pyrolysis.

5.4. Pyrolysis set up

The first step in setting up the pyrolysis equipment was to collect and prepare the necessary materials and waste. After finishing the construction of the body frame, the subsequent task is to assemble the pyrolysis equipment within it. In this study, a batch reactor was used for pyrolysis, which was made of stainless steel and had a sealed end and an outlet tube at the other end. This design facilitated the collection of volatile, gas, and oil products generated during the pyrolysis process. All the equipment within the reactor was sealed to prevent any leakage from or into the outside environment. The condenser system and heating source were also correctly set up, and the feedstock was weighed and mixed before being introduced into the reactor. The reactor was tightly sealed to prevent back leakage of gaseous hydrocarbons during pyrolysis, as illustrated in Figure 5-6.

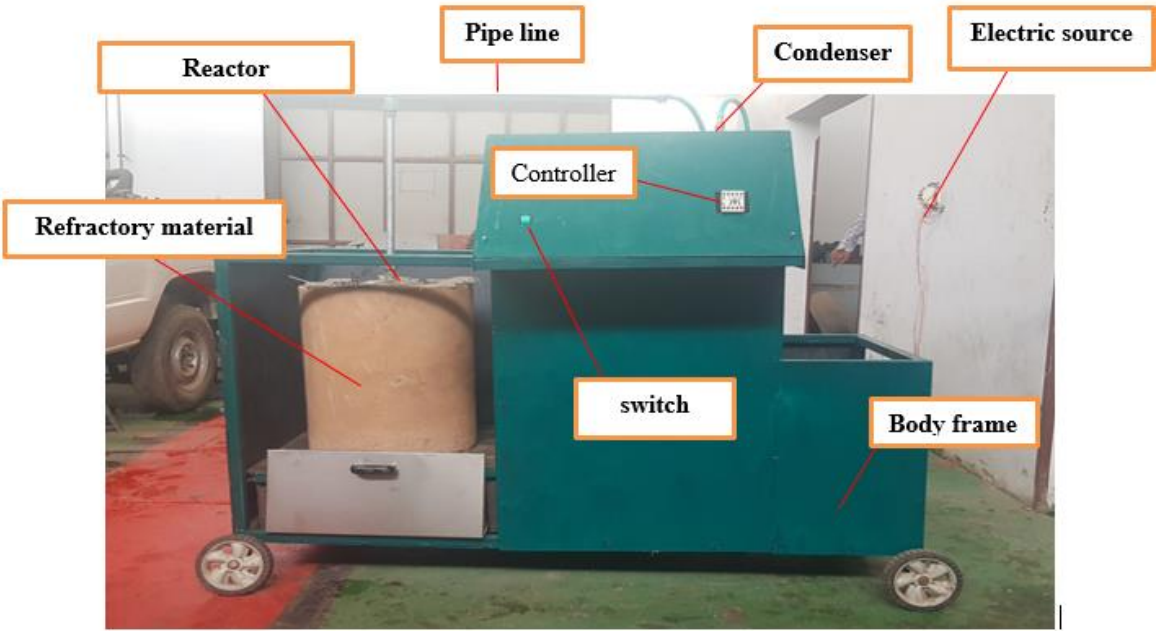

Figure 5-6: Experimental set up of pyrolysis machine.

5.5. Production of Pyrolysis oil

A cylindrical batch reactor was used to conduct pyrolysis of the feedstock at temperatures between 300 and 450°C in an oxygen-free environment for approximately 1 h and 9 min. The temperature was gradually increased from ambient to 300-450°C without a catalyst. The waste was gently cracked into gases that could be condensed into a series of gases, char, and distillate oil, which was the main focus of this study. The feedstock was loaded into the reactor to generate the target product in terms of both quantity and quality, which was then verified using the output obtained after pyrolysis. The produced waste oil was stored and prepared for analysis. Figure 5-7 provides an overview of the pyrolysis process.

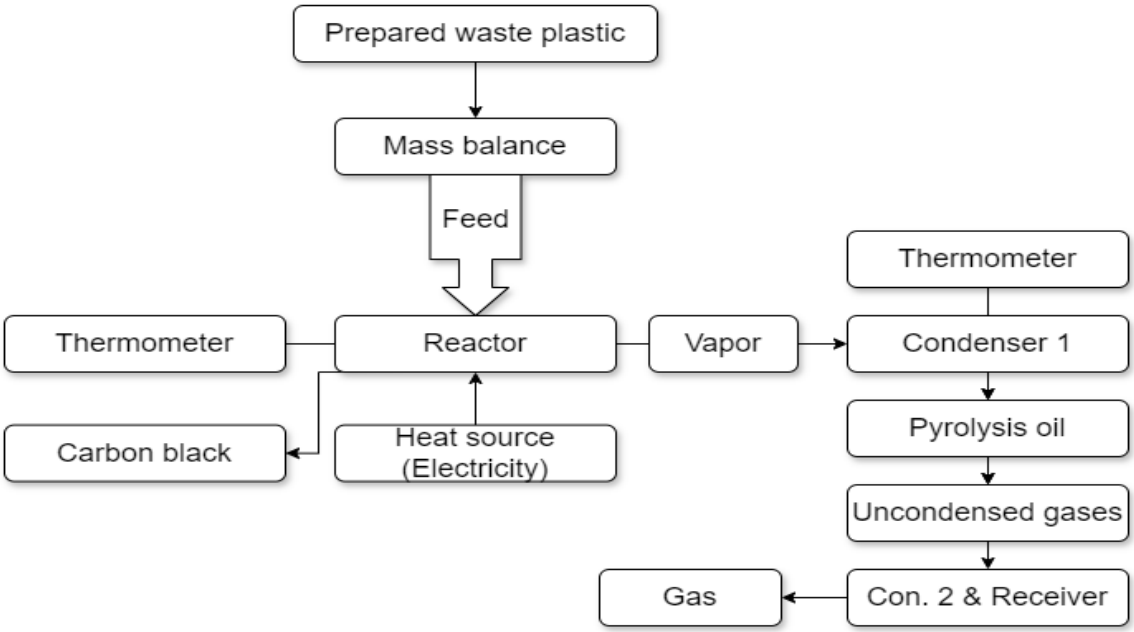

Figure 5-7:Over view of pyrolysis oil production.

5.6. Analysis of liquid fuel

Waste plastic fuel testing was conducted at the Material Science Engineering Laboratory of the Adama Science and Technology University and the Quality Assurance Service of the Ethiopian Petroleum Supply Enterprise. The fuel properties of the examined samples were determined using the American Standard for Testing Materials (ASTM) procedures for petroleum products, as outlined in ASTM 2002. Prior to assessing the liquid fuel properties under the operating conditions, the samples that yielded higher results were tested and compared to the standard outcomes. The yields of liquid fuel products were calculated using Equation below:

The percentage yield of condensable volatiles (in terms of weight) was determined using the following parameters:

- R1: Initial weight of the reactor before the experiment, measured in kilograms (kg).
- C1: Weight of condensers before experiment, measured in kilograms (kg).
- E1: Weight of the connectors before the experiment, measured in kilograms (kg).
- R2: Weight of the reactor after the experiment, measured in kilograms (kg).
- C2: Weight of condensers after experiment, measured in kilograms (kg).

- E2: Weight of the connectors after the experiment, measured in kilograms (kg).
- Ms: Weight of the feed sample measured in kilograms (kg).

$$\text{Condensate} = \frac{(R2+C2+E2)-(R1+C1+RC1)}{Ms} * 100\% \ldots\ldots\ldots\ldots\ldots\ldots\ldots\ldots 5.1$$

$$\text{Condensate} = \frac{15.2kg+10.3kg+0.87kg-13.9kg-4kg-0.37kg}{10kg} * 100\% = 81\%$$

The yields of oil and char are typically expressed as a percentage of the initial mass of plastic.

$$\text{Yield of plastic oil (Y-oil)} = \frac{Moil}{Ms} * 100\% \ldots\ldots\ldots\ldots\ldots\ldots\ldots\ldots\ldots\ldots\ldots\ldots\ldots\ldots 5.2$$

$$\text{Yield of plastic oil} = \frac{3.882kg}{10kg} * 100\% = 38.82\%$$

i.e. the fuel obtained from each kg of plastic waste used is 0.49 liter/kg

- the electric energy utilized for waste plastic oil production process

3kw*1.15hr = 3.45kwhr, which is equivalent to 12420KJ and the output energy from pyrolysis oil 41300KJ/kg and density are 0.78g/ml and volume are 4.9 liter

Mass(m) = 3.882kg

Then the output energy is 41300KJ/kg*3.882kg

= 160326.6KJ

Where M_{oil} is mass of liquid oil

$$\text{Yield of char (Y- char)} = \frac{M\ char}{Ms} * 100\% \ldots\ldots\ldots\ldots\ldots\ldots\ldots\ldots\ldots\ldots\ldots\ldots\ldots\ldots 5.3$$

$$\text{Yield of char} = \frac{0.8kg}{10kg} * 100\% = 8\%$$

Where M_{char} is mass of char

The calculation for the Gas yield(Y-gas) was derived by subtracting the condensable volatiles and char yield sum from 100 wt% as shown in equation 5.4 below.

$$\text{Y-gas} = 100\% - (\text{Y- condensate} + \text{Y- char}) \ldots\ldots\ldots\ldots\ldots\ldots\ldots\ldots\ldots 5.4$$

$$= 100\% - (81\% + 8\%) = 11\%$$

The conversion rate, which represents the proportion of feed that is ultimately converted into products during pyrolysis, was calculated using Equation 5.5, as shown below:

$$\text{Conversion efficiency} = \frac{Ms - Mc}{Ms} * 100\% \quad \text{.....5.5}$$

$$\text{Conversion efficiency} = \frac{10kg - .8kg - 5.318kg}{10kg} * 100\% = 38.8\%$$

After operation, the reactor was cleaned to remove the char product and solidified oil (wax) accumulated on its inner surface. The weights of these samples were then measured and used to calculate the amount of non-condensable (NC) gas produced, as shown in Equation 5.6.

$$N_c = M_s - M_c - M_{oil} \quad \text{.....5.6}$$

$$Nc = 10kg - 0.8kg - 3.882kg = 4.3kg$$

5.7. Conduct emission test

The emission test conducted at Adama Science and Technology University's automotive shop involved analyzing the emissions of gases such as CO, CO_2, NOx, and unburned HC from oil extracted from plastic waste and blended with diesel. This test was performed at various engine speeds using an exhaust gas analyzer, as illustrated in the Figure 5.8 below.

Figure 5-8: Analysis of emission test.

CHAPTER SIX

6. RESULTS AND DISCUSSIONS

In this section, we delve into an extensive experimental study centered around the extraction of plastic oil from waste plastic. The investigation encompasses critical elements such as determining the percentage yield of the extracted oil, a key metric for evaluating the efficiency and feasibility of the extraction process. Furthermore, the study meticulously examines the physical and chemical properties of the plastic oil, including density, kinematic viscosity, and calorific value. Additionally, the research extends to exploring the properties of blends comprising plastic oil and diesel fuel, essential for understanding their compatibility and potential applications as a fuel source.

Moreover, emission tests are conducted to evaluate the environmental impact and suitability of the extracted plastic oil as a fuel, ensuring compliance with environmental standards and pinpointing areas for enhancement.

6.1. Temperature Distribution

Temperature Distribution in the Reactor Wall as shown in Figure 6-1 below

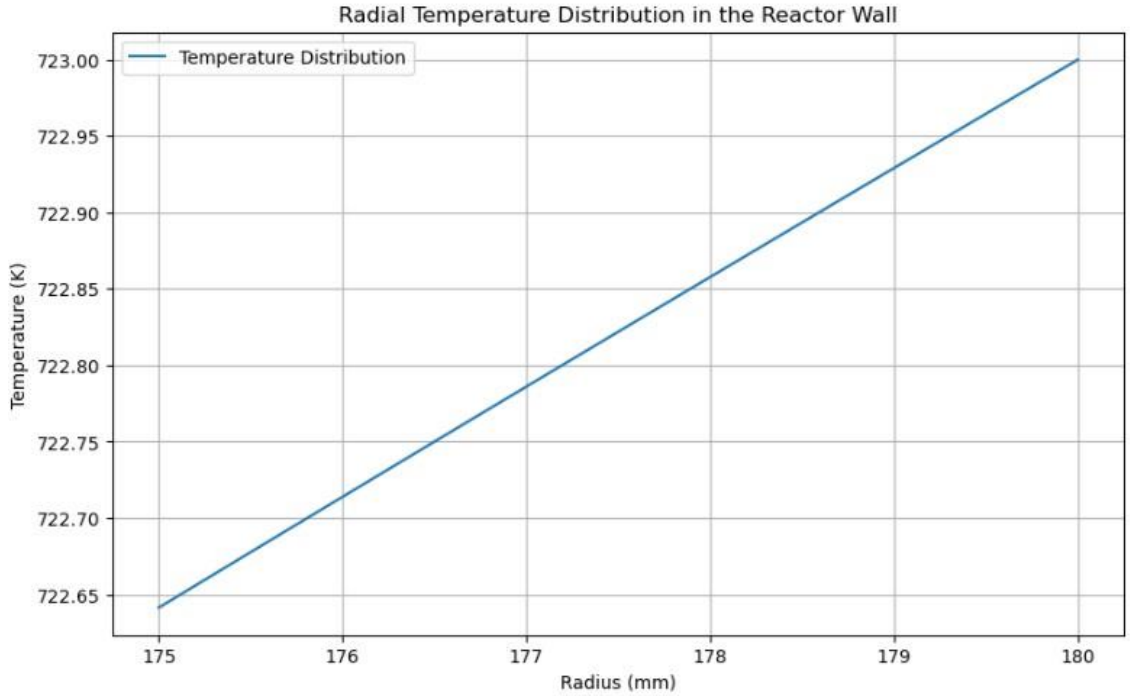

Figure 6-1:Radial temperature distribution in the reactor wall.

A graphical analysis of the temperature distribution in the mild steel reactor wall revealed a slight decrease in temperature from the outer surface (723 K) to the inner surface (approximately 722.64 K) over a thickness of 4 mm. This minimal temperature gradient indicates efficient heat conduction through the reactor wall, ensuring a nearly uniform temperature profile, which is crucial for the pyrolysis process. Uniformity in temperature minimizes the thermal stress within the reactor, thereby enhancing its structural integrity and operational reliability. The properties of mild steel, including good thermal conductivity, high tensile strength, and cost-effectiveness, contribute to efficient heat transfer and overall reactor performance, making it a suitable material for maintaining the stable high-temperature conditions necessary for efficient pyrolysis.

6.2. Heat map of Temperature Distribution

The heat of Radial temperature distribution in the reactor wall also illustrated in Figure 6-2 below

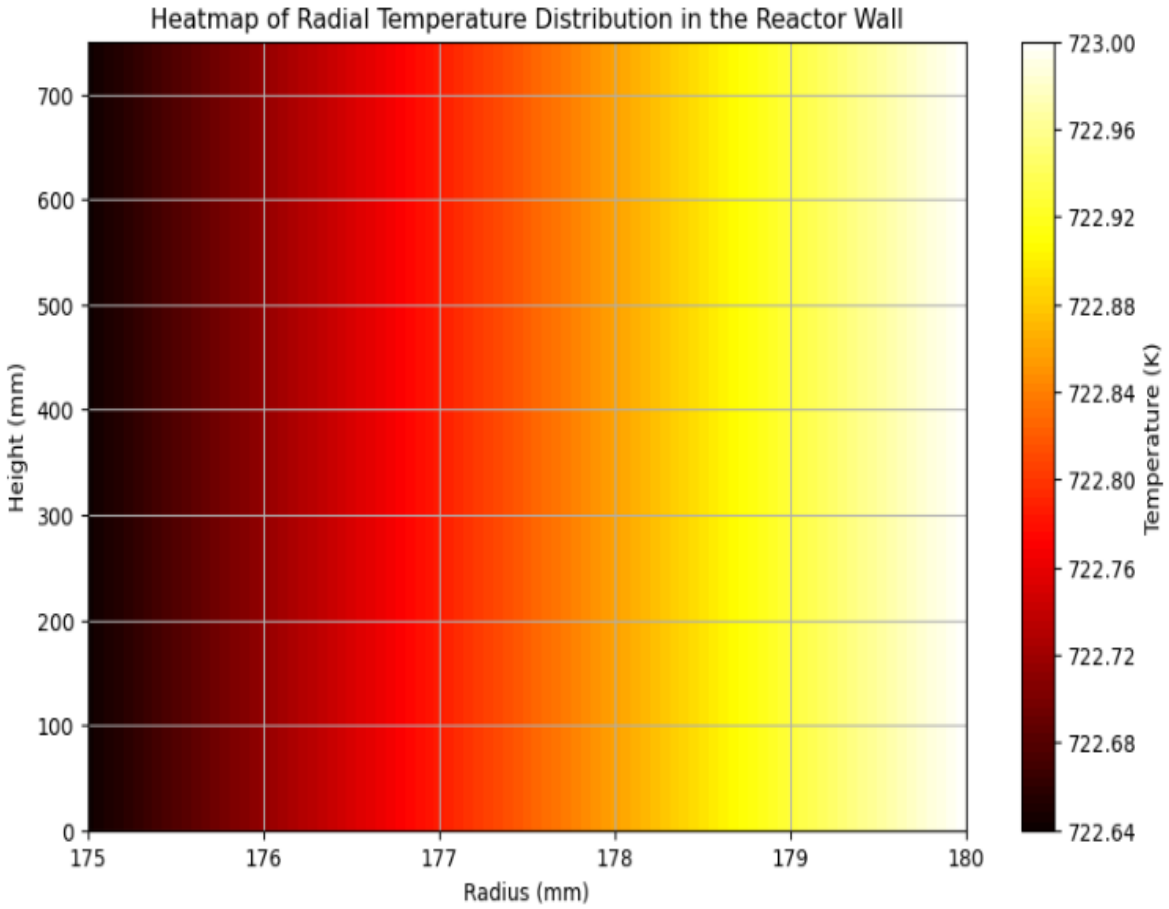

Figure 6-2:Heat map of radial temperature distribution

6.3. Percentage of product types

The percentage of product types obtained through plastic pyrolysis is illustrated in Figure 6-3, as shown below.

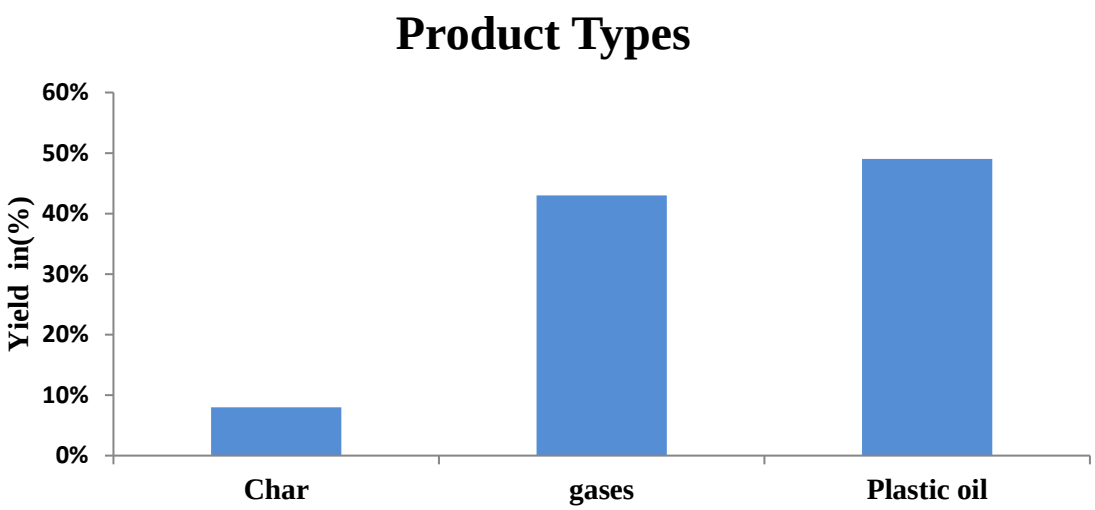

Figure 6-3:Percentage of product types.

The application of pyrolysis for the purpose of energy generation and recycling of mixed plastic waste, including HDPE, LDPE, PP, and PS, has been demonstrated to be a pioneering approach. As shown in the Figure above when applied to a 10 kg batch of plastic waste, the pyrolysis process produced impressive results: 8% char, 43% gas, and 49% liquid oil. This distribution underscores the substantial energy recovery potential embedded in plastic waste. The char generated during pyrolysis is not just a by-product; it holds significant value as a fuel or as a raw material for producing activated carbon, ceramics, and other industrial products. Gas, which is rich in methane, carbon dioxide, and hydrogen, is a versatile fuel source or feedstock for chemical and fuel production. Liquid oil, which has a high-value output, can replace fossil fuels.

Pyrolysis is a recycling method that has gained popularity due to its numerous advantages over traditional incineration, which often results in the emission of harmful pollutants. One of the key benefits of pyrolysis is its ability to process a wide variety of plastic materials, including mixed plastics, which are typically difficult to recycle. Additionally, pyrolysis has significant potential for energy recovery, with liquid oil that can be used as transportation fuel or to generate electricity, reducing reliance on fossil fuels and greenhouse gas emissions. Studies have demonstrated the effectiveness of pyrolysis in recycling plastic waste for example, research conducted on pyrolysis of polyethylene and polypropylene waste yields

char and gas, with a char yield of 0.5 kg and a gas yield of 3.5 kg per kilogram of waste(Suresh et al., 2021) Another study a char yield of 0.7 kg and a gas yield of 4.2 kg per kilogram of plastic waste(Suresh et al., 2021).These results suggest that optimizing the pyrolysis process can lead to increased yields of valuable char, gas, and liquid products.

6.4. Properties of waste plastic oil and its blends with diesel

The physical properties of the waste plastic oil and its blends with diesel were examined at the Materials Science and Engineering Department Laboratory of Adama Science and Technology University in accordance with ASMT standards. In addition to testing the density and kinematic viscosity of the waste plastic, its calorific value was evaluated. The Ethiopian Petroleum Supply Enterprise Quality Assurance Service conducted these tests. The outcomes are presented in Tables 6-1 and 6-2.

Table 6-1: Properties of tested plastic oil and its blends.

No	Property	Test method	Test Results				
			Diesel	WPO 10%	WPO 20%	WPO 30%	WPO
1	Density@15^0c (g/ml)	D4052	0.846	0.846	0.845	0.841	0.791
	Density@20^0c (g/ml)	D4052	0.842	0.842	0.841.2	0.838	0.784
2	Kinematic viscosity@32 °C(mm^2/s)	D562	4.5	4.4	4.2	3.42	2.15

Table 6-2: Properties of tested plastic oil.

No	Property	Test method ASTM	Limits	Test results
				WPO (Waste plastic oil)
1	Density@15^{0}C (g/ml)	D4052	Reports	0.789
	Density@20^{0}C (g/ml)	D4052	Reports	0.781
2	Kinematicviscosity@40°C(mm^2/s)	D445		2.31
3	Calorific value, Calc, MJ/kg	Calculated		41.31866

In the quest for sustainable energy sources, the utilization of waste plastic oil as a viable alternative to conventional fuels is gaining momentum. To ensure the practicality and effectiveness of this transition, it is imperative that the properties of waste plastic oil closely match or even surpass those of traditional fuels, such as diesel. In a comprehensive analysis comparing waste plastic oil with common diesel, three crucial properties stand out: density, kinematic viscosity, and calorific value. These properties serve as fundamental indicators of the performance and compatibility of waste-plastic oil as a fuel substitute. As shown in the above Table, the study revealed that by blending waste plastic oil with pure diesel in the range of 10% to 30%, significant improvements in property alignment with conventional diesel were observed. Notably, even at a 10% blending ratio, the resulting mixture exhibits properties similar to those of pure diesel, showing the potential for seamless integration of waste plastic oil into daily fuel usage. Furthermore, this research highlights a notable finding regarding the calorific value of pure plastic oil, surpassing previous studies and indicating a higher energy content. Additionally, the density of the waste plastic oil, which is initially higher than some previous research findings, aligns closely with the density of conventional diesel, emphasizing its suitability for fuel applications as illustrated in Figure 6-4 and 6-6 below. In conclusion, the data presented underscore the potential of waste plastic oil as a sustainable fuel alternative. By fine-tuning its properties to closely match or exceed those of traditional fuels, waste plastic oil has emerged as a viable solution for reducing environmental impacts and promoting energy sustainability in the future.

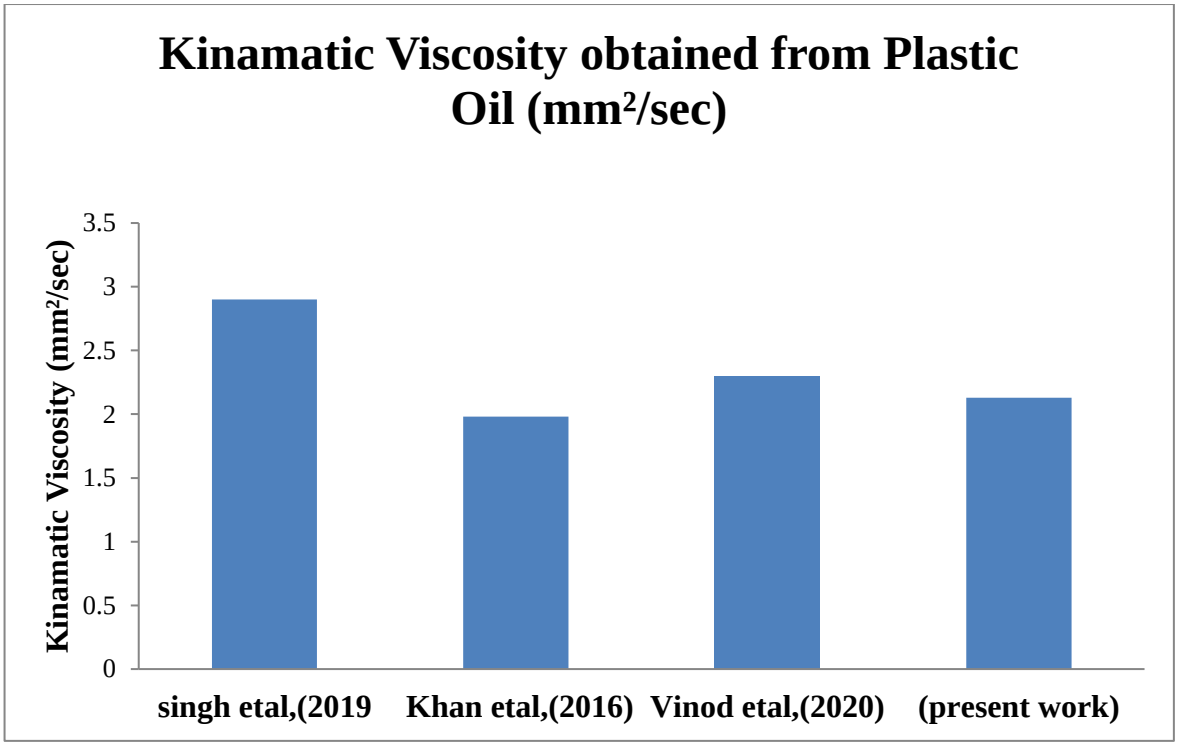

Figure 6-4: Kinematic Viscosity obtained from Plastic Oil.

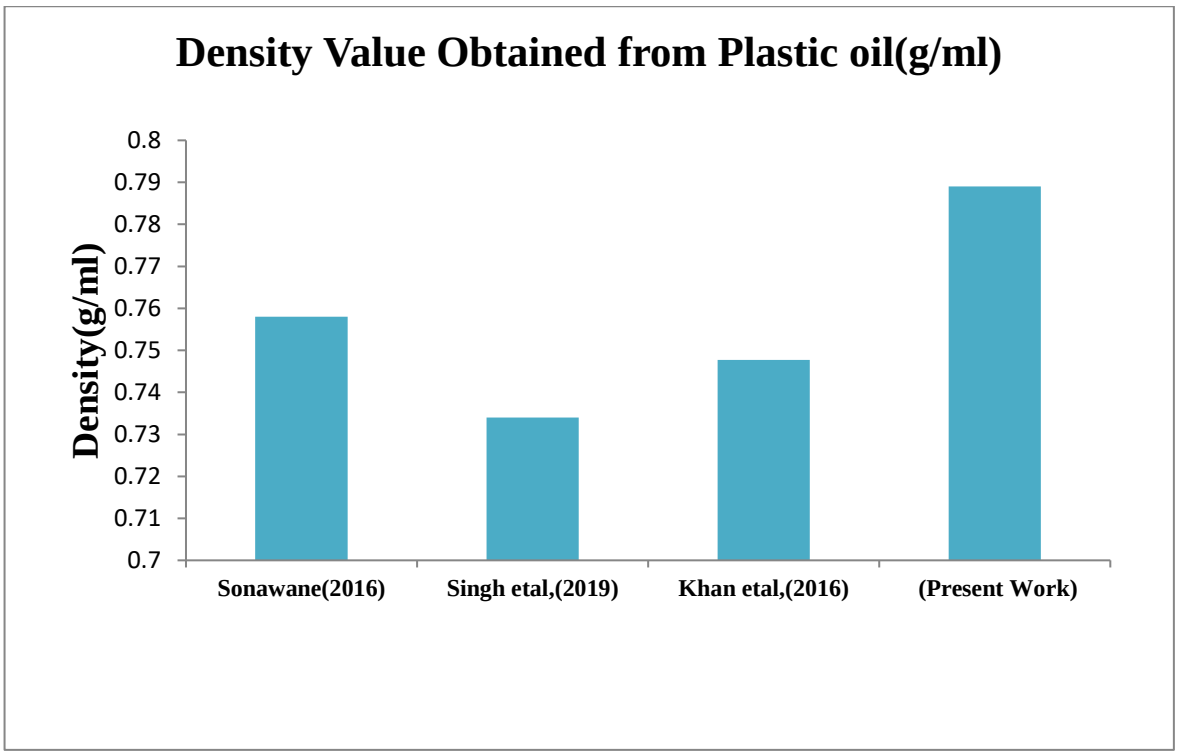

Figure 6-5: Density Value Obtained from Plastic oil.

6.5. Emissions test of waste plastic oil and its blends

6.5.1. Carbon monoxide emissions

The CO emissions (% vol) of pure diesel (B0) and its blends with waste plastic oil (B20, B30, and B50) at different engine speeds (rpm) exhibit distinct trends, as shown in Figure 6-1. At lower engine speeds (1000-1500 rpm), CO emissions increased with higher blend ratios of waste plastic oil. B50 had the highest CO emissions, followed by B30 and B20, compared with pure diesel (B0). However, at medium engine speeds (2000-2500 rpm), CO emissions were similar for all blends and pure diesel, with a slight increase for higher blend ratios. Interestingly, at higher engine speeds (3000-3800 rpm), CO emissions were higher for B50 than for the other blends and pure diesel, while B20 exhibited the lowest CO emission among the blends at these speeds.

Compared to pure diesel (B0), the CO emissions at lower speeds showed that B20 had similar levels to B0, whereas B30 and B50 had higher emissions. At medium speeds, all blends had comparable CO emissions to B0. However, at higher speeds, B20 had lower CO emissions than B0, while B30 and B50 had higher emissions.

Based on these findings, the recommended blend for different engine speed ranges is as follows:

- For lower engine speeds, B20 is recommended as it has the most similar CO emissions to pure diesel.
- For medium speeds, any blend can be used as they all have comparable CO emissions to pure diesel.
- For higher speeds, B20 is recommended as it has lower CO emissions than pure diesel.

These results are consistent with other studies on the use of waste plastic oil as a diesel substitute. A study by(Sharuddin et al., 2018) also found that blending waste plastic oil with diesel reduced CO emissions compared to pure diesel, with the lowest emissions at a 20% blend ratio. Furthermore,(Maithomklang et al., 2022) reported that CO emissions decreased with increasing engine speed for both pure diesel and plastic oil blends.

In conclusion, the 20% blend of waste plastic oil with diesel (B20) is the most suitable replacement for pure diesel across the tested engine speed range, as it has the most similar or lower CO emissions than pure diesel. These findings highlight the potential of using waste

plastic oil as a sustainable alternative to conventional diesel fuel while maintaining acceptable emission levels.

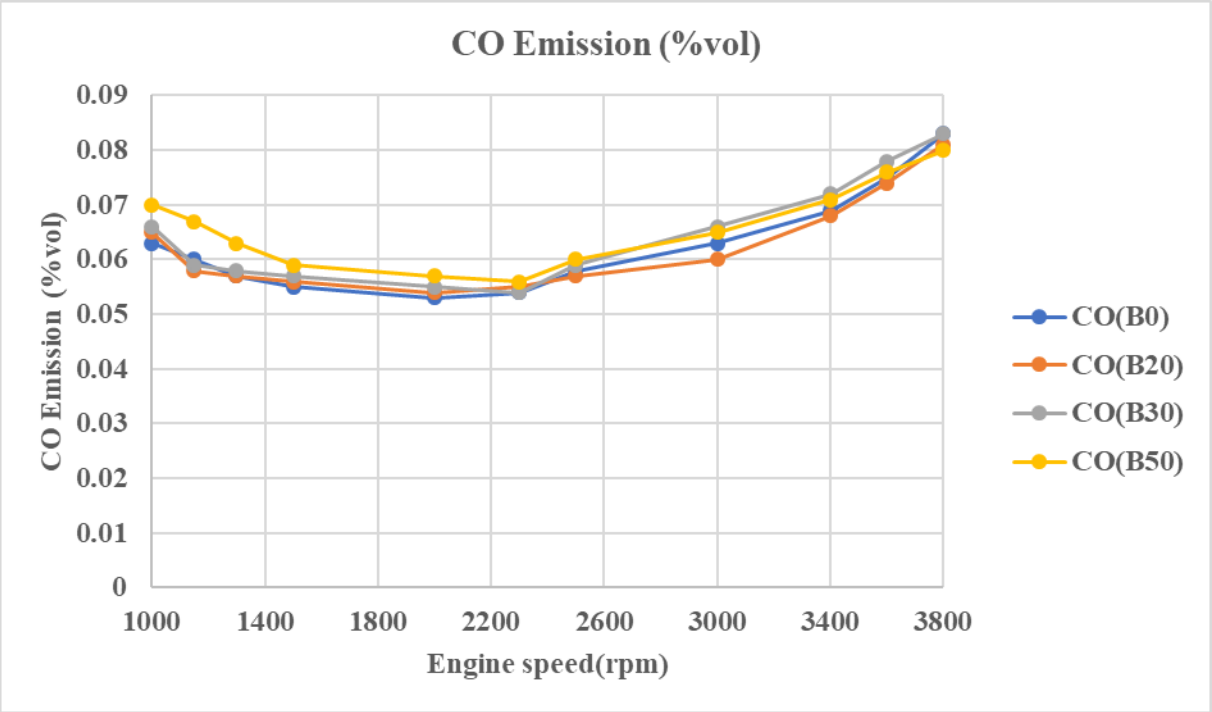

Figure 6-6: CO Emission result.

6.5.2. Carbon dioxide emissions

The CO_2 emissions from a diesel engine operating on pure diesel (B0) and its blends with waste plastic oil (B20, B30, and B50) were evaluated at various engine speeds ranging from 1000 to 3800 rpm, yielding an interesting pattern as shown in Figure 6-2: as the engine speed increased, the CO_2 emissions also increased for all fuel blends. At lower engine speeds (1000-1500 rpm), CO_2 emissions were notably lower for the blended fuels than for pure diesel. For instance, at 1500 rpm, B0 had CO_2 emissions of 2.56%, whereas B20, B30, and B50 had emissions of 2.47%, 2.42%, and 2.35%, respectively. This promising finding suggests that incorporating waste plastic oil into diesel fuel can significantly reduce the carbon footprint at lower engine speeds.

However, as the engine speed increased further (2000-3800 rpm), the difference in CO_2 emissions between the pure diesel and blended fuels decreased. At 3800 rpm, B0 had the highest CO_2 emissions at 3.30%, whereas B20, B30, and B50 had emissions of 3.18%, 3.01%, and 3.04%, respectively. Although the gap narrowed, the blended fuels still

maintained a slight advantage in terms of CO_2 emissions. The reduction in CO_2 emissions at lower engine speeds for the blended fuels can be attributed to the higher oxygen content and lower carbon content of the waste plastic oil compared with pure diesel. This unique composition promoted more complete combustion, resulting in lower CO_2 emissions. At higher engine speeds, the difference in CO_2 emissions between pure diesel and blended fuels becomes less significant, as the higher engine load and temperature lead to more complete combustion for all fuel blends. Mani et al. (2009) investigated diesel engines fuel with plastic pyrolysis oil-diesel blends and observed a similar trend of reduced CO_2 emissions with the addition of plastic pyrolysis oil, particularly evident at lower engine loads.(Padmanabhan et al., 2021) also reported decreased CO_2 emissions for waste plastic oil-diesel blends, especially at lower engine speeds. These studies collectively reinforce the potential of using waste plastic oil as a diesel fuel additive to reduce CO_2 emissions, particularly at low engine speeds. In conclusion, waste plastic oil has promising potential as a diesel fuel additive for reducing CO_2 emissions, especially at lower engine speeds.

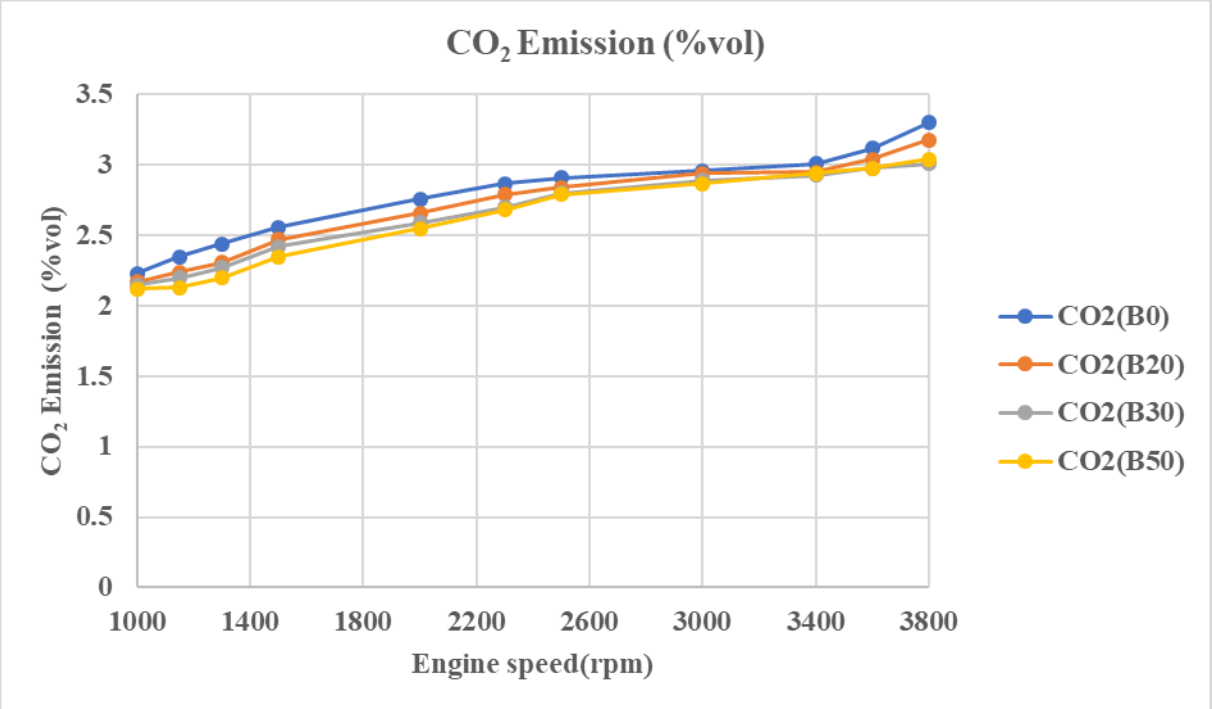

Figure 6-7: CO2 Emission result.

6.5.3. Nitrogen Oxide Emissions

The emissions of NOx from a diesel engine when using pure diesel fuel (B0) and blends of diesel and waste plastic oil (B20, B30, and B50), as illustrated in Figure 6-3, display a clear upward trend with increasing engine speed. The NOx emissions were relatively low at engine speeds of 1000-1500 rpm, NOx emissions were relatively low, ranging from 150 ppm for B0 to 220 ppm for B50. However, as the engine speed increased, the NOx emissions significantly increased, reaching 361 ppm for B50 at 3400 rpm.

This trend can be attributed to the higher cylinder temperatures and pressures experienced at higher engine speeds, which favor the formation of NOx through the thermal mechanism. In addition, the presence of nitrogen in waste plastic oil may contribute to increased NOx emissions through fuel mechanisms.

Interestingly, the B20 blend (20% waste plastic oil and 80% diesel) consistently exhibited lower NOx emissions than the other blends at all engine speeds. This finding suggests that B20 may be an optimal blend for reducing NOx emissions while still using plastic waste oil as a fuel source. In conclusion, the NOx emissions from a diesel engine fueled with waste plastic oil blends increased with engine speed, with B20 exhibiting the lowest NOx emissions among the tested blends. Further research is necessary to optimize the blend composition and engine parameters to minimize NOx emissions while maintaining the benefits of using waste plastic oil as a fuel source.

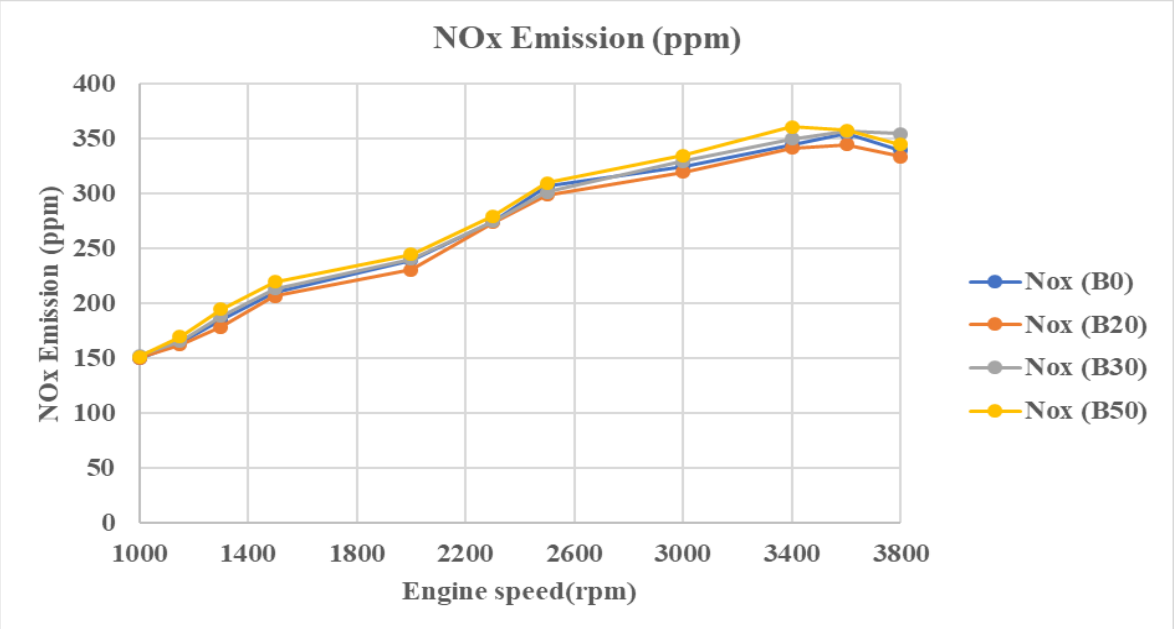

Figure 6-8: NOx Emission result.

6.5.4. Emission of unburned hydrocarbon

The investigation of unburned hydrocarbon (HC) emissions from a diesel engine running on pure diesel and various blends of diesel with waste plastic oil revealed a complicated relationship between the fuel composition, engine speed, and emissions. As illustrated in Figure 6-6, at lower engine speeds (1000-1500 rpm), the unburned HC emissions were relatively low for all the fuel blends. However, as the engine speed increased, there was a general trend of rising unburned HC emissions for all fuel blends, with the B50 blend (50% waste plastic oil and 50% diesel) consistently showing the highest emissions at each speed.

This trend suggests that the percentage of waste plastic oil in the blend has a significant impact on the unburned HC emissions, with higher proportions leading to increased emissions. These results align with those of previous studies that emphasized the influence of fuel composition on emissions. Although waste plastic oil can be used as an alternative to traditional fossil fuels, it may lead to higher unburned HC emissions than pure diesel.

The data also indicate that pure diesel (B0) is the most effective at minimizing unburned HC emissions across all engine speeds. This was likely due to the more complete combustion of diesel fuel, resulting in fewer unburned hydrocarbons being emitted. On the other hand, blends with higher proportions of waste plastic oil, such as B50, show elevated levels of HC emissions, potentially owing to the altered combustion characteristics of the fuel blend.

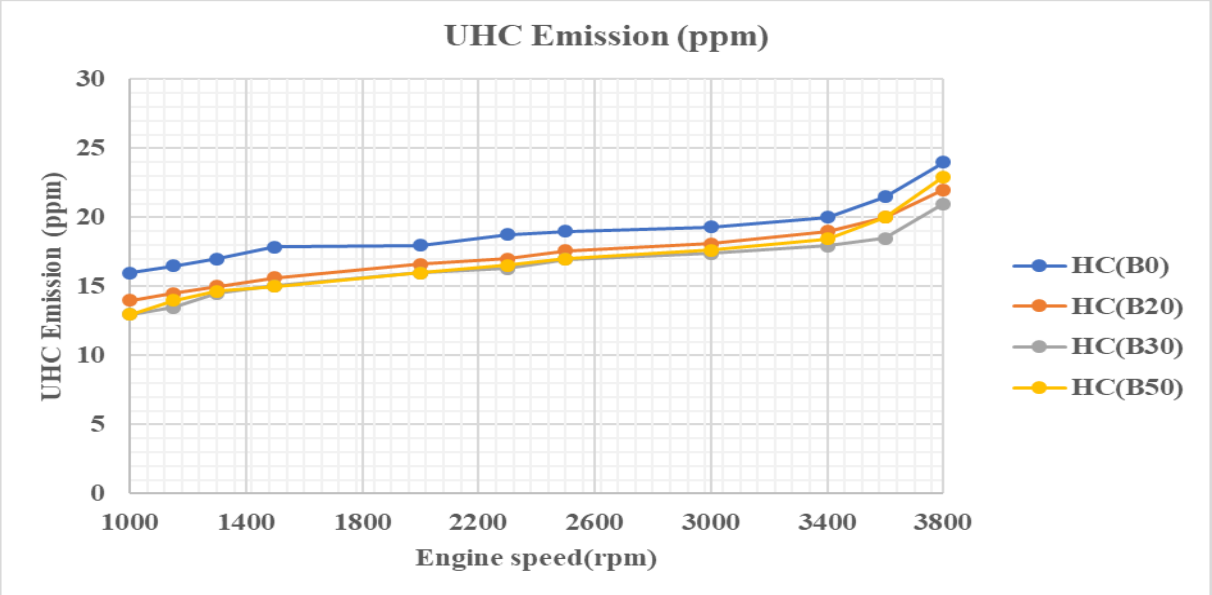

Figure 6-9: UHC Emission result.

6.6. Economic Analysis

List of raw materials with cost

The required raw materials with the specified cost and technical specification is presented in the table below

Table 6-3: list of raw materials with cost

No	Item descriptions	Technical specifications	Unit	Quantity	Total cost
1	Heater coil	3kw	PCs	4	120
2	Pipe	Stainless steel pipe (3/4inch)88	meter	2 meters	400
3	Angle bar	50mmX50mmX1080mmX5mm 88	PCs	2	1400
4	Flat bar	20 mmX300mmX3mm88	PCs	½	300
5	Sheet metal	46800mm^2X2mm88	PCs	1 ½	3075
6	Aluminium sheet metal	1000mm*1000mm88	PCs	1	2500
7	Stainless steel sheet metal	1000mm*1000mm88	PCs	1	2300
Total					10095

List of standard material with cost

The standard materials which are available in local market are listed as follows:

Table 6-4: list of standard materials with cost

No	Standard material	Specifications	Qnty	Total cost
1	Plug(mal)		1	35
2	Circuit interrupter		1	3812
3	Electric cable	Ø 5mm, 40amp	4 m	60
4	Gasket	35mmX35mmX2 mm	4	480
5	Switch		1	80
6	Bolt & nut	M12*1.75*40mm	10	80
7	Temperature controller		1	2016
8	JM26 Mullite insulation brick		20 kilos	900
9	LCD display	LCD 16X2	1	300
11	Elbow (3/4)		2	200
12	Pipe fitting		2	240
13	jumper cable		2	40
15	Paint		½	300
16	Electrode		2 pack	200
17	Rivet		2 pack	100
Total				7843

Manufacturing cost

For the fabrication process different tools are used

Table 6-5: List of cutting tools

No	Cutting tools	Specifications	Qnty	Total cost
1	Twist drill bit	Ø 4	1	10
2	Twist drill bit	Ø 8	1	15
3	Grinding disk	180mm	2	140
4	Cutter disk	180mm	3	210
Total				375

The machining cost for complete manufacturing is tabulated below

Table 6-6: machining cost.

No	Machining	Total price
1	Welding	750
2	Cutting	400
3	Grinding	120
4	Drilling	20
5	Rolling	120
Total		1410

Fixed Capital Investment

The capital investment required to supply manifesting and plant facilities is known as fixed capital investment. The subdivision of fixed capital investment is:

- ✓ Direct Cost
- ✓ Indirect Cost

Direct cost

The cost which is directly used in plant construction in addition to equipment cost is known as a direct cost.

Table 6-7: Direct cost of plastic pyrolysis machine

Item	Range	%	Cost (ETB)
Purchased equipment	---	100%	17938
Installation	4-5% of purchased equipment cost	5%	896.9
Electricity	4-5% of purchased equipment cost	4%	717.52
Building	3-4% of purchased equipment cost	3%	538.14
Yard Improvement	5-15% of purchase equipment cost	7%	1255.66
Total	---	---	**21,346.22**

Indirect Cost

Indirect costs are costs used by multiple activities, and which cannot therefore be assigned to specific cost objects. Examples of cost objects are products, services, geographical regions, distribution channels, and customers. Instead, indirect costs are needed to operate the business as a whole. It is useful to identify indirect costs, so that they can be excluded from short-term pricing decisions where management wants to set prices just above the variable costs of products. Indirect costs do not vary substantially within certain production volumes or other indicators of activities, and so are considered to be fixed costs. Examples of indirect costs are accounting and legal expenses, administrative salaries, office expenses, rent, security expenses, telephone expenses, and utilities.

Table 6-8: Indirect cost of the machine

Item	Range	%	Cost (ETB)
Contractor fee	2-8%	3%	538.14
Contingences	2-8%	2%	358.76
Power consumption	2-3%	2.3%	412.574
Total	----	----	**1309.474**

Fixed capital Investment = Direct cost + Indirect cost

Fixed capital Investment = $21346.22 + 1309.474 =$22655.694 ETB

Total capital investment

Total capital investment = Fixed capital investment + working capital investment

Working capital investment = 15% of fixed capital investment

Working capital investment = 3398.35ETB

Total capital Investment = 26,054.04ETB

- **Total production cost**

Total production cost = Variable Cost + Fixed Operating Cost + Overhead Cost +Electric cost

- ✓ **Variable cost**

Variable cost of plastic pyrolysis is shown in Table below

Table 6-9: Variable Cost of Plastic Pyrolysis.

Item	Cost (ETB)
Raw material	9000
Utilities	75
Variable Cost	9075

Variable Cost = Raw material Cost + Utilities Cost

Fixed operating cost

The fixed operating cost of pyrolysis plant is shown in Table below

Table 6-10: Fixed operating cost

Type	%FCI	Cost (ETB)
Maintenance	2	453.11
Operating Cost of Labour	3	679.67
Fixed Operating Cost	-	1132.78

Direct production cost = Variable Cost + Fixed Cost

Direct production cost = 31,730.694ETE

Overhead Charges

Overhead cost is 30% of direct production cost

Overhead Charges= 951.92ETE

- Electric cost per year

  = 9108Kwhr*2 ETB/ Kwhr = 18216 ETB

Total production cost = Direct Production Cost + Overhead Charges+ Electric cost

Total production cost = 50898.614ETB/year

- Total production rate

  = 39.2 liter/day = 8820 liter per year

Production Cost (ETB/liter) = $\frac{\text{Total production cost}}{\text{Total production rate}}$

Production Cost (ETE/liter) = 28 ETE per liter.

But the selling price of plastic oil per liter is 13 ETE per liter

Hence, the production cost of plastic oil is currently higher than its selling price, making the system economically unfeasible. As a result, its primary use is for waste management rather than profit generation. To improve the system's economic viability and reduce production costs, it is crucial to explore alternative energy sources. Utilizing biogas, for instance, instead of electricity can significantly lower energy expenses. By integrating biogas or other

renewable energy sources, the system can become more sustainable and cost-effective, thereby enhancing its overall efficiency and environmental benefits.

CHAPER SEVEN

7. CONCLUSIONS AND RECOMMENDATIONS

7.1. Summary

The study on creating a machine to transform plastic waste into fuel presents significant findings in the Results and Discussion section. The pyrolysis process successfully converted plastic waste into three main products, pyrolysis oil, char, and hydrocarbon gas, with 49% of the plastic waste transformed into oil, 8% into char, and 43% into gas. These results demonstrate the efficiency of the process in generating a considerable amount of liquid fuel, highlighting its potential for waste management and energy production.

The properties of the produced pyrolysis oil are comparable to those of conventional diesel. The oil had a calorific value of 41.318 MJ/kg, density of 0.789 g/ml at 15°C, and kinematic viscosity of 2.31 mm^2/s at 40°C. These characteristics suggest that pyrolysis oil is a suitable alternative to diesel with similar energy content and physical properties.

Emission tests showed that the environmental impact of using waste plastic oil as fuel was manageable. Carbon monoxide (CO) emissions were within acceptable limits, indicating that the combustion of oil did not significantly increase CO levels. Although carbon dioxide (CO2) emissions were slightly higher than diesel emissions, the increase was not substantial enough to offset the benefits of using oil as an alternative fuel. However, nitrogen oxide (NOx) emissions were higher because of the higher combustion temperatures required for pyrolysis oil, suggesting the need for mitigation measures such as catalytic converters. Unburned hydrocarbon (UHC) emissions were comparable to those of diesel, indicating efficient combustion of the pyrolysis oil.

7.2. Conclusions

This study presents the successful development of a fuel-extracting machine designed to convert plastic waste into usable fuel, demonstrating significant advancement in sustainable waste management and alternative fuel production. The machine effectively processes various types of plastics, including HDPE, LDPE, PS, and PP, and transforms them into valuable products, such as pyrolysis oil, char, and hydrocarbon gas. The produced pyrolysis oil exhibits a high calorific value and favorable properties, making it a viable substitute for traditional diesel fuel.

This innovation addresses two critical issues: the escalating plastic waste problem and reliance on diminishing fossil fuel resources. By converting plastic waste into valuable fuel, the machine not only mitigates the environmental impact of plastic disposal but also provides an alternative energy source, reducing dependency on conventional fossil fuels. This contributes to a circular economy and aids in decreasing greenhouse gas emissions, thereby promoting environmental sustainability.

The design and operation of the machine were meticulously planned and executed, optimizing the pyrolysis process to maximize fuel yield while maintaining high-quality output. Emission tests confirmed that the pyrolysis oil and its blends met environmental standards, further validating the potential of the machine for wider applications.

This study highlights the transformative potential of pyrolysis technology for waste management and energy production. The successful implementation of the fuel-extracting machine in Hossana City paves the way for similar initiatives in other regions, fostering sustainable practices and contributing to environmental conservation. As we strive for a greener future, such innovations will be crucial in addressing plastic waste challenges and ensuring energy security, making a significant impact on both the local and global scales.

7.3. Recommendations

In the pursuit of sustainable solutions for plastic waste management and alternative fuel production, optimizing waste plastic-to-oil conversion technology is crucial. By implementing key recommendations, advancements can be made to improve performance, efficiency, and environmental impact. The following are the essential recommendations to enhance the process.

- Optimize Reactor Design: Conduct a detailed two-dimensional transient heat transfer analysis and improve the agitation mechanism for uniform heating of plastics, preventing charring and incomplete pyrolysis.
- Diversify Feedstock Exploration: Research the pyrolysis potential of various plastic types, including PVC, and integrate a plastic shredder for finely ground feedstock.
- Enhance process efficiency: Implementing a continuous process pyrolysis plant, integrating distillation for refined output, and utilizing Computational Fluid Dynamics (CFD) simulations for precise analysis.

- Fuel Performance Evaluation: Investigate waste plastic oil as an alternative fuel for internal combustion engines and test properties such as flashpoint, fire point, cloud point, and total acidity.
- Innovative catalyst and nanoparticle testing: Experiments with different catalysts and nanoparticles to optimize production and assess performance and emissions.
- Blend Optimization and Scaling: Explore various fuel blends, analyze their characteristics, and evaluate cost-effective scaling of technology considering socioeconomic and environmental impacts.
- For large-scale production, alternative heating sources are used in addition to electricity to minimize operational costs and enhance energy efficiency. Options such as biogas, which can be produced from organic waste, should be considered as the primary heating source during pyrolysis. Biogas not only provides a renewable and cost-effective energy source but also aligns with the principles of circular economy by utilizing waste materials.

By focusing on these key recommendations, advancements in waste plastic-to-oil conversion technology can be achieved, contributing to a more sustainable approach towards plastic waste management and alternative fuel production.

REFERENCE

Aguado, J., Serrano, D. P., San Miguel, G., Castro, M. C., & Madrid, S. (2007). Feedstock recycling of polyethylene in a two-step thermo-catalytic reaction system. *Journal of Analytical and Applied Pyrolysis*, *79*(1–2), 415–423. https://doi.org/10.1016/j.jaap.2006.11.008

Babayemi, J. O., Nnorom, I. C., Osibanjo, O., & Weber, R. (2019a). Ensuring sustainability in plastics use in Africa: Consumption, waste generation, and projections. *Environmental Sciences Europe*, *31*(1), 60. https://doi.org/10.1186/s12302-019-0254-5

Babayemi, J. O., Nnorom, I. C., Osibanjo, O., & Weber, R. (2019b). Ensuring sustainability in plastics use in Africa: Consumption, waste generation, and projections. *Environmental Sciences Europe*, *31*(1), 60. https://doi.org/10.1186/s12302-019-0254-5

Bockhorn, H., Hornung, A., Hornung, U., & Schawaller, D. (1999). Kinetic study on the thermal degradation of polypropylene and polyethylene. *Journal of Analytical and Applied Pyrolysis*, *48*(2), 93–109. https://doi.org/10.1016/S0165-2370(98)00131-4

Damodharan, D., Rajesh Kumar, B., Gopal, K., De Poures, M. V., & Sethuramasamyraja, B. (2019). Utilization of waste plastic oil in diesel engines: A review. *Reviews in Environmental Science and Bio/Technology*, *18*(4), 681–697. https://doi.org/10.1007/s11157-019-09516-x

Darko, C., Yung, P. W. S., Chen, A., & Acquaye, A. (2023). Review and recommendations for sustainable pathways of recycling commodity plastic waste across different economic regions. *Resources, Environment and Sustainability*, *14*, 100134. https://doi.org/10.1016/j.resenv.2023.100134

Desidery, L., & Lanotte, M. (2022). 1 - Polymers and plastics: Types, properties, and manufacturing. In F. Giustozzi & S. Nizamuddin (Eds.), *Plastic Waste for Sustainable Asphalt Roads* (pp. 3–28). Woodhead Publishing. https://doi.org/10.1016/B978-0-323-85789-5.00001-0

Doboch Wanore, T., Abera Angello, Z., & Menberu Fetanu, Z. (2023). Optimized landfill site selection for municipal solid waste by integrating GIS and multicriteria decision analysis (MCDA) technique, Hossana town, southern Ethiopia. *Heliyon*, *9*(11), e21257. https://doi.org/10.1016/j.heliyon.2023.e21257

Ebenezer, O.-S., Osumanu, I. K., & Yahaya, A.-K. (2013). An Analysis of the Plastic Waste Collection and Wealth Linkages in Ghana. *International Journal of Current Research*, *5*.

Farayibi, P. K. (2017). Finite element analysis of plastic recycling machine designed for production of thin filament coil. *Nigerian Journal of Technology*, *36*(2), 411. https://doi.org/10.4314/njt.v36i2.13

Fojt, J., David, J., Přikryl, R., Řezáčová, V., & Kučerík, J. (2020). A critical review of the overlooked challenge of determining micro-bioplastics in soil. *Science of The Total Environment*, *745*, 140975. https://doi.org/10.1016/j.scitotenv.2020.140975

Gross, L., & Enck, J. (2021). Confronting plastic pollution to protect environmental and public health. *PLOS Biology*, *19*(3), e3001131. https://doi.org/10.1371/journal.pbio.3001131

Hogan, J. P., & Banks, R. L. (1986). History of Crystalline Polypropylene. In R. B. Seymour & T. Cheng (Eds.), *History of Polyolefins* (pp. 103–115). Springer Netherlands. https://doi.org/10.1007/978-94-009-5472-4_6

Jalilvand, A., Ghasemi, I., Karrabi, M., & Azizi, H. (n.d.). *Using Devulcanized EPDM in PP/HDPE/ EPDM Ternary Blend: Mechanical Properties and Morphology*.

Jastrzębska, I., & Szczerba, J. (2024). Design, Manufacturing and Properties of Refractory Materials. *Materials*, *17*(7), 1673. https://doi.org/10.3390/ma17071673

Jayswal, A., Arbind Kumarsah, Prabin Pradhananga, Rohit Sah, & Darlami, H. B. (2017). *Design, Fabrication and Testing of Waste Plastic Pyrolysis Plant*. https://doi.org/10.13140/RG.2.2.33682.15044

Jung, S.-H., Cho, M.-H., Kang, B.-S., & Kim, J.-S. (2010). Pyrolysis of a fraction of waste polypropylene and polyethylene for the recovery of BTX aromatics using a fluidized bed reactor. *Fuel Processing Technology*, *91*(3), 277–284. https://doi.org/10.1016/j.fuproc.2009.10.009

Kaiser, K., Schmid, M., & Schlummer, M. (2017). Recycling of Polymer-Based Multilayer Packaging: A Review. *Recycling*, *3*(1), 1. https://doi.org/10.3390/recycling3010001

Kaminsky, W., Predel, M., & Sadiki, A. (2004). Feedstock recycling of polymers by pyrolysis in a fluidised bed. *Polymer Degradation and Stability*, *85*(3), 1045–1050. https://doi.org/10.1016/j.polymdegradstab.2003.05.002

Khan, M. Z. H., Sultana, M., Al-Mamun, M. R., & Hasan, M. R. (2016). Pyrolytic Waste Plastic Oil and Its Diesel Blend: Fuel Characterization. *Journal of Environmental and Public Health*, *2016*, 1–6. https://doi.org/10.1155/2016/7869080

Kurniawan, A., Sugiarto, B., & Perdana, A. (2020). Design of a Simple Pyrolysis Reactor for Plastic Waste Conversion into Liquid Fuel using Biomass as Heating Source. *Eksergi*, *17*(1), 1. https://doi.org/10.31315/e.v17i1.3080

Maithomklang, S., Wathakit, K., Sukjit, E., Sawatmongkhon, B., & Srisertpol, J. (2022). Utilizing Waste Plastic Bottle-Based Pyrolysis Oil as an Alternative Fuel. *ACS Omega*, *7*(24), 20542–20555. https://doi.org/10.1021/acsomega.1c07345

Marcilla, A., Beltrán, M. I., & Navarro, R. (2008). Evolution of Products Generated during the Dynamic Pyrolysis of LDPE and HDPE over HZSM5. *Energy & Fuels*, *22*(5), 2917–2924. https://doi.org/10.1021/ef800229d

Miskolczi, N., Bartha, L., Deák, G., & Jóver, B. (2004). Thermal degradation of municipal plastic waste for production of fuel-like hydrocarbons. *Polymer Degradation and Stability*, *86*(2), 357–366. https://doi.org/10.1016/j.polymdegradstab.2004.04.025

Moriya, T., & Enomoto, H. (1999). Characteristics of polyethylene cracking in supercritical water compared to thermal cracking. *Polymer Degradation and Stability*, *65*(3), 373–386. https://doi.org/10.1016/S0141-3910(99)00026-9

Murthy, K., Shetty, R. J., & Shiva, K. (2023). Plastic waste conversion to fuel: A review on pyrolysis process and influence of operating parameters. *Energy Sources, Part A: Recovery, Utilization, and Environmental Effects*, *45*(4), 11904–11924. https://doi.org/10.1080/15567036.2020.1818892

Mutha, N. H., Patel, M., & Premnath, V. (2006). Plastics materials flow analysis for India. *Resources, Conservation and Recycling*, *47*(3), 222–244. https://doi.org/10.1016/j.resconrec.2005.09.003

Nofar, M., & Oğuz, H. (2019). Development of PBT/Recycled-PET Blends and the Influence of Using Chain Extender. *Journal of Polymers and the Environment*, *27*(7), 1404–1417. https://doi.org/10.1007/s10924-019-01435-w

Padmanabhan, S., Joel, C., Joel, L., Reddy, O. Y., Harsha, K. G. D. S., & Ganesan, S. (2021). Evaluation of Waste Plastic Pyrolysis Oil Performance with Diethyl Ether Additive

on Insulated Piston Diesel Engine. *Nature Environment and Pollution Technology*, *20*(5). https://doi.org/10.46488/NEPT.2021.v20i05.025

Panda, A. K., Singh, R. K., & Mishra, D. K. (2010). Thermolysis of waste plastics to liquid fuelA suitable method for plastic waste management and manufacture of value added products—A world prospective. *Renewable and Sustainable Energy Reviews*, *14*(1), 233–248. https://doi.org/10.1016/j.rser.2009.07.005

Pandey, P., Dhiman, M., Kansal, A., & Subudhi, S. P. (2023). Plastic waste management for sustainable environment: Techniques and approaches. *Waste Disposal & Sustainable Energy*, *5*(2), 205–222. https://doi.org/10.1007/s42768-023-00134-6

Pratama, A. W. & Winarko. (2020). Performance Test of A mixture of Polypropylene Plastic Fuel from Pyrolisis with Gasoline to Torque and engine Power. *Journal of Physics: Conference Series*, *1569*, 032045. https://doi.org/10.1088/1742-6596/1569/3/032045

Rapsing, E. C. (2016). *Design and Fabrication of Waste Plastic Oil Converter*. *4*(2).

Rasmussen, S. C. (2018). Revisiting the Early History of Synthetic Polymers: Critiques and New Insights. *Ambix*, *65*(4), 356–372. https://doi.org/10.1080/00026980.2018.1512775

Reif-Acherman, S. (2012). The contributions of Henri Victor Regnault in the context of organic chemistry of the first half of the nineteenth century. *Química Nova*, *35*(2), 438–443. https://doi.org/10.1590/S0100-40422012000200037

Ritchie, H., Samborska, V., & Roser, M. (2023). Plastic Pollution. *Our World in Data*. https://ourworldindata.org/plastic-pollution

Sarker, M. (2012). First Simple and Easy Process of Thermal Degrading Municipal Waste Plastics into Fuel Resource. *IOSR Journal of Engineering*, *02*(09), 38–49. https://doi.org/10.9790/3021-02923849

Seddegi, Z. S., Budrthumal, U., Al-Arfaj, A. A., Al-Amer, A. M., & Barri, S. A. I. (2002). Catalytic cracking of polyethylene over all-silica MCM-41 molecular sieve. *Applied Catalysis A: General*, *225*(1–2), 167–176. https://doi.org/10.1016/S0926-860X(01)00872-9

Sharuddin, S. D. A., Abnisa, F., Daud, W. M. A. W., & Aroua, M. K. (2018). Pyrolysis of plastic waste for liquid fuel production as prospective energy resource. *IOP Conference Series: Materials Science and Engineering*, *334*, 012001. https://doi.org/10.1088/1757-899X/334/1/012001

Shehata, N., Mohamed, H. S. H., Emam, H. M., & Ahmed, S. (2017). *FUEL PRODUCED FROM CATALYTIC PYROLYSIS OF WASTE PLASTIC*. *22*.

Shukla, Y., Singh, H., Sonkar, S., & Kumar, D. (n.d.). *Design Of Viable Machine To Convert Waste Plastic Into Mixed Oil For Domestic Purpose*.

Singh, N., Hui, D., Singh, R., Ahuja, I. P. S., Feo, L., & Fraternali, F. (2017). Recycling of plastic solid waste: A state of art review and future applications. *Composites Part B: Engineering*, *115*, 409–422. https://doi.org/10.1016/j.compositesb.2016.09.013

Sonawane, Y., Shindikar, M., & Khaladkar, M. (2014). Onsite Conversion of Thermoplastic Waste into Fuel by Catalytic Pyrolysis. *International Journal of Innovative Research in Science, Engineering and Technology*, *03*(09), 15903–15908. https://doi.org/10.15680/IJIRSET.2014.0309016

Suresh, A., Alagusundaram, A., Kumar, P. S., Vo, D.-V. N., Christopher, F. C., Balaji, B., Viswanathan, V., & Sankar, S. (2021). Microwave pyrolysis of coal, biomass and

plastic waste: A review. *Environmental Chemistry Letters*, *19*(5), 3609–3629. https://doi.org/10.1007/s10311-021-01245-4

Uddin, M. A., Koizumi, K., Murata, K., & Sakata, Y. (1997). Thermal and catalytic degradation of structurally different types of polyethylene into fuel oil. *Polymer Degradation and Stability*, *56*(1), 37–44. https://doi.org/10.1016/S0141-3910(96)00191-7

Varma, A. K., & Mondal, P. (2017). Pyrolysis of sugarcane bagasse in semi batch reactor: Effects of process parameters on product yields and characterization of products. *Industrial Crops and Products*, *95*, 704–717. https://doi.org/10.1016/j.indcrop.2016.11.039

Wilke, G. (2003). Fifty Years of Ziegler Catalysts: Consequences and Development of an Invention. *Angewandte Chemie International Edition*, *42*(41), 5000–5008. https://doi.org/10.1002/anie.200330056

Wongkhorsub, C., & Chindaprasert, N. (2013). A Comparison of the Use of Pyrolysis Oils in Diesel Engine. *Energy and Power Engineering*, *05*(04), Article 04. https://doi.org/10.4236/epe.2013.54B068

APPENDICES

Appendix A: Pipe schedule ASME B36.19M

Schedule is the value used to determine outside diameter for stain less pipe and its value depicted in Table A.

Table A- 1: Pipe schedule ASME B36.19M

PIPE NPS	OUTSIDE DIAMETER O.D	PIPE SCHEDULE													MEASURE Top: Wall thickness (in) Bottom: Pipe weight (lb/ft)
	inches	5s	5	10	10s	40s STD	40	60	80s XH(XS)	80	100	120	140	160	XXH (XXS)
1/8	0.405		0.035 *0.1383*	0.049 *0.186*	0.049 *0.186*	0.068 *0.245*	0.068 *0.2447*		0.095 *0.315*	0.095 *0.315*					
1/4	0.54		0.049 *0.257*	0.065 *0.33*	0.065 *0.33*	0.088 *0.425*	0.088 *0.4248*		0.119 *0.535*	0.119 *0.535*					
3/8	0.675		0.049 *0.3276*	0.065 *0.424*	0.065 *0.424*	0.091 *0.568*	0.091 *0.5676*		0.126 *0.734*	0.126 *0.734*					
1/2	0.84	0.065 *0.538*	0.065 *0.5383*	0.083 *0.671*	0.083 *0.671*	0.109 *0.851*	0.109 *0.851*		0.147 *1.088*	0.147 *1.088*				0.188 *1.304*	0.294 *1.714*
3/4	1.05	0.065 *0.684*	0.065 *0.6838*	0.083 *0.857*	0.083 *0.857*	0.113 *1.131*	0.113 *1.131*		0.154 *1.474*	0.154 *1.474*				0.219 *1.937*	0.308 *2.441*
1	1.315	0.065 *0.868*	0.065 *0.8678*	0.109 *1.404*	0.109 *1.404*	0.133 *1.679*	0.133 *1.679*		0.179 *2.172*	0.179 *2.172*				0.25 *2.844*	0.358 *3.659*
1-1/4	1.66	0.065 *1.107*	0.065 *1.107*	0.109 *1.806*	0.109 *1.806*	0.14 *2.273*	0.14 *2.273*		0.191 *2.997*	0.191 *2.997*				0.25 *3.765*	0.382 *5.214*
1-1/2	1.9	0.065 *1.274*	0.065 *1.274*	0.109 *2.085*	0.109 *2.085*	0.145 *2.718*	0.145 *2.718*		0.2 *3.631*	0.2 *3.631*				0.281 *4.859*	0.4 *6.408*
2	2.375	. *1.604*	0.065 *1.604*	0.109 *2.638*	0.109 *2.638*	0.154 *3.653*	0.154 *3.653*		0.218 *5.022*	0.218 *5.022*				0.344 *7.444*	0.436 *9.029*
2-1/2	2.875	0.083 *2.475*	0.083 *2.475*	0.12 *3.531*	0.12 *3.531*	0.203 *5.793*	0.203 *5.793*		0.276 *7.661*	0.276 *7.661*				0.375 *10.01*	0.552 *13.7*
3	3.5	0.083 *3.029*	0.083 *3.029*	0.12 *4.332*	0.12 *4.332*	0.216 *7.576*	0.216 *7.576*		0.3 *10.25*	0.3 *10.25*				0.438 *14.32*	0.6 *18.58*
3-1/2	4	0.083 *3.472*	0.083 *3.472*	0.12 *4.973*	0.12 *4.973*	0.226 *9.109*	0.226 *9.109*		0.318 *12.51*	0.318 *12.51*					0.636 *22.85*
4	4.5	0.083 *3.915*	0.083 *3.915*	0.12 *5.613*	0.12 *5.613*	0.237 *10.79*	0.237 *10.79*	0.281 *12.66*	0.337 *14.98*	0.337 *14.98*		0.438 *19.01*		0.531 *22.51*	0.674 *27.54*

Appendix B: Constants for tube bank in counter flow and correction factor

The constants for tube bank in counter flow as depicted in Table B-1.

Table B-1: Constants for tube bank in counter flow.

Configuratio	$Re_{D,max}$	C_1	m
Aligned	$10–10^2$	0.80	0.40
Staggered	$10–10^2$	0.90	0.40
Aligned	$10^2–10^3$	Approximate as a single (isolated) cylinder	
Staggered	$10^2–10^3$		
Aligned $(S_T/S_L > 0.7)^a$	$10^3–2 \times 10^5$	0.27	0.63
Staggered $(S_T/S_L < 2)$	$10^3–2 \times 10^5$	$0.35(S_T/S_L)^{1/5}$	0.60
Staggered $(S_T/S_L > 2)$	$10^3–2 \times 10^5$	0.40	0.60
Aligned	$2 \times 10^5–2 \times 10^6$	0.021	0.84
Staggered	$2 \times 10^5–2 \times 10^6$	0.022	0.84

The correction factor that used during condenser design as depicted in Table B-2.

Table B- 2: Correction factor.

N_L	1	2	3	4	5	7	10	13	16
Aligned	0.70	0.80	0.86	0.90	0.92	0.95	0.97	0.98	0.99
Staggered	0.64	0.76	0.84	0.89	0.92	0.95	0.97	0.98	0.99

Appendix C: Dimensional and Cross-sectional properties for SSAB

The dimensional and cross-sectional properties for SSAB that used for body design as depicted in Table C.

Table C-1: Dimensional and cross-sectional properties for SSAB.

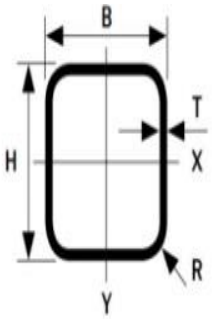

M = Weight
A = Cross-section area
A_u = External surface area
I = Moment of inertia
W = Section modulus

W_p = Plastic section modulus
i = Radius of gyration
I_v = Torsion modulus
W_v = Section modulus in torsion

Theoretical density = 7.85 kg/dm³

The cross-sectional properties have been calculated by using nominal dimensions H, B and T and corner outer radius R.

R = 2.0 x T. when T ≤ 6.0 mm
R = 2.5 x T. when 6.0 mm < T ≤ 10.0 mm
R = 3.0 x T. when T > 10.0 mm

H x B mm	T mm	M kg/m	A $mm^2 \times 10^2$	A_u m^2/m	$I_x = I_y$ $mm^4 \times 10^4$	$W_x = W_y$ $mm^3 \times 10^3$	$W_{px} = W_{py}$ $mm^3 \times 10^3$	$i_x = i_y$ mm x 10	I_v $mm^4 \times 10^4$	W_v $mm^3 \times 10^3$
25x25	2.0	1.36	1.74	0.093	1.48	1.19	1.47	0.92	2.53	1.80
25x25	2.5	1.64	2.09	0.091	1.69	1.35	1.71	0.90	2.97	2.07
25x25	3.0	1.89	2.41	0.090	1.84	1.47	1.91	0.87	3.33	2.27
30x30	2.0	1.68	2.14	0.113	2.72	1.81	2.21	1.13	4.54	2.75
30x30	2.5	2.03	2.59	0.111	3.16	2.10	2.61	1.10	5.40	3.20
30x30	3.0	2.36	3.01	0.110	3.50	2.34	2.96	1.08	6.15	3.58
40x40	2.0	2.31	2.94	0.153	6.94	3.47	4.13	1.54	11.28	5.23
40x40	2.5	2.82	3.59	0.151	8.22	4.11	4.97	1.51	13.61	6.21
40x40	3.0	3.30	4.21	0.150	9.32	4.66	5.72	1.49	15.75	7.07
40x40	4.0	4.20	5.35	0.146	11.07	5.54	7.01	1.44	19.44	8.48
50x50	2.0	2.93	3.74	0.193	14.15	5.66	6.66	1.95	22.63	8.51
50x50	2.5	3.60	4.59	0.191	16.94	6.78	8.07	1.92	27.53	10.22
50x50	3.0	4.25	5.41	0.190	19.47	7.79	9.39	1.90	32.13	11.76
50x50	4.0	5.45	6.95	0.186	23.74	9.49	11.73	1.85	40.42	14.43
50x50	5.0	6.56	8.36	0.183	27.04	10.82	13.70	1.80	47.46	16.56
60x60	2.0	3.56	4.54	0.233	25.14	8.38	9.79	2.35	39.79	12.59

Appendix D: Properties of waste plastic oil

The properties of waste plastic oil sample choosen for the study was done in Ethiopian petroleum supply Enterprise quality assurance service as depicted in Figure D.

Company Name:

ETHIOPIAN PETROLEUM SUPPLY ENTERPRISE
QUALITY ASSURANCE SERVICE

Document No: OF/EPSE/QAS/033
Page 1 of 1

TITLE: CERTIFICATE OF TEST REPORT

Issue No.: 2 | Date of Issue: May ,2024
Prepared by: QT | Approved by: Tadesse H/Mariam

Sample Originator: ADAMA SCIENCE &TECHNOLOGY UNIVERSITY	Request No:7/2-1-1/7mgo/38/73/16
Sample Type: Wpo	Analytical Method: ASTM /IP/ISO.
Sample Number: 01	Analytical Result: Interpreted with stds.
Lab. Number: 2024- ADO-EXT-38	Report No: QA/0042/2024
Sample Submitted By: CUSTOMER HABTAMU	Test date: 02/05/2024
Date Submitted: 1/05/2024	Issued Date: 10/05/2024
Customer Address: ADAMA	Telephone. 0916-881967

S.N	Property	Test method ASTM	Limits	Test results of the sample	
				WPO100	
1	Density@15°C, g/mL	D4052	Report	0.789	
	Density@20°C, g/mL	D4052	Report	0.781	
2	Kinematic viscosity @ 40 °c, mm^2/sec	D 445		2.31	
3	Calorific value, calc, BTU/LB	Calculated		41318.66	

Liability:- Ethiopian Petroleum supply Enterprise, its Laboratory, its Servants or agents Shall not be held liable for any damages, loss, claims or expenses direct or indirect howsoever caused, arising in connection with the laboratory test carried out on waste plastic oil sample submitted to it for analysis whether in tort or in contract, due to any act, omission or error of whatever nature, whether or not negligence and howsoever caused. Furthermore all expenses and implied warranties are specifically disclaimed. This test report shall not be reproduced or given to a third party without written approval of the Petroleum Quality Assurance Service.

Lab. Expert Name- Signature-

Senior expert Name- Signature-

Quality Control Head Name- Signature-

Ethiopian Petroleum Supply Enterprise 1966

PLEAS MAKE SURE THAT THIS IS THE CORRECT ISSUE BEFORE USE

CONFIDENTIAL

Figure D-1: Properties of waste plastic oil.

Appendix E: Visual Documentation of Research Work in Shop

Figure E-1: Visual documentation of research work.

Appendix F: Visual documentation of research work at laboratory

Figure F-1: Visual documentation of research work at laboratory.

Appendix G: Emission tests results

Table G-1: Emission test result for CO.

CO emission(%vol)				
Engine speed(rpm)	CO(B0)	CO(B20)	CO(B30)	CO(B50)
1000	0.0632	0.0651	0.0661	0.072
1150	0.061	0.0583	0.0592	0.0674
1300	0.0572	0.0572	0.0581	0.0631
1500	0.0553	0.0565	0.0573	0.0592
2000	0.0531	0.0544	0.0552	0.0571
2300	0.0541	0.0553	0.0544	0.0564
2500	0.0582	0.0572	0.0591	0.063
3000	0.0632	0.0633	0.0663	0.0651
3400	0.0694	0.0681	0.0721	0.0712
3600	0.0753	0.0742	0.0782	0.0761
3800	0.0832	0.0814	0.0831	0.083

Table G-2: Emission test result for CO2.

Co_2 emission (%vol)				
Engine speed(rpm)	CO_2(B0)	CO_2(B20)	CO_2(B30)	CO_2(B50)
1000	2.231	2.171	2.151	2.123
1150	2.353	2.243	2.22	2.131
1300	2.441	2.311	2.273	2.22
1500	2.562	2.473	2.422	2.353
2000	2.761	2.662	2.592	2.551
2300	2.873	2.791	2.73	2.683
2500	2.912	2.842	2.82	2.792
3000	2.962	2.941	2.894	2.871
3400	3.013	2.952	2.931	2.942
3600	3.121	3.041	2.982	2.983
3800	3.31	3.182	3.012	3.041

Table G-3: Emission test result for NOx.

Nox emission (ppm)				
Engine speed(rpm)	Nox (B0)	Nox (B20)	Nox (B30)	Nox (B50)
1000	149	150	152	151
1150	164	162	165	169
1300	184	178	188	194
1500	209	206	213	219
2000	239	230	240	244
2300	274	273	274	279
2500	306	298	301	309
3000	324	319	329	334
3400	344	341	349	360
3600	354	344	356	357
3800	339	333	354	344

Table G-4: Emission test result for HC.

HC emission (ppm)				
Engine speed(rpm)	HC(B0)	HC(B20)	HC(B30)	HC(B50)
1000	16.2	14.05	13.1	13.1
1150	16.51	14.53	13.5	14
1300	17.011	15	14.5	14.67
1500	17.827	15.65	15.04	15
2000	18.2	16.62	16	15.98
2300	18.725	17	16.32	16.55
2500	19.3	17.58	16.98	17.1
3000	19.32	18.09	17.4	17.65
3400	20.22	19.5	17.93	18.44
3600	21.53	20.3	18.5	20.2
3800	24.23	22.2	21	22.90

Appendix H: Some of Instruments that used

Figure H-1: Some of instruments used.

Appendix I: Code for radial temperature distribution

```
import numpy as np
import matplotlib.pyplot as plt
# giving boundary condition and  constants , heater is applied at the outer surface
radius_inner = 175  # mm (inner radius)
radius_outer = 180  # mm (outer radius)
height = 750  # mm
power = 3000  # W
k = 50  # W/m·K, thermal conductivity of steel
T_outer = 450 + 273  # K

# Converting mm to meters
height_m = height / 1000
radius_inner_m = radius_inner / 1000
radius_outer_m = radius_outer / 1000

# Calculate the inner temperature
Q = power
A = 2 * np.pi * radius_outer_m * height_m  # Outer surface area in m^2
T_inner = T_outer - (Q / (2 * np.pi * k * height_m)) * np.log(radius_outer_m / radius_inner_m)

# Radial temperature distribution of wall
r = np.linspace(radius_inner_m, radius_outer_m, 100)
T = T_outer - (Q / (2 * np.pi * k * height_m)) * np.log(radius_outer_m / r)

# Plotting
plt.figure(figsize=(10, 6))
plt.plot(r * 1000, T, label='Temperature Distribution')
plt.xlabel('Radius (mm)')
plt.ylabel('Temperature (K)')
plt.title('Radial Temperature Distribution in the Reactor Wall')
plt.legend()
plt.grid(True)
plt.show()

T_inner  # Display the inner temperature in Kelvin for reference
```

```python
import numpy as np
import matplotlib.pyplot as plt
# Given boundary condition and constants, heater is applied at the outer surface
radius_inner = 175  # mm (inner radius)
radius_outer = 180  # mm (outer radius)
height = 750  # mm
power = 3000  # W
k = 50  # W/m·K, thermal conductivity of steel
T_outer = 450 + 273  # K
# Converting mm to meters
height_m = height / 1000
radius_inner_m = radius_inner / 1000
radius_outer_m = radius_outer / 1000
# Calculate the inner temperature
Q = power
A = 2 * np.pi * radius_outer_m * height_m  # Outer surface area in m^2
T_inner = T_outer - (Q / (2 * np.pi * k * height_m)) * np.log(radius_outer_m / radius_inner_m)
# Radial temperature distribution of wall
r = np.linspace(radius_inner_m, radius_outer_m, 100)
T = T_outer - (Q / (2 * np.pi * k * height_m)) * np.log(radius_outer_m / r)
# 2D Grid for heatmap
z = np.linspace(0, height_m, 100)
R, Z = np.meshgrid(r, z)
T_2d = T_outer - (Q / (2 * np.pi * k * height_m)) * np.log(radius_outer_m / R)
# Plotting
plt.figure(figsize=(10, 6))
plt.contourf(R * 1000, Z * 1000, T_2d, 100, cmap='hot')
plt.colorbar(label='Temperature (K)')
plt.xlabel('Radius (mm)')
plt.ylabel('Height (mm)')
plt.title('Heatmap of Radial Temperature Distribution in the Reactor Wall')
plt.grid(True)
plt.show()
# Display the inner temperature in Kelvin for reference
T_inner
```